AD 409 302

WATERTOWN ARSENAL LABORATORIES

LOW TEMPERATURE FLOW AND FRACTURE CHARACTERISTICS OF SOME IRON-BASE ALLOYS

TECHNICAL REPORT WAL TR 834.2/9

BY

JOHN NUNES

AND

FRANK R. LARSON

DATE OF ISSUE - MAY 1963

AMS CODE 5011.11.838
BASIC RESEARCH IN PHYSICAL SCIENCES
D/A PROJECT 1-A-0-10501-B-010

WATERTOWN ARSENAL
WATERTOWN 72, MASS.

The findings in this report are not to be construed as an official Department of the Army position.

Plastic flow

Fracture

Iron alloys

LOW TEMPERATURE FLOW AND FRACTURE CHARACTERISTICS OF SOME IRON-BASE ALLOYS

Technical Report WAL TR 834.2/9

by

John Nunes

and

Frank R. Larson

Date of Issue - May 1963

AMS Code 5011.11.838
Basic Research in Physical Sciences
D/A Project 1-A-0-10501-B-010

WATERTOWN ARSENAL
WATERTOWN 72, MASS.

WATERTOWN ARSENAL LABORATORIES

TITLE

LOW TEMPERATURE FLOW AND FRACTURE CHARACTERISTICS OF SOME IRON-BASE ALLOYS

ABSTRACT

Temperature dependent functions of various tensile flow stress and fracture parameters were investigated on iron and low composition alloys of Fe-C, Fe-Cr, Fe-Mn, and Fe-Ni. Data were obtained over a range of test temperatures from 200 to -196 C at an initial strain rate of .01 min^{-1}.

It was found that the strain hardening exponent, n, for the Fe-Ni alloys exhibited a considerable improvement at very low testing temperatures with increased alloy addition. Also, the stress and strain at fracture followed a predictable transitional type of behavior. Some anomalous yield point and strengthening effects were also observed.

The flow stress-temperature dependence was evaluated employing the relation:

$$\sigma = \frac{M}{T} + \sigma_0$$

where it is shown that along with crystallographic structure composition can strongly influence the constant M. An empirical formula describing this effect is as follows:

$$M = m_1 \text{ (equivalent At. \% Ni)}^{-1/3}.$$

Some preliminary tests were run on several commercial steels to test the generality of this relationship.

JOHN NUNES
Materials Engineer

FRANK R. LARSON
Supervisory Physical Metallurgist

APPROVED:

J. F. SULLIVAN
Director
Watertown Arsenal Laboratories

CONTENTS

INTRODUCTION

One of the phenomenological explanations of the ductile-to-brittle transition encountered in body-centered cubic metals is based upon the difference in the temperature dependence of the flow and fracture stresses.[1,2] It states simply that the fracture stress is relatively insensitive to temperature and that the yield or flow stress rises rapidly with decreasing temperature so that when the flow stress reaches the fracture stress, brittle fracture occurs without appreciable plastic deformation. This behavior is illustrated schematically in Figure 1 where the ductile-to-brittle transition is shown to occur at two possible temperatures. The lowest temperature (T_B) represents essentially completely brittle behavior while the higher temperature (T_N) represents

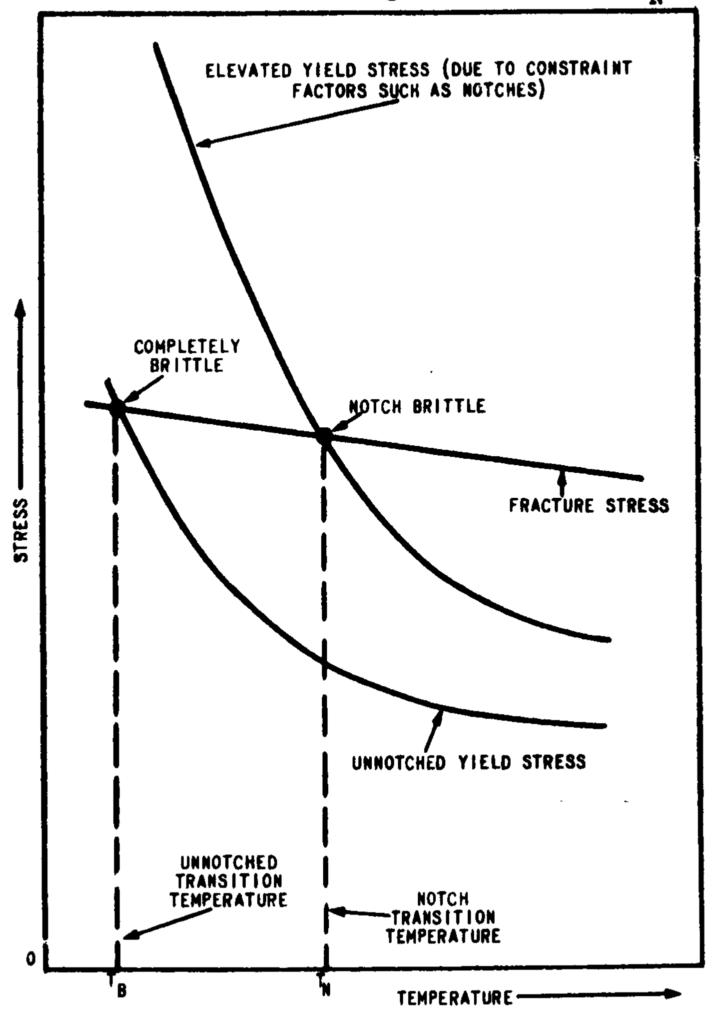

Figure 1. SCHEMATIC REPRESENTATION OF THE FLOW STRESS-TEMPERATURE DEPENDENCE RELATIONSHIP TO THE DUCTILE-BRITTLE TRANSITIONAL BEHAVIOR OF BCC METALS

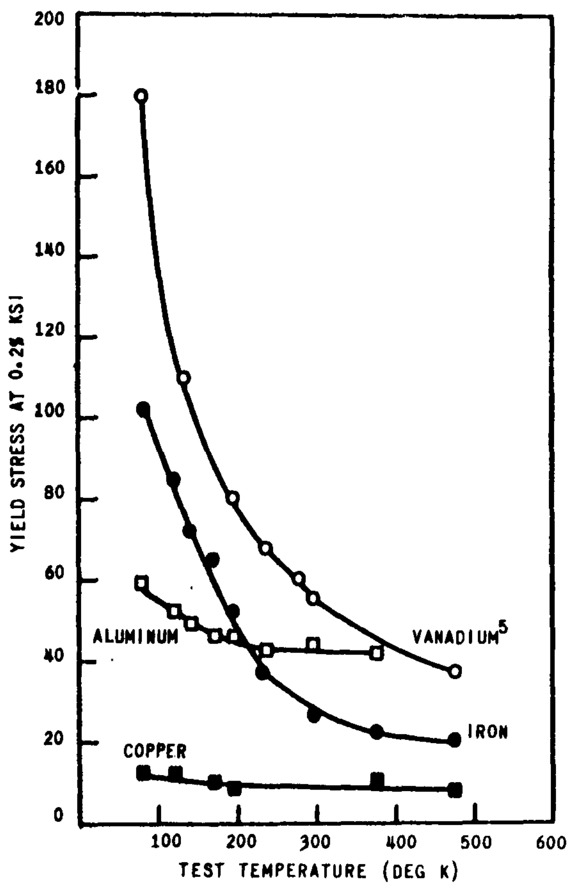

Figure 2. REPRESENTATIVE YIELD STRESS VERSUS TEMPERATURE CURVES FOR BCC Fe AND V AND FOR FCC Al AND Cu METALS

"notch" brittle behavior. Support for this theory is obtained when it is observed that face-centered cubic metals, which do not commonly have a ductile-to-brittle transition, also do not commonly exhibit any strong temperature dependence of the yield stress. This apparent causality of yield or flow stress behavior with the ductile-to-brittle transition has been generally observed for most metals representative of these two crystallographic structures. One exception to this generalization appears in the case of tantalum[3,4] where no apparent ductile-to-brittle transition has been observed. However, this may simply be an indication that this type of behavior is not directly related to the flow stress and that some other mechanism such as twinning must also be operative. A comparison of the typical temperature dependence of the yield stress of some representative metals is shown in Figure 2.

In the study of the temperature dependence of the strength of metallic materials, considerable effort has been devoted to the yield strength. These studies along with dislocation theory have indicated that, within certain limitations, the yield strength should be a linear function of the reciprocal of absolute temperature. The equation to represent this in a simplified form is as follows:

$$\sigma = \frac{M}{T} + \sigma_0 \Bigg|_{\text{Constant } \epsilon \, + \, \dot{\epsilon}.}$$

The above equation was utilized to study the plastic flow properties of a 4340 steel in a previous investigation.[5] In that study the true stress-strain tests were run over a range of testing temperatures and heat treatments. Figure 3 illustrates the compliance of the data to the above relationship. One of the important features of the work was the demonstration of the fact that the slope M was independent of microstructure and strength level.

Further examination of other alloy steels,[6,7] copper,[8] aluminum,[6] titanium,[6] iron,[6,8] and vanadium[9] revealed that this slope M (the

temperature dependence of the yield or flow stress) was not only sensitive to crystal structure but also to composition. Some of these metals which were shown in Figure 2 are now shown in Figure 4 where the yield stress is replotted versus the reciprocal of absolute temperature. It can be seen from this plot and the other data in Figure 3 that although the slope M is primarily influenced by crystal structure, it is also affected by composition. The particular study being reported here will be concerned with the effect of composition only.

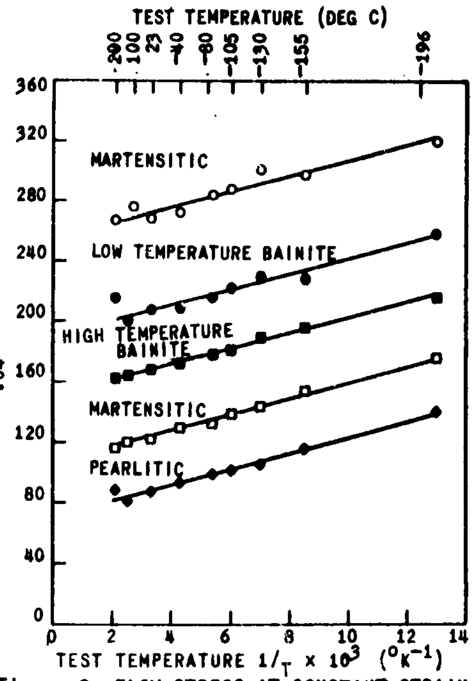

Figure 3. FLOW STRESS AT CONSTANT STRAIN OF .04 VERSUS THE RECIPROCAL OF ABSOLUTE TEMPERATURE FOR HEAT-TREATED AISI 4340 STEELS

Many studies have been conducted on both the effects of alloying elements and temperature on the mechanical properties of iron and its alloys. One of the earlier, more comprehensive analyses of these effects was that of Bain.[10] This was followed by more quantitative studies on the influence of composition in some iron binary alloys as influenced by alloying elements on heat treatment,[11] annealing,[12] and tension testing.[13] Although these alloys were not of the highest purity, the property data obtained from them were sufficient to predict property data on more complex iron-base alloys, such as low-carbon alloy steels. More recently studies have been conducted on iron alloys with such alloying elements as carbon,[14,15,16] manganese,[17] aluminum,[18] oxygen,[19] and phosphorous.[20] Work related to effects of alloying elements on low-carbon steels has also received considerable attention.[21,22,23] However, the most significant amount of work on mechanical property determinations in recent years has been focussed upon the base metal itself, iron. Besides its obvious commercial importance, the impetus created by such theoretical work as Cottrell's

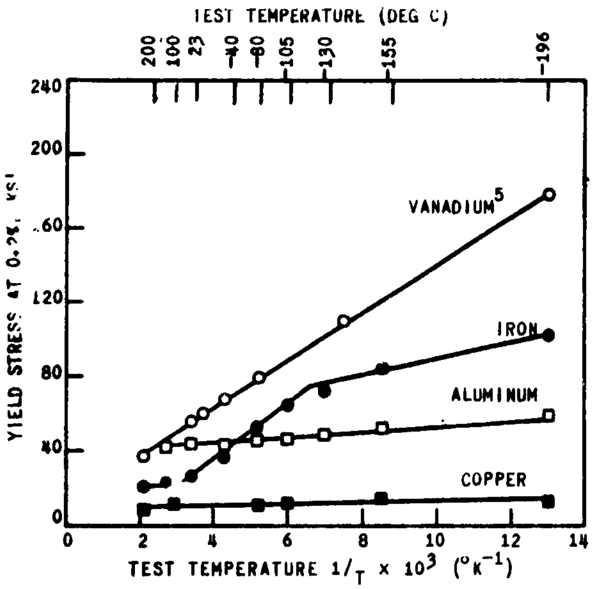

Figure 4. YIELD STRESS VERSUS THE RECIPROCAL ABSOLUTE TEMPERATURE FOR THE BCC Fe AND V AND THE FCC Al AND Cu METALS SHOWN IN FIGURE 2

on yielding[24] has probably been a major factor in generating this interest. Furthermore, the availability of significant amounts of mechanical property data on increasingly higher purities of iron[25,26,27] has also made such studies more feasible. These and other works have resulted in considerable advancés in the theoretical treatment of plastic flow[28,29,30] and fracture[31,32,33] of iron. The preceding summary of investigations is representative of the work which has gone on in this area, although no attempt has been made to make a complete literature survey.

In spite of this prior work, there is a need for generating more basic tensile data on the simpler, single-phase iron alloys in order that such significant factors as the flow stress-temperature dependence can be studied and correlated with more complex alloy systems. With this in mind, it was necessary to obtain such information by first studying the effect of composition and test temperature on some selected iron-binary alloys. True stress-true strain data was obtained to fracture in order to evaluate other related parameters such as strain hardening, fracture stress, and fracture strain over a temperature range of 200 to -196 C.

EXPERIMENTAL PROCEDURE

The materials employed in this study consist of the base metal iron, iron-binary alloys, iron-carbon alloys, some low-alloy carbon steels, and a 301 stainless steel. All the iron and iron-base alloys were laboratory heats of 900-gram cubes. These heats were made by melting with a tungsten arc under an argon atmosphere. Four re-melts were made of each heat to insure homogeneity of the alloy. A chill cast structure was obtained by employing a water-cooled copper crucible. Four basic alloying elements, chromium, manganese, nickel, and carbon, were used to make up the single-phase iron-binary and iron-carbon alloys which were initially prepared using electrolytic iron. However, it became necessary to make up new heats of the Fe-Ni alloys due to the severe cracking which was encountered as a result of cold working. It was concluded that the relatively high oxygen content may have been the major factor causing this embrittlement. This conclusion was further strengthened when the new heats of Fe-Ni which were made up of a higher purity, vacuum-melted iron were processed without any difficulty.

All the cubes were press forged at 800 C except the Fe-Ni alloys which were forged at 1000 C. The forgings were then vacuum annealed at 950 C, air cooled and swaged at room temperature to a final diameter of 0.375 inch. This resulted in an 80 percent reduction of area for all the alloys which were then recrystallized for one hour at 704 C under vacuum and furnace cooled, except for the 2.5 percent Ni alloy which was recrystallized at 600 C for two hours and the 5.0 percent Ni alloy which was recrystallized at 500 C for four hours. Thus all the materials were recrystallized from the cold-worked condition essentially in a single-phase "alpha" condition except the Fe-C alloys which contained Fe_3-C spheroidized in the alpha matrix. Chemical analyses for all materials

are shown in Table I. Grain size determinations and equivalent atomic percentages are tabulated in Table II for the iron and iron alloys. Relatively constant grain sizes within each alloy system were found in most cases, although no effort was made to establish a constant grain size.

True stress-true strain tension data were obtained from continuous load-profile curves over a range of testing temperatures of 200 to -196 C. A 30,000-pound capacity mechanical testing machine was used at a constant platen displacement of 0.01 in./in. All test temperatures were obtained by employing a liquid bath such as nitrogen, isopentane, alcohol, or oil, depending on the temperature range. More complete details pertaining to the testing method can be found in a previous publication.[34] The tension specimen geometry employed in this study was 0.252-inch diameter, untapered, with a 1-inch gage section.

True stress-true strain curves for the iron and iron alloys tested are shown in Appendix A. Due to the relatively large amount of highly localized deformation occurring in the necked region of most of the iron alloy specimens, the measurements which were obtained employing the diameter gage assembly beyond 65 percent reduction of area were in error because of the bluntness of the measuring fingers used to detect the changes in diameter. However, it was found that this could be compensated for and corrected diameter values could be obtained if a load-diameter curve was constructed and extrapolated to the small diameter values in question. This method was actually checked by running an interrupted test.

RESULTS AND DISCUSSION

Several significant plastic flow and fracture parameters were selected from the true stress-true strain data. These parameters are (a) flow stress at a constant strain ($\sigma_{.04}$) of .04; (b) stress and strain at maximum load (σ_{ml} and ϵ_{ml}); (c) stress and strain at fracture (σ_f and ϵ_f); and (d) the strain hardening exponent (n). Although this study was primarily concerned with the effect of alloy additions on the flow stress-temperature dependence parameter, several other interesting composition and temperature effects were observed for other plastic flow and fracture parameters. Also included in this study are the upper and lower yield point data obtained from load-platen displacement curves which are tabulated for all the iron alloys in Tables III to VII. Some anomalous behavior was noted in these data which could not readily be understood in relation to current theory. This was noticed in an Fe-1 Mn alloy at 23 C where the upper yield point effect observed on testing in air could be eliminated simply by testing a specimen in alcohol or isopentane. These tests were repeated several times and in all cases the observed anomaly was reproduced. Furthermore, tests at -40 C and lower in these liquid baths saw the yield point effect return. The only thing peculiar about this alloy, which had to be eventually

discarded, was the relatively high amount of nitrogen present, in the order of 50 ppm compared to 10 to 20 ppm found for all the other alloys. The high amount of nitrogen did effect the strength level of this material, raising it considerably above predicted values based upon the other alloys. Because of this anomalous behavior a new heat of Fe-1 Mn alloy was made up of lower nitrogen content which did not exhibit any large yield point effects in alcohol at room or low temperature. This is shown in Table V. However, these findings should be considered inconclusive until a more comprehensive study is made on this particular alloy system, especially on the effect of nitrogen and testing environment. Another finding, although not as dramatic, was the suppression of the typical serrated-type load-elongation curve that is usually observed in iron alloys that are strain aged in the temperature region of 200 C. This was noted for the Fe-.4 C and the Fe-2 Cr alloys where a combination of alloy addition and lowered oxygen may have been responsible for this effect.

Flow Stress and Strain at Maximum Load

Generally speaking, it is first necessary to assume that the base metal being studied here will not vary significantly because of the residual alloy elements normally found present and that the alloying element added will be the primary contributing factor to any changes in properties observed.

This approach has been employed successfully in the past[13,35] to evaluate and predict various solid solution effects in iron and will be used in the analysis of all the properties studied here.

Plots illustrating the effect of test temperature for the vacuum-melted iron, Fe-C, Fe-Cr, Fe-Mn, and Fe-Ni alloys are shown in Appendix B. Referring to the stress at maximum load (σ_{ml}), it can be seen that it is essentially a linear function over the range of test temperatures studied. This may be attributed in part to the relatively small variation in the slope M for the strain range at which maximum load occurred. Hence, this could then be considered as an approximate iso-strain parameter for these strain values. In cases where the alloys were made from the electrolytic iron, it can be seen that there is also an embrittling effect at the lowest temperatures of approximately -130 C for the Fe-C alloys and -155 C for the Fe-Mn and the Fe-Cr alloys. This can be partially attributable to the high oxygen content for the solid solution alloys as indicated by recent work showing severe embrittling effects obtained at these levels of oxygen.[19] The Fe-C embrittlement has generally been attributed to the brittle second phase present. It is interesting to note that none of the Fe-Ni alloys exhibited this loss of ductility and that these alloys have the lowest oxygen concentration next to that of the Fe-C. In the case of the Fe-C alloys, we may conclude that previously proposed factors, such as carbon content and grain size, are primarily responsible for this type of embrittlement in this two-phase system.

Another point of interest observed for all the compositions studied was the apparently constant value of stress at maximum load at the lowest temperatures which remained independent of composition for any particular alloy system. This is in contradiction with observations at the higher temperatures, particularly at room temperature, where a definite strengthening effect can be observed. Figure 5 illustrates this effect

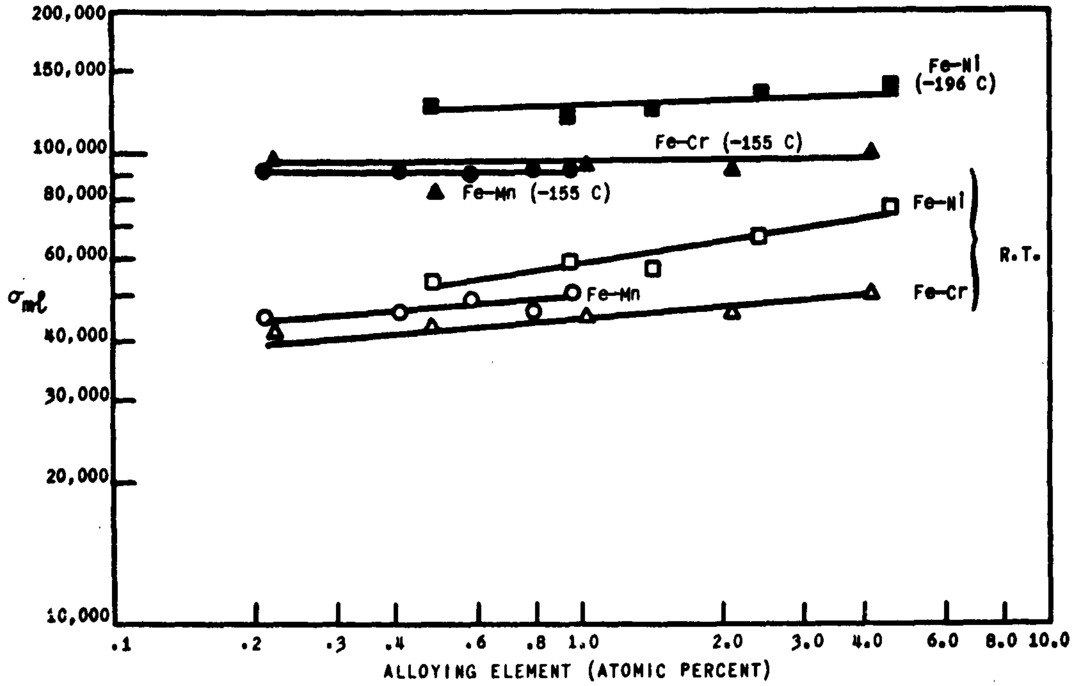

Figure 5. VARIATION OF THE STRESS AT MAXIMUM LOAD, σ_{ml}, VERSUS ATOMIC PERCENT ALLOY ADDITION AT R. T. AND SOME SELECTED LOW TEMPERATURES

quite dramatically. It can be seen that thermal effects can definitely erase any strengthening effects produced by solute additions at the higher temperatures. The slight differences in slope observed between the Fe-Ni and the other alloys can be attributed to the smaller grain size and higher carbon content in the vacuum-melted iron.

Generally speaking, the strain at maximum load (ϵ_{ml}) behaves in a manner similar to the strain hardening exponent (n). This would be expected, particularly as the n measurements were made in the uniform strain region at maximum load and both parameters reflect strain hardening behavior. A more detailed description of n will follow, which will in effect cover ϵ_{ml}, also.

Strain Hardening Exponent

For the Fe-C alloys, it can be shown in Figures B2 to B6 that n, the strain hardening exponent, decreased with increasing carbon content and that this decrease was most severe at the higher temperatures and least severe at the lower temperatures. Looking at the effect of temperature on any

one of the Fe-C alloys, it can be seen why this is so; first, at the lower carbon contents, the strain hardening exponent changes abruptly from a value of about 0.25 to a constant value of 0.15 between temperatures of 23 C and -80 C. Secondly, at the highest carbon studied, 1 percent C, this variation was considerably less and had an average n value of 0.15. It is interesting to note that the relatively high values of n exist only in the region of room temperature.

Of the three solid solution alloys, the Fe-Ni alloy which had the smallest grain size and the lowest oxygen content exhibited the most dramatic improvement in n values for the lower test temperatures and higher alloy additions. Referring to Figures B17 to B21 this trend can be seen for the Fe-Ni alloys, where at the lower (1% Ni) composition n decreases from approximately 0.30 to 0.13 and at the higher (5% Ni) composition n is relatively constant, varying from .27 to .25. To illustrate the trend exhibited by n at various compositions and several temperatures, Figure 6 was constructed. The strong influence of Ni at additions of over 1 percent can be easily seen when room temperature and -196 C n values are

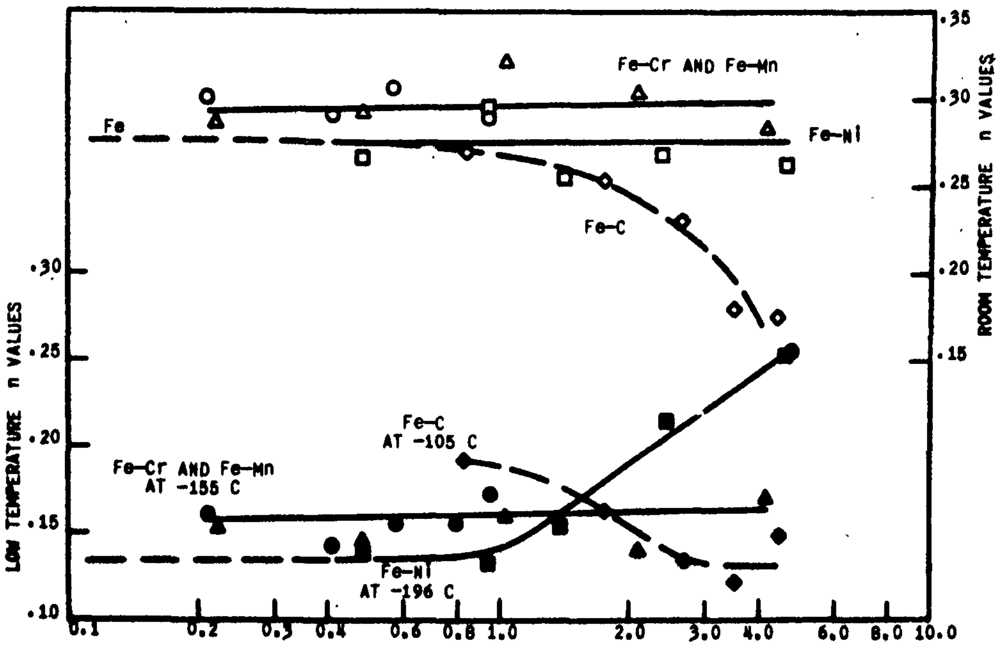

Figure 6. VARIATION OF THE STRAIN HARDENING EXPONENT, n, VERSUS ATOMIC PERCENT ALLOY ADDITION AT R. T. AND SOME SELECTED LOW TEMPERATURES

compared. The behavior of Fe-C is illustrated for room temperature and -105 C. Another interesting point is the apparent constancy of n values for the Fe-Cr and Fe-Mn at room temperature and -155 C. That the other solid solution alloys might behave similarly to the Fe-Ni if there were less oxygen and smaller grain size is an obvious conclusion. Yet there is an alternative explanation which is that at higher amounts of alloy

addition, i.e., greater than 1 percent for the Mn and greater than 4 percent for the Cr, there will be a tendency for the n value to change. However, there has been some indication that simply by lowering the oxygen content, an improvement in n can be obtained at the lower test temperatures for high purity Fe-Mn alloys.[17]

Fracture Stress and Strain

There are some rather interesting observations that can be made concerning the stress and strain parameters at fracture versus temperature as is shown in Appendix B. First, the strain of fracture, ϵ_f, remains constant, as the stress at fracture, σ_f, is decreasing. Second, ϵ_f decreases during the same time that σ_f is relatively constant. This general trend was observed in all the compositions and over the range of test temperatures studied. Others have observed this general trend in polycrystalline metals[36] and have sought to establish the transition point that would occur going from a constant ϵ_f to constant σ_f (the transition occurring at some specific temperature or range of temperatures in this case, although variation in strain rate and strength level have also been used). It has been pointed out[37] that with this transition defined, one could have a material at its optimum strength and ductility. For most of the solid solution alloys here, this region apparently occurs at about the same test temperature, i.e., -40 C. However, when approaching the higher Ni alloys one can see a definite decrease in this transition temperature. It is apparent that a definite analogy between this and what has been reported for Charpy impact tests on low-carbon steels having these percentages (2.5 to 5.0 percent) of Ni can be drawn.[38] Although the general effect of Ni on producing increased toughness is known, the relationship between the tensile flow stress and such tests as the Charpy V-notch impact tests which are used to evaluate this increased toughness has not been established. However, recent work has shown that some general correlations may be obtained in the ductile region of plastic flow just prior to transition behavior as exhibited in the impact test.[39] More specifically, it has been shown that a functional relation could be obtained between increased toughness and an increase in the strain hardening exponent, n.

Flow Stress at Constant Strain

In evaluating the flow stress dependence at constant strain, several important parameters are held constant or assumed to be ineffective at the range of strains studied. These factors are: (1) strain rate at any given strain is constant; (2) iso-strain values chosen represent instantaneous values of flow stress; (3) homogeneous and uniform strain is occurring; and (4) essentially isothermal conditions exist.

There is another factor, the slope M, which is assumed to be constant here, i.e., the flow stress at a constant strain will vary linearly when plotted versus the reciprocal of absolute temperature. Of course, there will be limitations to this function that are relatively obvious, such as (1) metallurgical transformation, (2) changes in deformation mechanism, and (3) prior history (stress, strain, or metallurgical) which will define a

temperature range over which a particular value of M will be valid. These limitatioms are only too obvious when reference is made to the Fe and Fe alloy curves in Appendix B. Here it can be seen that there are apparent discontinuities at approximately 200 C, the strain aging effect, and at -130 C, the start of twinning. Both of these changes are indicative of a change in deformation mechanism. If tests had been run at 910 C, discontinuities due to a change in crystal structure would also have been manifested by a change in the M value. Such factors as strength level and structure do not appear to affect the M value appreciably if at all.[5] With this in mind, the M values have been determined for the iron and iron alloys studied here at an iso-strain of .04. These are shown in Table VIII along with the temperature ranges over which they are considered valid. Also tabulated is the intercept value of σ_0, which can be considered as an indicator of strength level, such as yield strength, even though it exists at an imaginary temperature of $1/T = 0$.

The flow stress M value which is taken at ϵ.04 in this case also could have been determined as easily for any other iso-strain provided the initial assumptions made previously are met. This type of generalization relationship where various constant strains have been considered appears to take the following form:

$$T\,(\sigma - \sigma_0) = K\epsilon^A \qquad \text{Constant } \dot{\epsilon}$$

where $K\epsilon^A = M$. (M here is a variable with respect to ϵ.)

However, referring back to the iso-strain curve at .04, the following observations on the values of M can be made. Carbon and chromium do not appreciably lower M with increasing alloy content. Manganese and nickel definitely lower M with increased alloy content. Figure 7 shows this relationship between M and the atomic percent alloy addition for the various iron alloys. It can be seen that the Fe-C and Fe-Cr slopes vary little, while the Fe-Mn and Fe-Ni vary considerably over the same composition ranges. From these curves it is possible to determine an empirical equation relating the M value with the atomic percent alloy element. It is first assumed that an equivalent nickel curve can be constructed such as was done by Gensamer.[35] This was made possible by assuming that the Fe-C and the Fe-Cr contribute a fixed amount to the M value independent of composition over the range of compositions studied, and that the Fe-Mn and Fe-Ni slopes were parallel. With these considerations the following equation was derived:

$$M = m_1(\text{equivalent Ni})^{-1/3}$$

where $m_1 = 94 \text{ psi} \times 10^{-5} \text{ degrees K}$

$$(\text{equivalent Ni}) = 2.3\,(\text{At. \% Mn}) + C + \text{At. \% Ni}.$$

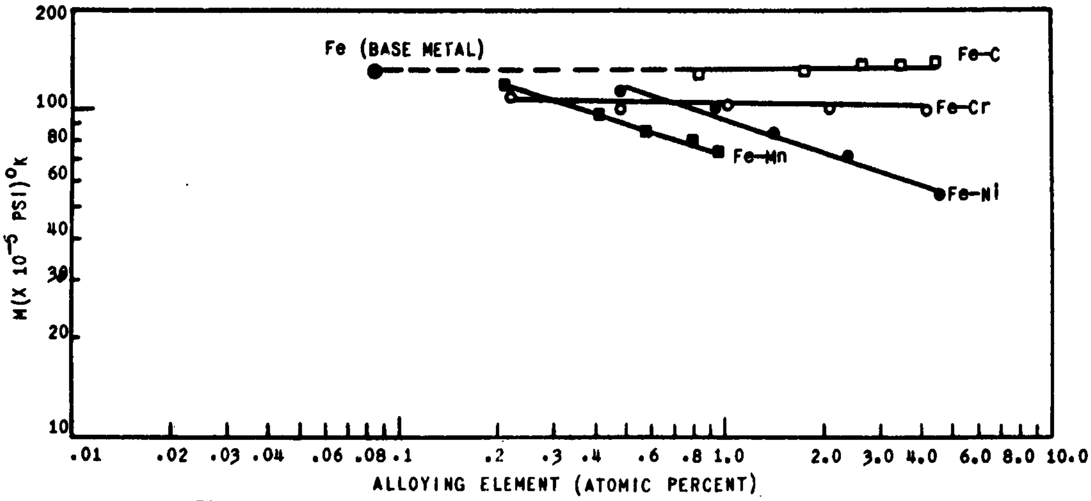

Figure 7. FLOW STRESS TEMPERATURE DEPENDENCE SLOPE, M, VERSUS ATOMIC PERCENT ALLOY ADDITION

As carbon did not affect the M value, it is ignored. However, C_1 equals 0.7 for steels containing Cr within the ranges specified here.

In order to check the effectiveness of this equation toward predicting M values on more highly alloyed steels, some commercial steels were tested and the M values experimentally determined. The flow stress iso-strain curves are shown in Figures 8a and 8b. These values are also shown in Table VIII. Their chemical analyses can be found in Table I. From these chemical analyses, the M values were calculated using the formula derived here. These calculated values are compared with the experimental values in Figure 9. It can be seen that within a ±5 percent deviation band, these values correlate remarkably well. The higher slope values which do not fit as nicely as the rest of the data points are from the plain carbon steels where there may have been some minor alloying elements contributing to effectively lower the slopes.

As much of the data referred to here is not generally made available, tables were made up containing these various parameters along with some "engineering" tensile stress data. These are shown for the iron and iron alloys in Tables IX to XIII. Table XIV shows the iso-strain data for the alloy steels used here.

Significance of Iso-Strain Flow Stress-Dependent Curves

Referring back to the experimental data shown here, the flow stress ($\sigma_{.04}$) may be described by a linear function with the reciprocal absolute temperature parameter. This curve, which can be considered as representing

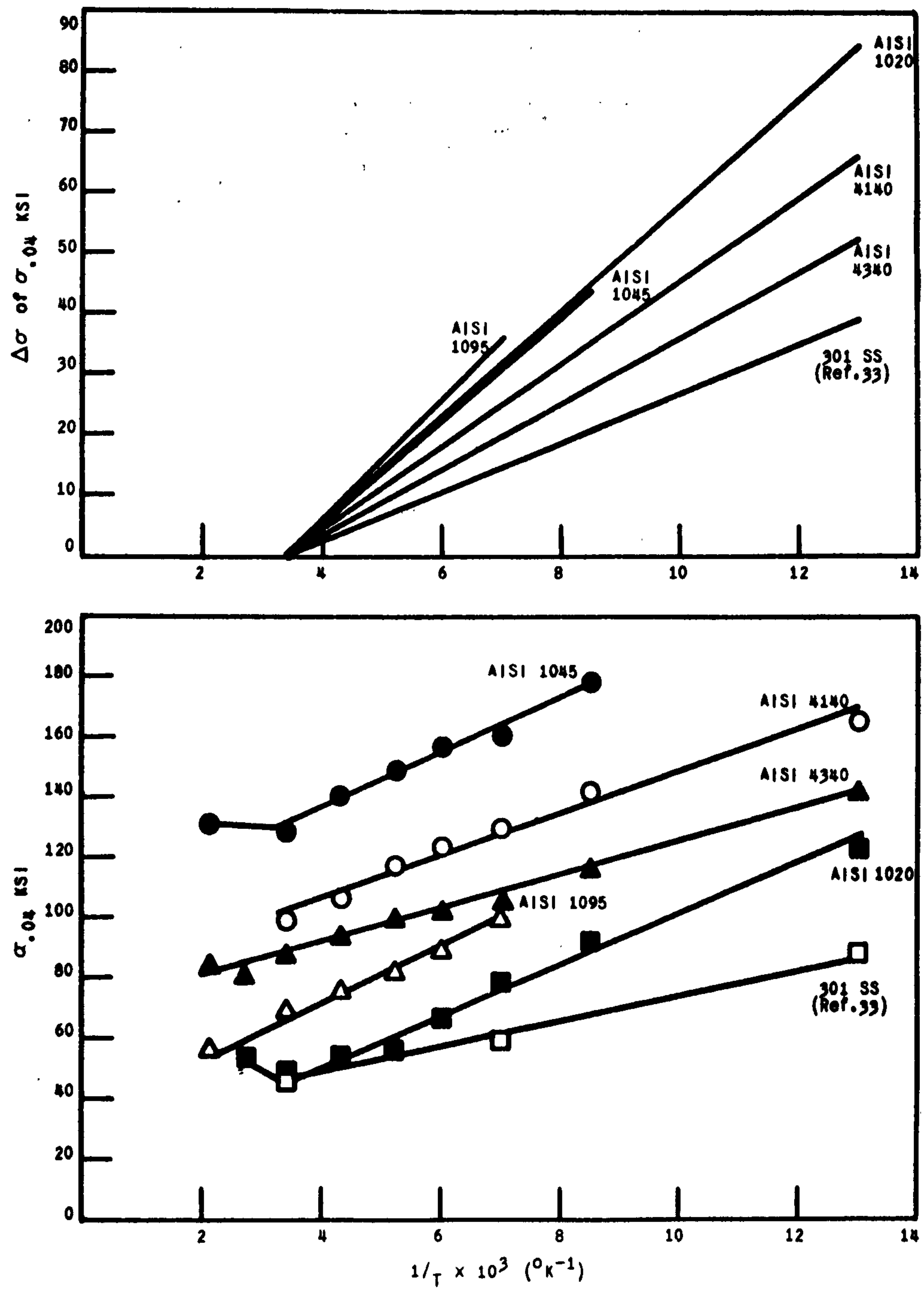

Figure 8. FLOW STRESS, $\sigma_{.04}$ VERSUS THE RECIPROCAL OF ABSOLUTE TEMPERATURE FOR SOME COMMERCIAL ALLOY STEELS

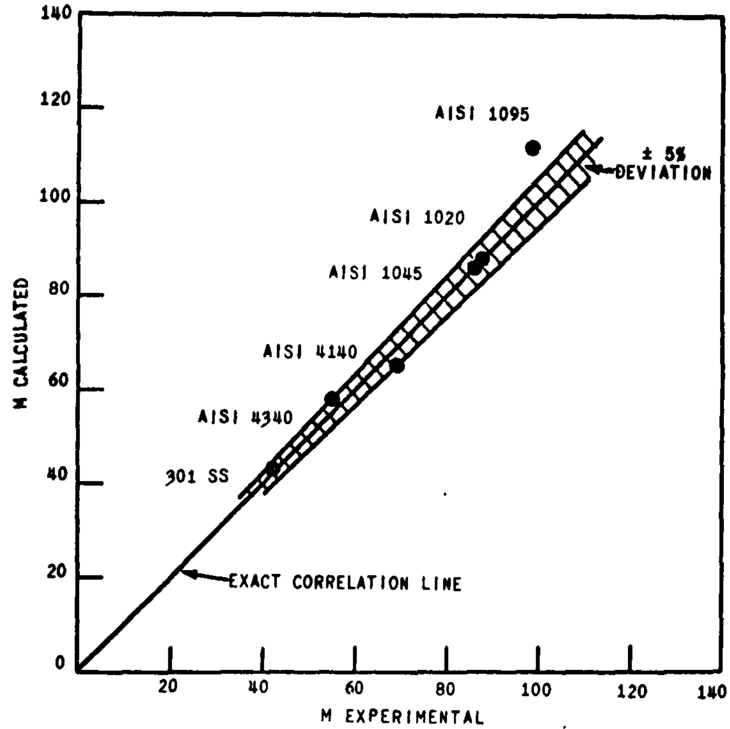

Figure 9. CALCULATED M VALUE VERSUS EXPERIMENTAL M VALUES FOR SOME COMMERCIAL ALLOY STEELS

yield stress conditions, will at some temperature reach a critical stress level which could result in brittle failure. Analysis of this type of idealized failure by Gensamer[1] and Orowon[2] has shown that many variables, such as specimen geometry, strain rate, microstructure, etc., will influence this transitional temperature. That such a stress level must be reached is shown in the torsion test which results in ductile failures at temperatures to -196 C.[40] Body-centered cubic (bcc) materials which show high M values generally exhibit a ductile-brittle transition as a result of reaching these critical points while the opposite can be said of face-centered cubic (fcc) metals whose flow stress appear to increase much more slowly, resulting in low M values.

Restated more simply it can be said that the critical stress to fracture which apparently increases at a much slower rate is reached much sooner by the bcc metals as evidenced by yield or flow stress curves which rapidly increase with decreasing temperature. Although this type of analysis is generally accepted today, it is restated here to emphasize the importance which can be attached to obtaining a quantitative measure for the flow stress-temperature dependence. The slope measurement M gives this value, apparently with good validity. This can be demonstrated by comparing the relative toughness of the materials tested here. Metals that had the highest slopes, such as the plain carbon steels, are known to behave in a brittle manner much more easily than

the 301 and AISI 4340 steels, which had the lowest M values and the highest toughness. Furthermore, the alloying elements of Mn and Ni, which are gamma stabilizers, acted most effectively in lowering M.

CONCLUSIONS

Based upon the experimental evidence gathered here the following significant conclusions are drawn:

1. At maximum load the flow stress and strain behave in a fairly predictable manner, resulting in increased values of flow stress with decreasing temperature. However, at the low temperatures the flow stress properties relating to solid solution strengthening are apparently uninfluenced by alloy composition at these composition levels.

2. The Fe-Ni alloys exhibited considerable improvement in low temperature strain hardening properties as evidenced by the increased n values with increased alloy addition.

3. Stress and strain at fracture followed a predictable manner versus temperature, i.e., strain at fracture decreased with constant fracture stress at low temperature while stress at fracture decreased at constant fracture strains for the higher test temperatures. In the solid solution alloys the strain at fracture remained reasonably the same at any particular test temperature except for the two highest Fe-Ni alloys, where a large improvement in fracture strain was observed at the lowest test temperature.

4. For the materials studied here the iso-strain flow stress temperature dependence was shown to follow the formula:

$$\sigma = \frac{M}{T} + \sigma_o$$

for constant strain of .04 and strain rate.

5. It was shown that the M value is influenced by composition and that its value can be predicted from a formula of the following form:

$$M = m_1 \text{ (equivalent Ni)}^{-1/3}.$$

6. Ni and Mn, which are primarily gamma stabilizers in iron, are the most beneficial of the alloying elements studied here for lowering this M value (flow stress temperature dependence).

7. The lower M values, which can be related to the alloying elements used in a steel such AISI 4340, may be regarded as a measure of toughness.

TABLE I

CHEMICAL ANALYSES OF MATERIALS TESTED

Alloy	Weight %						ppm				
	C	Cr	Mn	Ni	Mo	Si	O	H	N	P	S
Base Metal - Electrolytic Iron											
Fe	.013	<.01	<.01	.02	.003	<.01	114	0.6	10	20	20
Fe-.2C	.183	<.01	nil	.03	.009	-	12	0.7	10	-	40
-.4C	.383	<.01	nil	.03	.008	.009	1	<0.1	10	-	40
-.6C	.578	<.01	nil	.03	.008	.002	10	0.1	10	-	60
-.8C	.769	<.01	nil	.03	.007	.010	3	<0.1	10	-	40
-1C	.987	<.01	nil	.03	.007	.009	2	0.4	10	-	40
Fe-.25Cr	.013	.21	nil	.04	.008	.027	256	<0.1	10	-	50
-.5Cr	.012	.45	nil	.03	.004	-	203	<0.1	10	-	40
-1Cr	.011	.95	nil	.04	.005	-	172	<0.1	10	-	40
-2Cr	.014	1.96	nil	.03	.009	.002	162	0.3	10	-	50
-4Cr	.012	3.88	nil	.03	.013	.012	263	<0.1	10	-	70
Fe-.2Mn	.019	<.01	.21	.03	.008	.005	165	0.5	10	-	50
-.4Mn	.021	<.01	.40	.03	.009	.002	192	0.2	20	-	50
-.6Mn	.014	<.01	.57	.03	.008	.008	158	0.2	10	-	50
-.8Mn	.014	<.01	.78	.03	.005	.007	206	0.7	10	-	50
-1Mn	.009	<.01	.95	<.01	<.01	<.01	223	0.3	20	20	50
Base Metal - Vacuum-Melted Iron											
Fe	.018	<.01	<.01	<.01	<.01	<.01	9.7	0.5	10	30	40
Fe-.5Ni	.019	<.01	<.01	.51	<.01	<.01	4.4	<0.1	10	40	40
-1Ni	.017	<.01	<.01	.99	<.01	<.01	6.8	0.6	10	40	30
-1.5Ni	.018	<.01	<.01	1.50	<.01	<.01	3.8	0.3	10	30	-
-2.5Ni	.020	<.01	<.01	2.53	<.01	<.01	3.9	0.4	20	30	40
-5Ni	.020	<.01	<.01	4.83	<.01	<.01	3.1	0.5	20	30	40
Commercial Steels											
1020	.21	-	.50	-	-	-	-	-	-	110	330
1045	.48	-	.72	-	-	-	-	-	-	150	420
1095	1.01	-	.25	-	-	-	-	-	-	130	300
4140	.40	.93	.94	.21	.19	.30	-	-	-	200	360
4340	.38	.80	.76	1.78	.25	.32	-	-	-	220	80
301SS	.80	16.93	1.14	7.04	-	.49	-	-	-	280	180

TABLE I

CHEMICAL ANALYSES OF MATERIALS TESTED

Alloy	Weight %						ppm				
	C	Cr	Mn	Ni	Mo	Si	O	H	N	P	S
Base Metal - Electrolytic Iron											
Fe	.013	<.01	<.01	.02	.003	<.01	114	0.6	10	20	20
Fe-.2C	.183	<.01	nil	.03	.009	-	12	0.7	10	-	40
-.4C	.383	<.01	nil	.03	.008	.009	1	<0.1	10	-	40
-.6C	.578	<.01	nil	.03	.008	.002	10	0.1	10	-	60
-.8C	.769	<.01	nil	.03	.007	.010	3	<0.1	10	-	40
-1C	.987	<.01	nil	.03	.007	.009	2	0.4	10	-	40
Fe-.25Cr	.013	.21	nil	.04	.008	.027	256	<0.1	10	-	50
-.5Cr	.012	.45	nil	.03	.004	-	203	<0.1	10	-	40
-1Cr	.011	.95	nil	.04	.005	-	172	<0.1	10	-	40
-2Cr	.014	1.96	nil	.03	.009	.002	162	0.3	10	-	50
-4Cr	.012	3.88	nil	.03	.013	.012	263	<0.1	10	-	70
Fe-.2Mn	.019	<.01	.21	.03	.008	.005	165	0.5	10	-	50
-.4Mn	.021	<.01	.40	.03	.009	.002	192	0.2	20	-	50
-.6Mn	.014	<.01	.57	.03	.008	.008	158	0.2	10	-	50
-.8Mn	.014	<.01	.78	.03	.005	.007	206	0.7	10	-	50
-1Mn	.009	<.01	.95	<.01	<.01	<.01	223	0.3	20	20	50
Base Metal - Vacuum-Melted Iron											
Fe	.018	<.01	<.01	<.01	<.01	<.01	9.7	0.5	10	30	40
Fe-.5Ni	.019	<.01	<.01	.51	<.01	<.01	4.4	<0.1	10	40	40
-1Ni	.017	<.01	<.01	.99	<.01	<.01	6.8	0.6	10	40	30
-1.5Ni	.018	<.01	<.01	1.50	<.01	<.01	3.8	0.3	10	30	-
-2.5Ni	.020	<.01	<.01	2.53	<.01	<.01	3.9	0.4	20	30	40
-5Ni	.020	<.01	<.01	4.83	<.01	<.01	3.1	0.5	20	30	40
Commercial Steels											
1020	.21	-	.50	-	-	-	-	-	-	110	330
1045	.48	-	.72	-	-	-	-	-	-	150	420
1095	1.01	-	.25	-	-	-	-	-	-	130	300
4140	.40	.99	.94	.21	.19	.30	-	-	-	200	360
4340	.38	.80	.76	1.78	.25	.32	-	-	-	220	80
301SS	.80	16.93	1.14	7.04	-	.49	-	-	-	280	180

TABLE II

EQUIVALENT ATOMIC PERCENTAGES FOR THE FE ALLOYS STUDIED WITH THE AVERAGE ASTM GRAIN SIZE NUMBERS

Alloy	Series	Weight % Element	Atomic Weight % Element	ASTM Grain Size
Fe-.2C	18	.18	.83	8
-.4C	19	.38	1.74	4-8
-.6C	17	.58	2.64	5-6
-.8C	23	.77	3.48	11-12
-1.0C	21	.99	4.44	12
Fe-.25Cr	12	.21	.22	4-5
-.5Cr	13	.45	.48	4-6
-1.0Cr	14	.95	1.02	3-5
-2.0Cr	16	1.96	2.10	3-5
-4.0Cr	15	3.88	4.15	4-6
Fe-.2Mn	3	.21	.21	3-5
-.4Mn	2	.40	.41	0-5
-.6Mn	4	.57	.58	4-5
-.8Mn	1	.78	.79	4-5
-1.0Mn	Z	.95	.96	3-5
Fe-.5Ni	N1	.51	.48	6-8
-1.0Ni	N2	.99	.94	7-8
-1.5Ni	N3	1.50	1.43	7-8
-2.5Ni	N4	2.53	2.41	8-10
-5.0Ni	N5	4.83	4.61	7-8
Fe*	Vacuum Melt	.018	.084	4-8

*Percentages are given for the carbon content

TABLES III to VII

UPPER AND LOWER YIELD POINTS OBSERVED IN THE IRON-BASE ALLOYS (IN PSI)

		Test Temperature (deg C)								
TABLE III Fe-C Alloys		200*	100	23	-40	-80	-105	-103	-155	-196
Fe-.2C	Upper	(1)	42,000	46,400	60,600	73,600	85,800	87,500	104,800	(2)
	Lower	(1)	24,300	32,400	49,200	61,800	70,800	78,000	95,400	(2)
Fe-.4C	Upper	-	36,000	40,800	64,800	84,000	92,000	98,000	(2)	-
	Lower	-	30,000	39,600	55,200	70,800	78,000	86,000	(2)	-
Fe-.6C	Upper	(1)	52,200	61,200	70,100	95,400	97,000	-	-	-
	Lower	(1)	39,000	45,600	57,300	79,000	85,000	-	-	-
Fe-.8C	Upper	(1)	46,000	60,000	84,000	96,000	105,000	126,100	(2)	-
	Lower	(1)	45,000	54,000	69,000	81,000	92,000	105,100	(2)	-
Fe-1C	Upper	(1)	64,800	70,200	94,000	108,000	122,300	(2)	-	-
	Lower	(1)	54,000	60,000	76,800	91,000	99,400	(2)	-	-
TABLE IV Fe-Cr Alloys										
Fe-.25Cr	Upper	(1)	14,200	(1)	30,400	48,600	56,400	61,200	70,000	89,800
	Lower	(1)	11,000	(1)	26,400	43,200	48,000	58,000	68,000	76,400
Fe-.5Cr	Upper	(1)	(1)	(1)	(1)	(1)	42,000	60,600	62,400	80,400
	Lower	(1)	(1)	(1)	(1)	(1)	41,000	58,000	60,800	76,000
Fe-1Cr	Upper	(1)	(1)	(1)	32,400	(1)	(1)	55,200	74,400	69,000
	Lower	(1)	(1)	(1)	30,000	(1)	(1)	50,800	63,600	68,000
Fe-2Cr	Upper	(1)	(1)	(1)	(1)	(1)	(1)	(1)	(1)	(1)
	Lower	(1)	(1)	(1)	(1)	(1)	(1)	(1)	(1)	(1)
Fe-4Cr	Upper	(1)	(1)	(1)	27,600	60,000	59,400	82,800	83,000	102,000
	Lower	(1)	(1)	(1)	26,400	46,800	53,400	70,000	80,000	99,600
TABLE V Fe-Mn Alloys										
Fe-.2Mn	Upper	(1)	(1)	16,000	33,600	44,600	59,000	70,000	70,800	88,800
	Lower	(1)	(1)	15,000	27,800	40,400	50,600	63,000	69,600	83,400
Fe-.4Mn	Upper	13,800	19,000	20,200	36,600	47,000	60,000	63,600	73,600	89,800
	Lower	12,000	13,600	17,400	26,000	42,600	51,600	59,000	66,000	82,200
Fe-.6Mn	Upper	10,500	(1)	(1)	26,400	41,400	54,000	64,200	75,000	74,800
	Lower	10,000	(1)	(1)	25,800	34,800	50,400	54,000	66,000	72,000
Fe-.8Mn	Upper	13,800	13,400	24,600	30,000	40,200	57,000	66,400	(1)	74,400
	Lower	12,000	12,000	17,400	24,000	39,000	50,400	57,600	(1)	72,600
Fe-1Mn	Upper	(1)	(1)	(1)	-	(1)	-	59,200	70,000	-
	Lower	(1)	(1)	(1)	-	(1)	-	54,000	66,600	-
TABLE VI Fe-Ni Alloys										
Fe-.5Ni	Upper	27,000	40,200	39,000	49,200	62,800	74,800	93,600	102,000	110,000
	Lower	24,000	26,000	28,800	38,400	51,600	60,000	78,000	82,800	100,000
Fe-1Ni	Upper	30,600	40,400	44,000	52,800	57,600	76,000	85,200	104,400	118,000
	Lower	26,000	26,400	31,200	40,000	50,400	61,200	69,600	82,000	106,000
Fe-1.5Ni	Upper	30,000	33,600	46,000	46,200	52,800	70,000	90,000	98,400	112,800
	Lower	26,000	28,800	32,400	38,000	50,400	55,200	69,200	78,000	99,600
Fe-2.5Ni	Upper	45,600	46,400	49,800	48,000	64,800	71,000	82,200	98,800	126,000
	Lower	34,000	33,000	38,400	43,200	51,600	58,800	67,200	78,000	110,000
Fe-5Ni	Upper	44,400	41,800	50,800	61,600	62,000	69,600	82,800	90,000	112,500
	Lower	38,000	40,800	46,800	52,000	56,000	62,000	66,000	76,000	96,000
TABLE VII Unalloyed Vacuum-Melted Iron										
	Upper	22,200	32,400	32,400	51,600	68,400	76,000	94,000	108,000	117,000
	Lower	20,000	23,400	25,800	36,000	52,800	66,000	72,000	84,000	100,800

Most curves exhibited typical serrated behavior at this temperature, the exceptions being the Fe-.4C and the Fe-2Cr alloys.

(1) No clear yield points discernible

(2) Broke prior to yielding

TABLE VIII

SLOPE (M) OF THE FLOW STRESS ($\sigma_{.04}$)–RECIPROCAL ABSOLUTE TEMPERATURE CURVE AND INTERCEPT (σ_0)

Material	*Temperature Range (deg K)	M (psi deg K)	σ_o (psi)
Fe-.2C	373 to 118	128.4 x 10^5	-7,700
-.4C	373 to 143	129.0	-2,600
-.6C	373 to 168	137.1	2,000
-.8C	473 to 143	136.7	13,000
-1.0C	473 to 168	139.2	20,000
Fe-.25Cr	296 to 118	109.0	-17,000
-.5Cr	373 to 118	100.0	-12,800
-1.0Cr	373 to 143	101.5	-10,200
-2.0Cr	473 to 118	100.0	-8,000
-4.0Cr	473 to 118	98.5	-3,900
Fe-.2Mn	296 to 143	118.5	-17,800
-.4Mn	373 to 118	95.5	-7,700
-.6Mn	373 to 118	84.8	-1,700
-.8Mn	373 to 118	79.6	0
-.1.0Mn	373 to 118	73.6	5,000
Fe-.5Ni	373 to 118	113.5	-8,000
-1.0Ni	373 to 118	100.0	0
-1.5Ni	373 to 118	83.6	7,000
-2.5Ni	373 to 77	71.5	17,000
-5.0Ni	473 to 77	54.2	30,000
Fe	296 to 143	130.8	-13,100
AISI 1020	296 to 77	87.5	15,000
AISI 1045	296 to 118	86.0	102,000
AISI 1095	296 to 143	98.4	32,000
AISI 4140	296 to 77	69.3	80,000
AISI 4340	373 to 77	54.5	70,000
SS 301	296 to 77	42.1	32,000

*Constants are valid over temperature range indicated.

TABLE IX

MECHANICAL PROPERTY DATA ON FE-C ALLOYS

Fe-.2C Specimen	Test Temp. (deg. C)	$\sigma_{.04}$ (psi)	σ_{ml} (psi)	σ_f (psi)	ϵ_{ml}	ϵ_f	n	Y.S. 0.2% (psi)	UTS (psi)	R.A. (%)
18-9	200	36,000	47,800	87,200	.187	1.355	.173	18,000	39,500	76.2
18-8	100	29,200	53,200	112,600	.300	1.500	.292	24,300	40,000	78.4
18-1	23	33,400	55,700	106,800	.277	1.450	.270	31,200	42,000	78.2
18-2	-40	50,100	65,700	128,100	.231	1.418	.202	47,400	52,000	74.9
18-3	-80	62,600	72,100	128,600	.165	1.263	.171	61,000	61,000	72.9
18-4	-105	75,400	81,600	138,200	.210	1.190	.193	68,400	66,000	70.5
18-5	-130	79,300	91,800	139,500	.187	1.065	.150	74,000	76,000	69.5
18-6	-155	97,100	103,100	138,800	.153	.787	.137	94,000	88,000	58.7
18-7A*	-196	-	-	134,200	-	-	-	-	134,200	0
Fe-.4C Specimen										
19-9	200	41,800	54,200	99,600	.198	1.248	.182	20,000	44,000	71.0
19-8	100	31,300	55,600	101,400	.254	1.248	.258	30,000	43,000	74.1
19-1	23	40,200	63,300	104,400	.254	1.147	.253	38,800	49,000	72.2
19-2	-40	55,300	74,100	115,200	.209	1.105	.192	52,800	60,000	67.0
19-3	-80	73,100	79,500	132,200	.131	1.051	.121	69,000	69,500	70.6
19-4	-105	79,300	93,800	136,100	.209	.959	.161	75,000	76,000	65.1
19-5	-130	83,500	91,900	140,300	.148	.934	.133	80,000	79,000	61.4
19-6A*	-155	-	-	114,600	-	-	-	-	114,600	0
Fe-.6C Specimen										
17-9	200	45,900	60,900	91,600	.193	.959	.180	33,000	50,000	62.8
17-8	100	39,700	60,700	102,600	.254	1.161	.225	37,800	47,000	69.8
17-1	23	47,500	73,400	111,700	.255	1.024	.230	44,400	56,500	64.8
17-2A	-40	61,300	81,800	124,000	.188	.954	.190	57,300	67,700	65.3
17-3	-80	77,200	91,000	135,900	.165	.884	.143	74,400	77,000	60.4
17-4	-105	84,600	97,700	137,400	.148	.811	.130	81,000	84,000	57.8
Fe-.8C Specimen										
23-9	200	45,900	62,500	86,200	.170	.762	.159	39,600	52,500	58.4
23-8	100	48,000	65,300	92,300	.187	.811	.185	44,500	54,000	59.9
23-1	23	58,500	79,800	122,000	.187	.859	.178	54,000	66,000	58.7
23-2	-40	71,500	87,500	122,200	.165	.787	.152	67,600	74,000	57.4
23-3	-80	83,500	94,000	125,000	.170	.684	.140	79,000	79,000	51.5
23-4	-105	92,900	104,000	139,400	.131	.618	.121	90,000	91,000	48.0
23-5A*	-130	112,600	115,000	158,200	.061	.576	.058	105,100	108,300	41.4
23-6A*	-155	-	-	123,600	-	-	-	-	123,600	0
Fe-1C Specimen										
21-9	200	54,300	69,800	90,400	.165	.651	.170	47,200	59,000	48.6
21-8	100	54,300	70,300	95,500	.165	.706	.170	53,400	59,500	52.0
21-1	23	62,500	80,600	106,500	.166	.640	.176	60,000	68,000	51.5
21-2	-40	79,300	95,700	120,000	.165	.597	.150	74,000	81,000	47.4
21-3	-80	90,800	99,000	124,100	.114	.544	.122	87,000	88,000	41.6
21-4A*	-105	107,600	123,100	139,300	.188	.446	.148	99,400	101,900	39.4
21-5A*	-130	-	-	114,600	-	-	-	-	114,600	0

*0.200" diameter specimen used in place of standard specimen that originally broke at threads.

TABLE X

MECHANICAL PROPERTY DATA ON FE-CR ALLOY

Fe-.25Cr Specimen	Test Temp. (deg. C)	$\sigma_{.04}$ (psi)	σ_{ml} (psi)	σ_f (psi)	ϵ_{ml}	ϵ_f	n	Y.S. 0.2% (psi)	UTS (psi)	R.A. (%)
12-9	200	26,700	36,900	90,100	.170	1.951	.188	10,200	31,000	89.6
12-8	100	18,800	37,200	75,300	.277	1.868	.320	10,800	28,000	90.2
12-1	23	20,900	41,000	79,300	.277	1.808	.284	16,800	31,000	91.4
12-2	-40	26,600	53,600	123,500	.370	1.997	.321	24,400	37,000	91.0
12-3	-80	43,800	58,500	147,500	.165	2.104	.166	40,800	49,500	89.4
12-4	-105	50,700	69,900	140,800	.210	1.751	.207	46,200	56,500	87.6
12-5	-130	59,500	82,000	141,500	.156	1.552	.153	56,400	70,000	82.0
12-6	-155	69,400	96,400	142,500	.183	1.024	.184	67,200	80,000	66.5
12-7A	-196	88,900	-	116,100	-	.134	.207	77,400	101,300	45.8
Fe-.5Cr Specimen										
13-9	200	18,800	32,600	78,100	.254	2.059	.250	6,600	25,200	89.2
13-8	100	18,800	33,200	88,000	.300	2.294	.284	8,400	24,500	91.6
13-1	23	23,000	43,100	114,000	.277	2.174	.291	12,600	32,500	91.6
13-2	-40	28,700	46,400	107,700	.277	2.037	.249	25,200	35,000	88.4
13-3	-80	44,100	59,100	105,900	.165	1.770	.168	40,000	50,000	86.2
13-4	-105	44,900	60,400	107,500	.187	1.676	.186	42,000	50,000	87.2
13-5	-130	61,600	78,100	120,300	.136	1.147	.150	57,600	68,000	70.5
13-6	-155	66,800	80,500	126,200	.123	.884	.143	62,400	71,000	59.1
13-7	-196	87,200	-	87,200	-	.040	-	80,000	83,500	4.2
Fe-1Cr Specimen										
14-9	200	20,000	33,100	78,000	.254	2.128	.279	8,400	25,600	91.4
14-8	100	16,100	35,900	88,900	.323	2.222	.350	9,900	26,000	92.6
14-1	23	20,900	43,700	102,900	.309	1.997	.320	14,800	32,000	92.0
14-2	-40	32,400	50,700	121,000	.280	2.082	.267	29,400	38,000	90.2
14-3	-80	45,900	54,000	125,000	.116	2.059	.141	44,000	48,000	90.4
14-4	-105	54,800	68,400	128,100	.162	1.828	.143	52,400	58,000	87.8
14-5	-130	56,900	71,500	139,800	.140	1.676	.149	50,600	62,000	81.4
14-6	-155	66,800	92,600	135,700	.188	1.355	.157	62,400	76,500	77.4
14-7	-196	93,000	-	126,500	-	.174	.167	78,000	106,000	17.7
Fe-2Cr Specimen										
16-9	200	16,700	30,300	77,200	.300	2.174	.298	7,800	22,400	92.6
16-8	100	19,800	37,300	109,100	.299	2.197	.308	7,200	27,600	92.0
16-1	23	23,000	45,100	112,900	.277	2.082	.302	10,400	34,000	90.6
16-2	-40	30,300	51,000	115,400	.254	2.037	.255	22,400	39,500	91.0
16-3	-80	45,900	57,600	130,400	.178	1.972	.163	38,400	48,000	90.4
16-4	-105	52,700	68,000	154,900	.165	1.951	.159	46,800	57,500	88.6
16-5	-130	65,200	88,900	144,200	.209	1.568	.151	60,400	72,000	81.0
16-6	-155	75,200	90,900	121,400	.156	.884	.139	68,800	77,500	65.5
16-7	-196	98,100	-	122,400	-	.123	.179	87,600	108,000	11.8
Fe-4Cr Specimen										
15-9	200	20,000	36,500	103,500	.304	2.174	.299	11,200	26,800	89.2
15-8	100	23,200	42,300	112,100	.277	2.016	.294	12,600	32,000	87.2
15-1	23	25,100	50,300	125,400	.277	1.951	.280	16,000	38,000	89.0
15-2	-40	31,300	59,400	141,700	.254	1.930	.294	27,400	46,000	86.8
15-3	-80	46,500	65,900	164,100	.254	2.059	.224	45,200	51,000	88.4
15-4	-105	55,300	69,700	162,200	.165	1.910	.163	52,000	59,000	85.8
15-5	-130	67,800	80,000	160,900	.161	1.751	.154	67,200	68,000	84.2
15-6	-155	81,400	100,200	157,200	.174	1.092	.170	78,600	84,000	68.3
15-7	-196	101,800	131,600	160,500	.193	.513	.183	101,400	108,000	38.6

TABLE XI

MECHANICAL PROPERTY DATA ON FE-MN ALLOY

Fe-.2Mn Specimen	Test Temp. (deg. C)	$\sigma_{.04}$ (psi)	σ_{ml} (psi)	σ_f (psi)	ϵ_{ml}	ϵ_f	n	Y.S. 0.2% (psi)	UTS (psi)	R.A. (%)
3-9	200	24,600	37,500	69,000	.209	1.751	.203	10,400	30,400	91.6
3-8	100	20,400	39,500	70,100	.322	1.808	.286	11,600	28,500	91.6
3-1	23	22,500	44,600	119,000	.298	2.478	.299	15,600	33,000	92.8
3-2	-40	31,400	49,400	112,100	.255	2.150	.251	27,800	38,000	90.4
3-3	-80	44,900	56,300	115,900	.153	1.972	.164	40,400	48,000	90.6
3-4	-105	55,300	66,300	113,600	.131	1.732	.124	50,600	58,000	89.4
3-5	-130	66,800	82,900	151,500	.140	1.622	.128	63,600	72,000	81.0
3-6	-155	71,500	91,600	139,400	.179	1.105	.161	69,600	78,000	64.5
3-7	-196	93,900	124,200	127,500	.174	.200	.183	86,000	104,000	18.2
Fe-.4Mn Specimen										
2-9	200	27,800	43,900	105,800	.240	1.972	.217	12,600	34,400	88.4
2-8	100	21,400	45,100	105,600	.281	1.951	.318	13,600	34,000	91.4
2-1A	23	23,500	45,700	114,800	.299	2.222	.288	17,600	33,800	92.0
2-2	-40	29,500	51,800	112,700	.254	1.951	.269	26,400	40,000	91.4
2-3	-80	44,600	63,200	139,700	.242	1.997	.195	42,600	50,000	89.4
2-4	-105	54,300	64,000	134,100	.114	1.808	.127	51,600	57,000	87.6
2-5	-130	62,100	73,100	149,400	.123	1.751	.133	59,000	64,500	82.0
2-6	-155	68,900	91,500	151,300	.157	1.434	.142	66,000	78,000	78.2
2-7A*	-196	91,900	125,000	134,700	.189	.303	.180	86,000	103,500	25.2
Fe-.6Mn Specimen										
4-9	200	25,900	36,600	83,300	.232	1.930	.213	10,200	29,000	90.6
4-8	100	20,400	43,700	101,600	.371	2.082	.344	11,000	30,000	91.6
4-1	23	25,100	48,000	131,100	.299	2.104	.305	15,000	35,500	91.0
4-2	-40	28,700	54,700	123,200	.299	1.972	.300	25,800	40,500	91.0
4-3	-80	40,700	61,000	132,200	.276	1.751	.242	34,200	46,500	90.4
4-4	-105	52,000	65,000	152,200	.165	1.972	.159	49,800	55,000	88.4
4-5	-130	56,700	71,900	147,700	.114	1.732	.122	54,000	64,000	83.2
4-6	-155	71,000	89,600	137,700	.161	1.092	.155	66,000	76,000	67.7
4-7A*	-196	-	-	85,200	-	.030	-	80,600	82,800	2.9
Fe-.8Mn Specimen										
1-9	200	25,100	40,800	101,600	.254	2.082	.239	10,800	31,600	90.6
1-8	100	19,100	41,000	93,800	.308	2.059	.298	12,600	30,000	91.2
1-1	23	26,100	45,700	121,300	.236	2.104	.258	18,300	36,000	91.6
1-2	-40	27,100	56,400	120,000	.282	1.889	.298	24,000	42,000	90.4
1-3	-80	43,700	62,200	138,500	.236	1.910	.208	39,800	49,000	89.2
1-4	-105	48,500	63,100	141,200	.145	1.751	.168	48,800	54,500	87.6
1-5	-130	56,100	73,300	142,200	.156	1.518	.178	55,800	62,500	78.8
1-6A*	-155	74,500	92,000	125,900	.155	.772	.156	68,800	78,800	53.8
1-7B*	-196	-	-	83,000	-	.008	-	82,200	82,500	1.0
Fe-1Mn Specimen										
Z-6	200	30,100	-	-	-	-	-	16,800	38,400	85.8
Z-5	100	25,700	-	-	-	-	-	16,800	33,600	89.6
Z-1	23	28,000	49,700	124,200	.276	2.016	.288	16,800	37,600	90.2
Z-2	-80	39,700	64,600	140,200	.254	1.808	.275	34,600	50,000	89.2
Z-3	-130	58,500	76,700	139,600	.178	1.500	.181	51,600	64,000	83.0
Z-4	-155	68,900	92,300	158,600	.178	1.234	.173	66,000	77,000	70.2

*0.200" diameter specimen used in place of standard specimen that originally broke at the threads.

TABLE XII

MECHANICAL PROPERTY DATA ON FE-NI ALLOY

Fe-.5Ni Specimen	Test Temp. (deg. C)	$\sigma_{.04}$ (psi)	σ_{ml} (psi)	σ_f (psi)	ϵ_{ml}	ϵ_f	n	Y.S. 0.2% (psi)	UTS (psi)	R.A. (%)
N1-9	200	32,300	55.200	128.100	.245	1.808	.236	24,000	43.100	84.2
N1-8	100	31,200	52,500	126.500	.281	1.789	.272	24,600	39.400	86.2
N1-1	23	31,300	52,900	132.400	.277	1.951	.265	27,600	40,000	89.0
N1-2	-40	39,700	61,000	140,800	.277	1.951	.274	36,600	46,000	88.6
N1-3	-80	52,200	67,900	153,800	.254	1.848	.243	49,200	52,500	90.6
N1-4	-105	61,600	68,600	163,600	.148	1.868	.160	58,000	59,000	90.2
N1-5	-130	75,200	79,400	155,000	.123	1.604	.108	72,600	70.000	83.6
N1-6	-155	82.500	91,000	177.000	.140	1.484	.101	79.500	79.000	78.2
N1-7	-196	104.400	126.500	157.200	.165	.513	.140	100,000	107.000	41.0
Fe-1Ni Specimen										
N2-10	200	37,200	58,200	126,800	.245	1.808	.232	27,600	45.300	83.4
N2-9	100	30,900	53,800	137,800	.227	1.848	.271	26,000	42,800	85.2
N2-1A	23	32,100	58,300	160,000	.304	2.037	.295	30,600	42,600	87.2
N2-2	-40	42,100	64,500	153,800	.281	1.848	.300	38,400	46,800	86.4
N2-3	-80	48,000	73,600	166,700	.299	1.930	.270	48,000	54,400	87.5
N2-4A	-105	63,100	73,600	188,300	.209	2.059	.217	58,000	59,600	87.5
N2-5	-130	73,000	84,100	184,800	.174	1.694	.162	69,000	70,500	83.4
N2-7	-155	86,000	92,300	192,700	.123	1.586	.112	81,600	81,400	83.8
N2-8	-196	103,300	118,100	180,400	.145	.946	.133	102,000	102,000	62.4
Fe-1.5Ni Specimen										
N3-9	200	35.700	57,800	129,300	.227	1.751	.232	27,000	45,700	82.6
N3-8	100	33,800	58,300	134.100	.286	1.770	.282	28,800	43,700	84.0
N3-1	23	35,500	56,300	135,000	.273	1.868	.252	29,600	42,500	87.6
N3-2	-40	38,200	66,400	165,200	.281	2.016	.277	37,200	49,800	87.5
N3-3	-80	52,200	75,500	180,000	.273	1.972	.276	49,200	57,000	86.4
N3-4A	-105	57,600	80,100	185,700	.286	1.888	.270	52,000	60,100	86.1
N3-5	-130	70,000	86,100	195,100	.245	1.808	.221	64,800	67,300	83.6
N3-6	-155	79,000	101,900	191,300	.245	1.568	.219	76,800	79,700	79.2
N3-11	-196	106,500	123,300	171,200	.148	.823	.153	100,000	106,000	58.8
Fe-2.5Ni Specimen										
N4-9	200	38,800	64,200	148,700	.262	1.848	.242	33,600	49,300	85.7
N4-8	100	37,200	60,000	151,000	.227	1.848	.246	32,400	47,800	86.0
N4-1B	23	40,700	66,800	164,800	.263	1.951	.267	38,000	51,300	91.0
N4-2	-40	44,700	75,900	179,700	.281	1.910	.258	42,600	57,200	87.5
N4-3	-80	53,200	87,300	188,400	.277	1.868	.262	49,000	66,000	86.4
N4-4	-105	58,200	92,300	207,300	.247	1.808	.271	56,000	69,300	86.2
N4-5	-130	68,600	104,900	225,600	.327	1.848	.273	64,800	75.500	85.0
N4-6.	-155	81,000	106,000	233,000	.245	1.732	.227	76,800	82,400	83.6
N4-7	-196	108,900	133.500	242,900	.227	1.263	.214	105,500	106,300	71.8
Fe-5Ni Specimen										
N5-9	200	46,900	69,700	173,600	.227	1.930	.233	38,000	55,400	85.6
N5-8	100	42,500	69,100	168,800	.245	1.930	.252	40,800	54,000	87.0
N5-1	23	47,800	77,000	190,100	.263	1.951	.260	46,000	59,100	86.8
N5-2	-40	53,100	86,900	207,400	.263	1.910	.269	50,800	66,700	85.8
N5-3	-80	60,000	99,500	206,500	.254	1.694	.255	56,000	77,000	85.6
N5-4	-105	63,100	101,800	218,400	.281	1.751	.271	60,600	76,300	84.0
N5-5	-130	69,000	106,600	221,700	.263	1.694	.263	65,400	81,800	82.4
N5-6	-155	78,500	114,000	238,700	.249	1.676	.250	75,000	89,100	81.4
N5-7	-196	100,300	133,900	239,800	.245	1.218	.252	96,000	104,700	72.2

TABLE XIII

MECHANICAL PROPERTY DATA ON UNALLOYED VACUUM-MELTED IRON

Vacuum-Melted Iron Specimen	Test Temp. (deg. C)	$\sigma_{.04}$ (psi)	σ_{ml} (psi)	σ_f (psi)	ϵ_{ml}	ϵ_f	n	Y.S. 0.2% (psi)	UTS (psi)	R.A. (%)
B-9	200	35.100	-	-	-	-	-	19.800	42.000	82.4
B-8	100	28.800	-	-	-	-	-	22.200	39.200	85.0
B-1	23	28.800	49.200	121.700	.299	1.972	.275	25.800	36.400	89.0
B-2	-40	38.200	55.700	133.300	.263	1.930	.261	38.800	42.800	88.4
B-3	-80	54.300	60.300	135.100	.144	1.810	.127	52.000	52.000	87.6
B-4	-105	69.400	72.600	139.800	.153	1.876	.121	64.800	82.000	87.2
B-5	-130	75.200	82.100	156.500	.157	1.534	.125	72.000	70.800	83.4
B-6	-155	87.400	95.500	161.600	.106	1.218	.128	85.200	85.800	73.7
B-16	-196	104.400	126.000	168.000	.156	.762	.137	102.600	108.000	54.8

TABLE XIV

CONSTANT FLOW STRESS VALUES ($\sigma_{.04}$) FOR SOME COMMERCIAL ALLOY STEELS AT VARIOUS TEST TEMPERATURES (200 TO -196 C) (IN PSI)

Material	Test Temperature (deg C)								
	200	100	RT	-40	-80	-105	-130	-155	-196
AISI 1020	-	53,600	48.400	54.600	54.800	65.600	78.100	91.800	123.100
AISI 1045	130.500	-	127.300	139.900	148.200	156.600	159.700	177.400	-
AISI 1095	58.400	-	68.900	75.200	81.400	87.700	98.100	-	-
AISI 4140	-	-	98.100	106.500	116.900	124.200	129.400	142.000	184.900
AISI 4340	83.500	80,200	87.200	93.400	97.700	101.000	103,800	115.500	141.400
AISI 301 S.S.	-	-	47.000	-	-	58.700	-	-	88.700

APPENDIX A

FIGURES A-1 THROUGH A-21. TRUE STRESS-TRUE STRAIN TENSION CURVES FOR VARIOUS IRON-BASE ALLOYS OVER A RANGE OF TEST TEMPERATURES. EACH FIGURE SHOWS AN ALLOY AND THE APPROPRIATE TEMPERATURE RANGE.

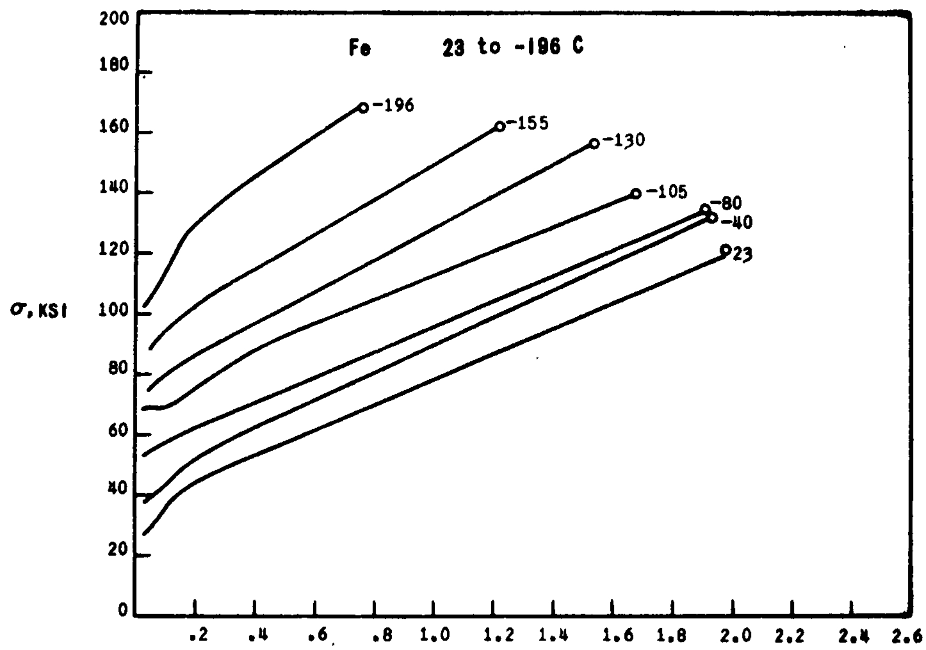

Figure A-1

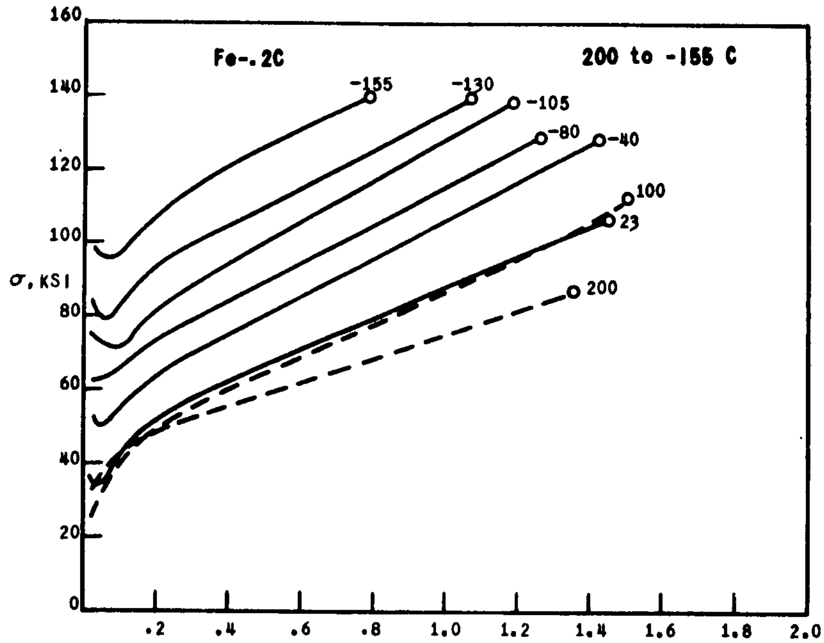

Figure A-2

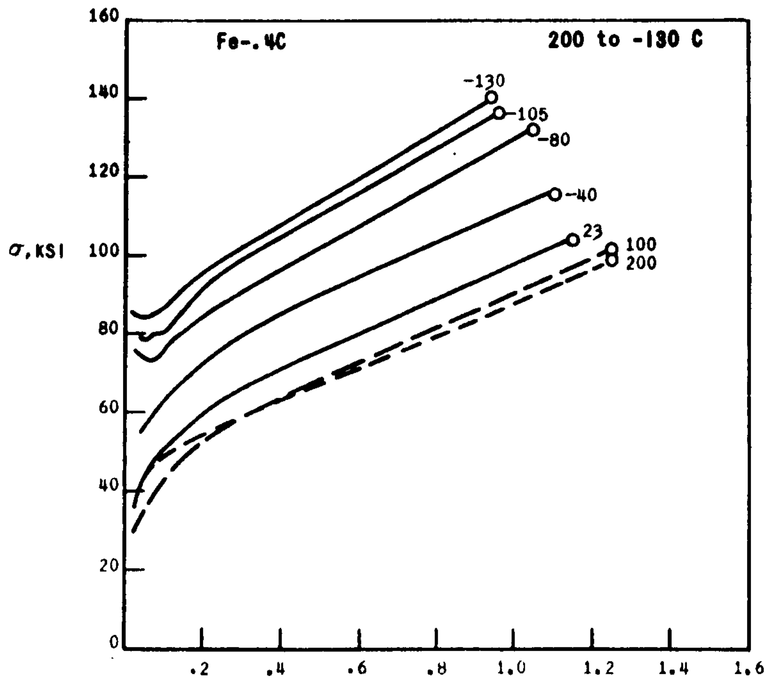

Figure A-3

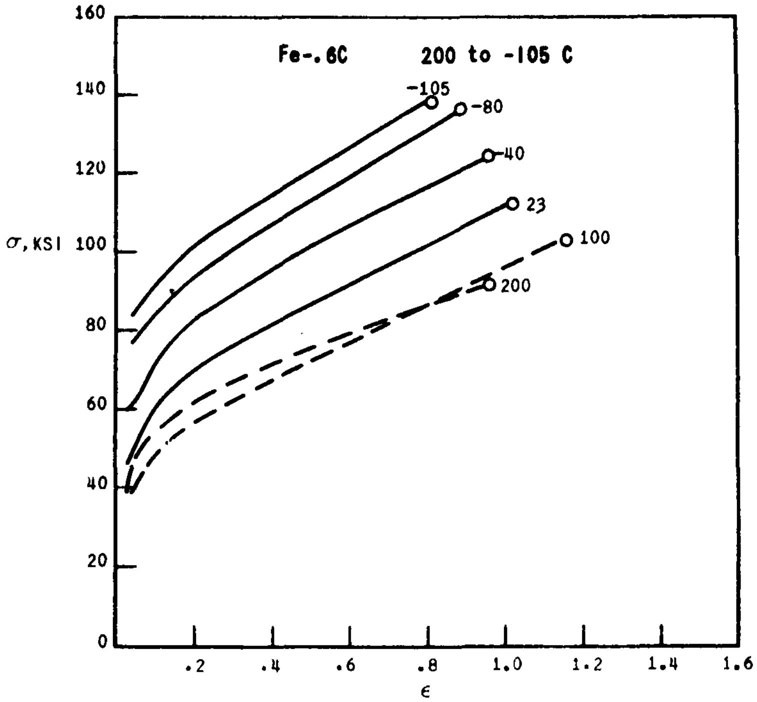

Figure A-4

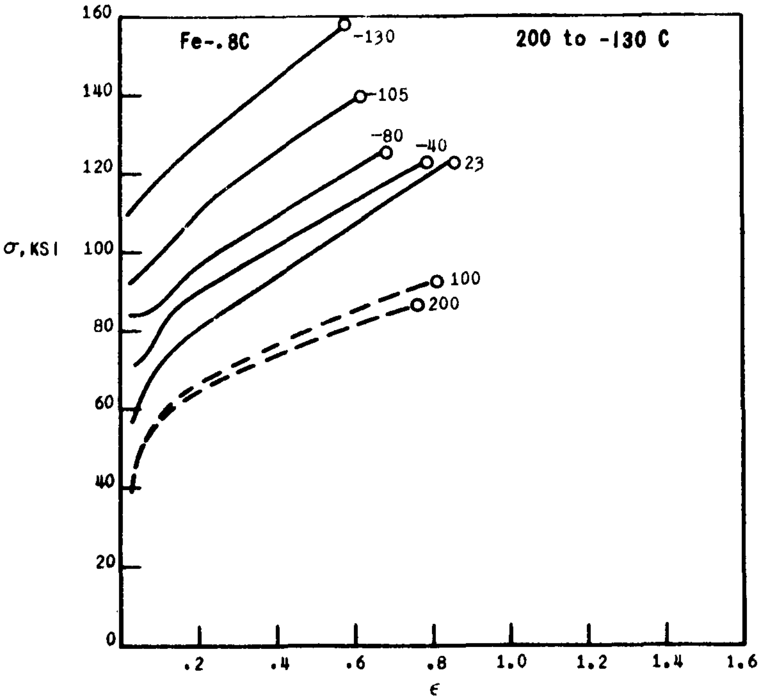

Figure A-5

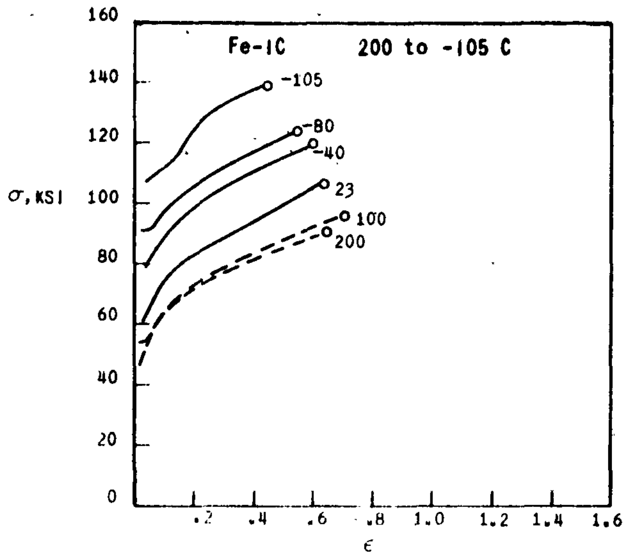

Figure A-6

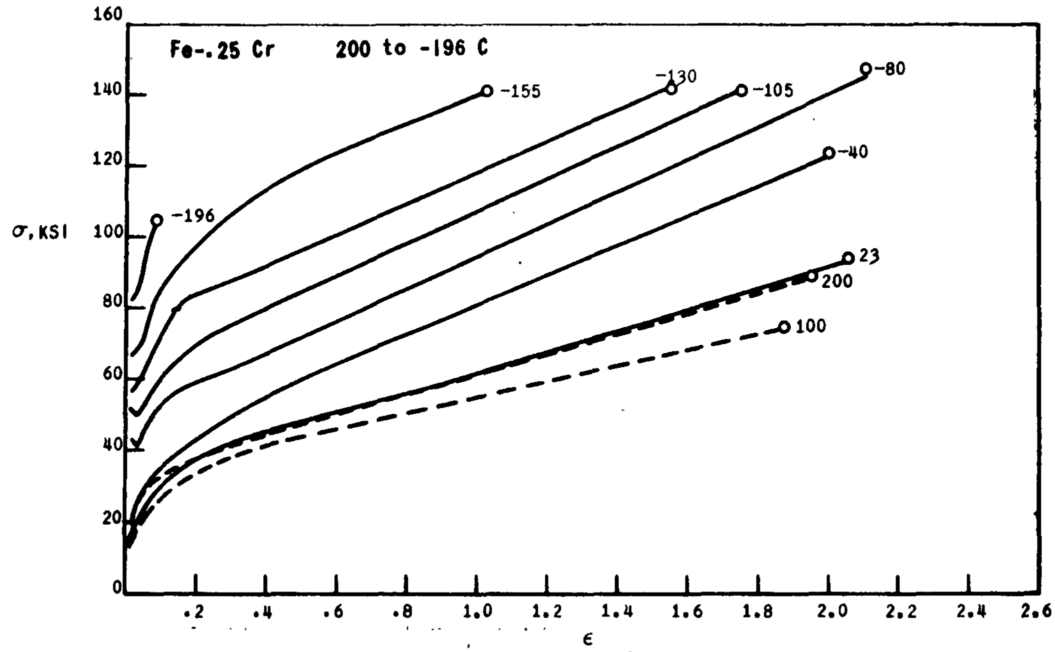

Figure A-7

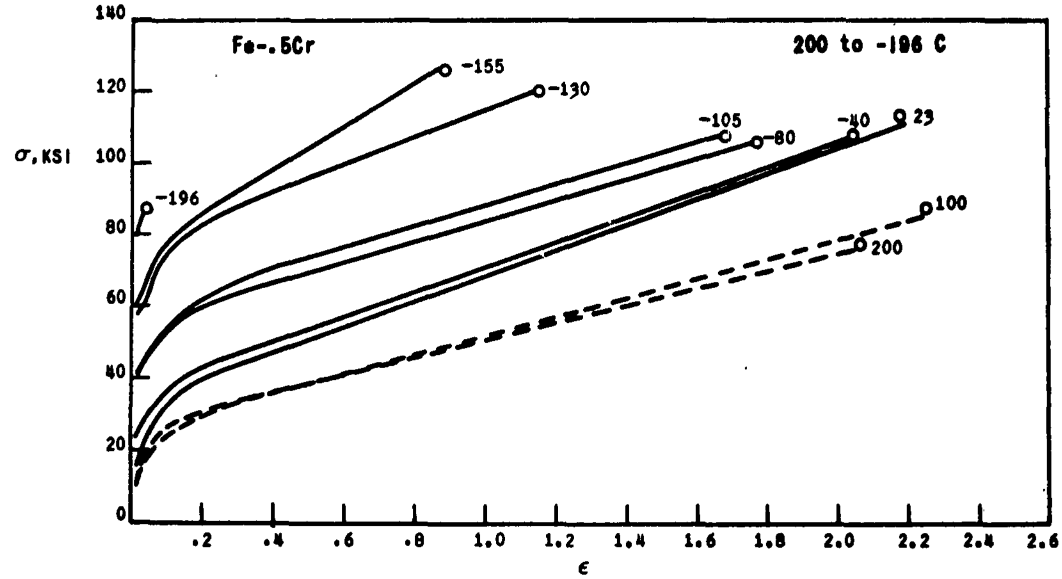

Figure A-8

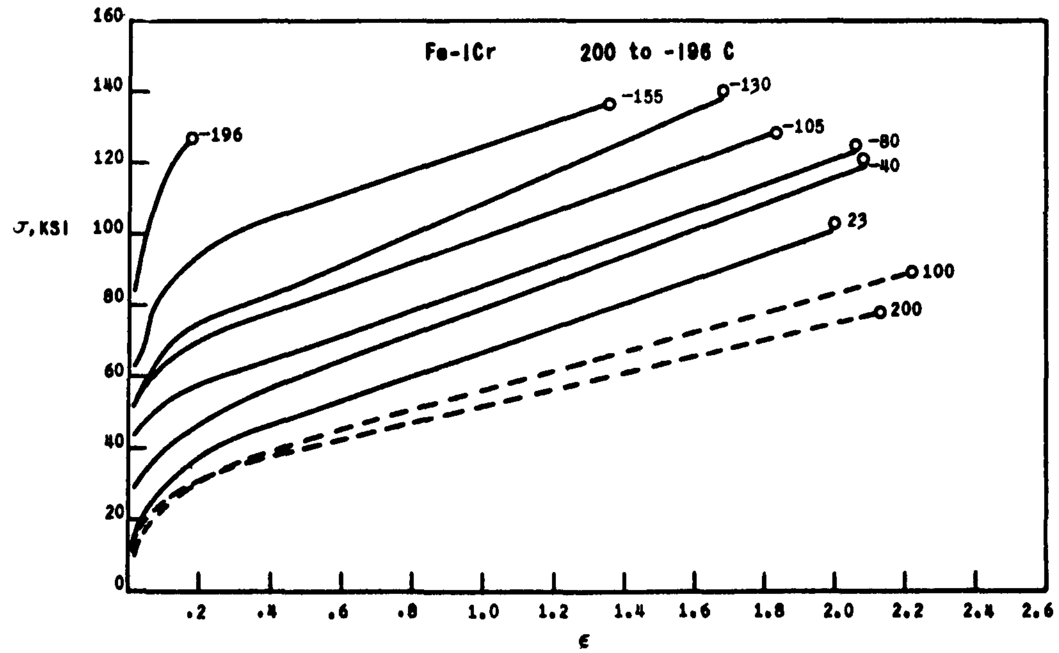

Figure A-9

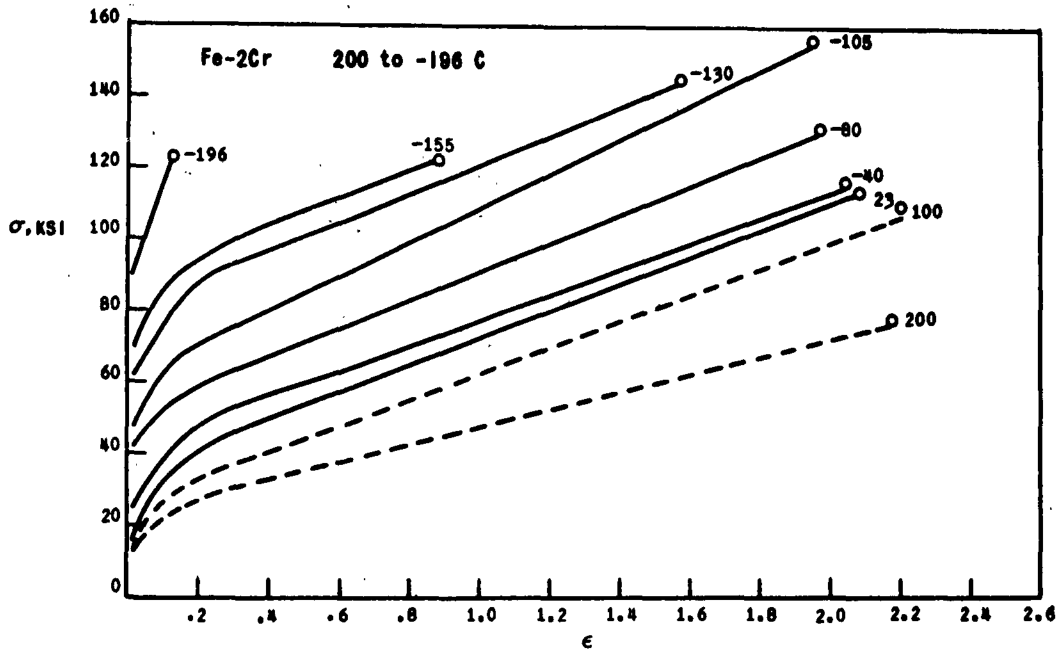

Figure A-10

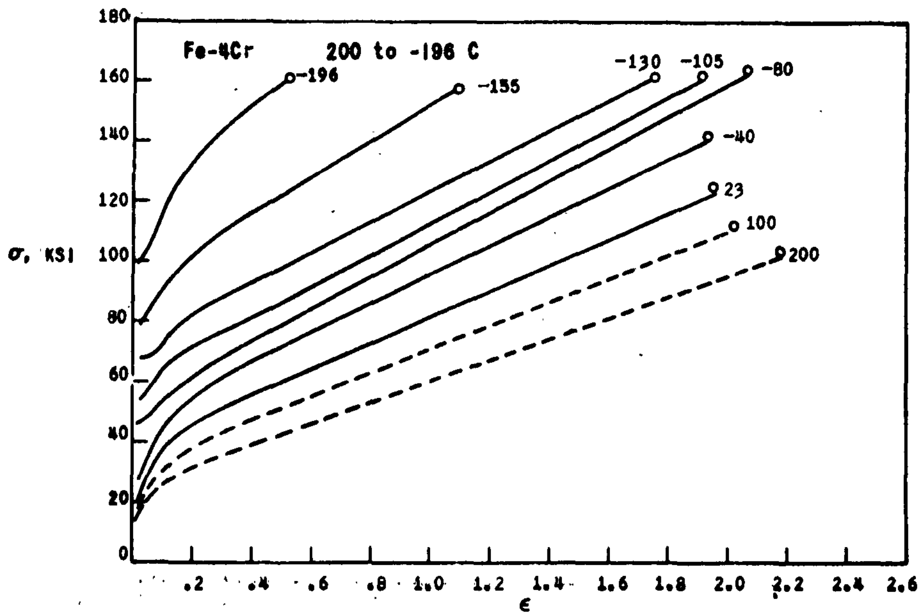

Figure A-11

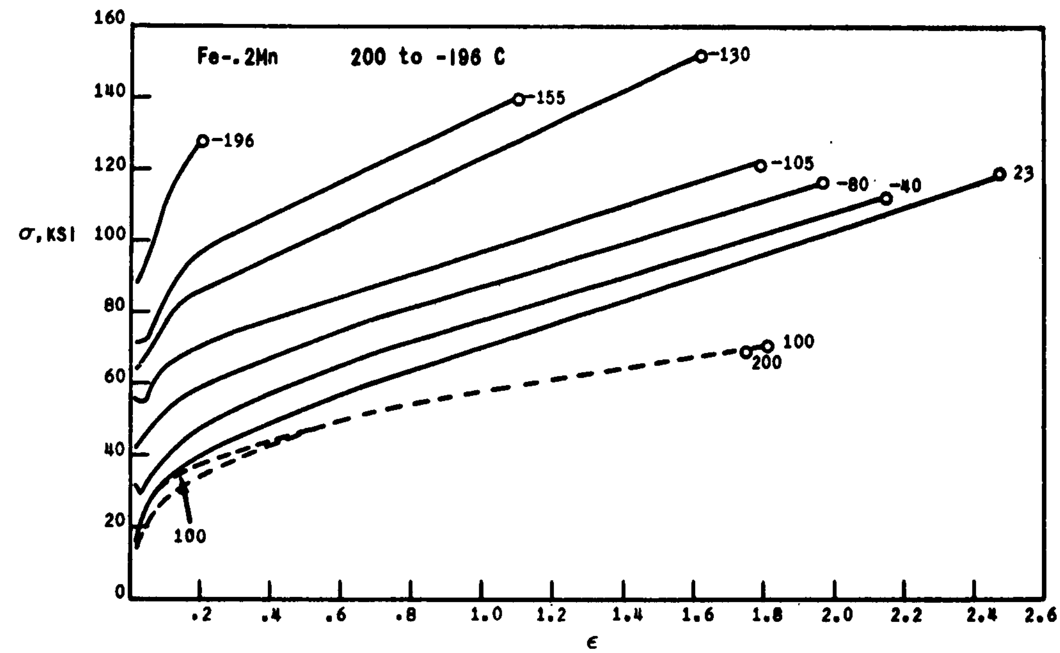

Figure A-12

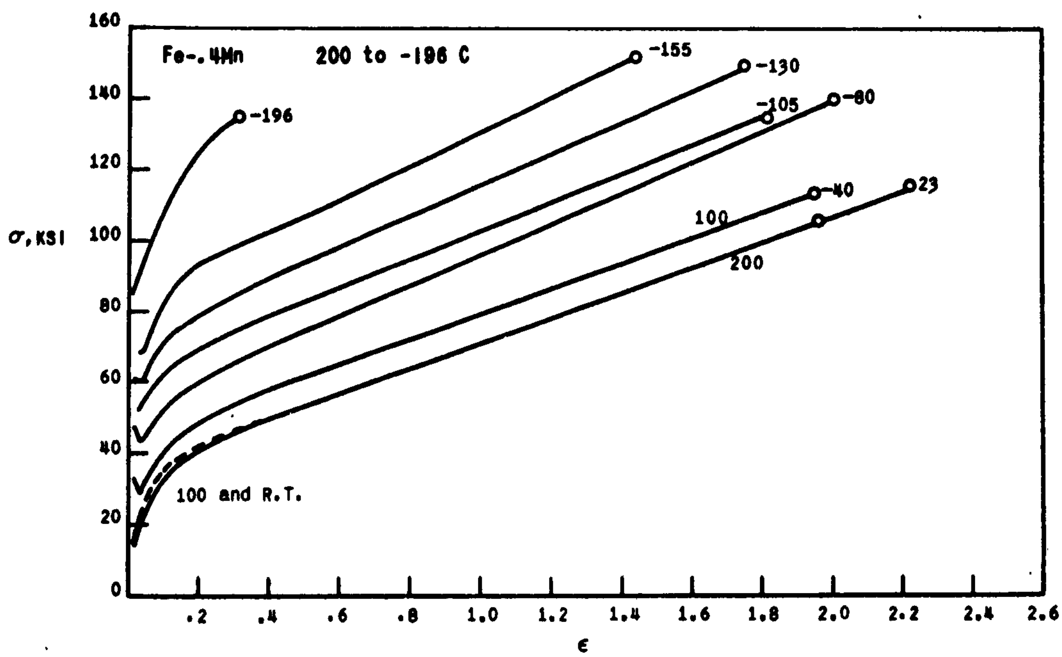

Figure A-13

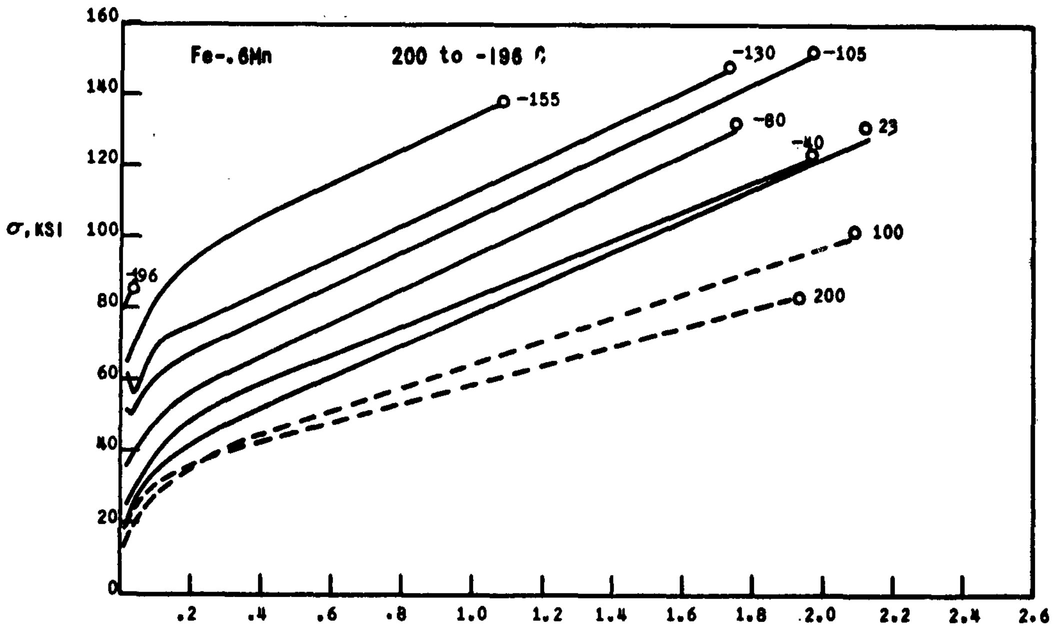

Figure A-14

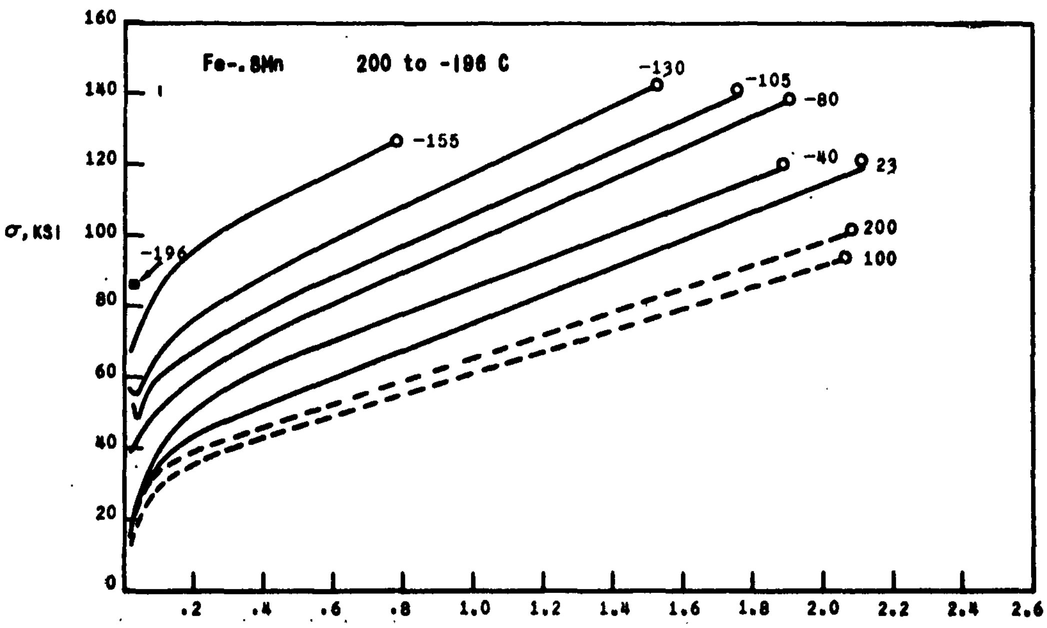

Figure A-15

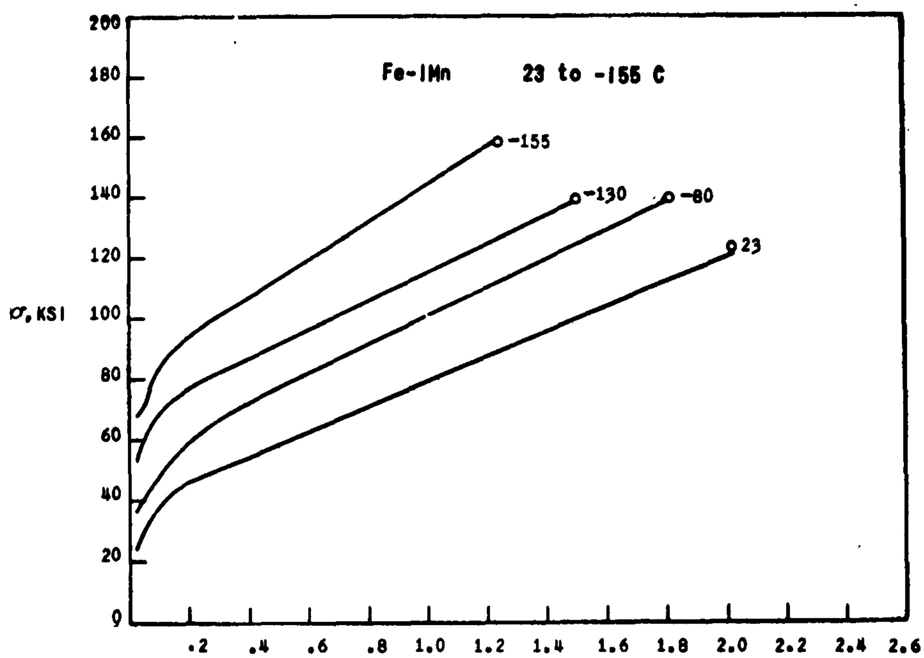

Figure A-16

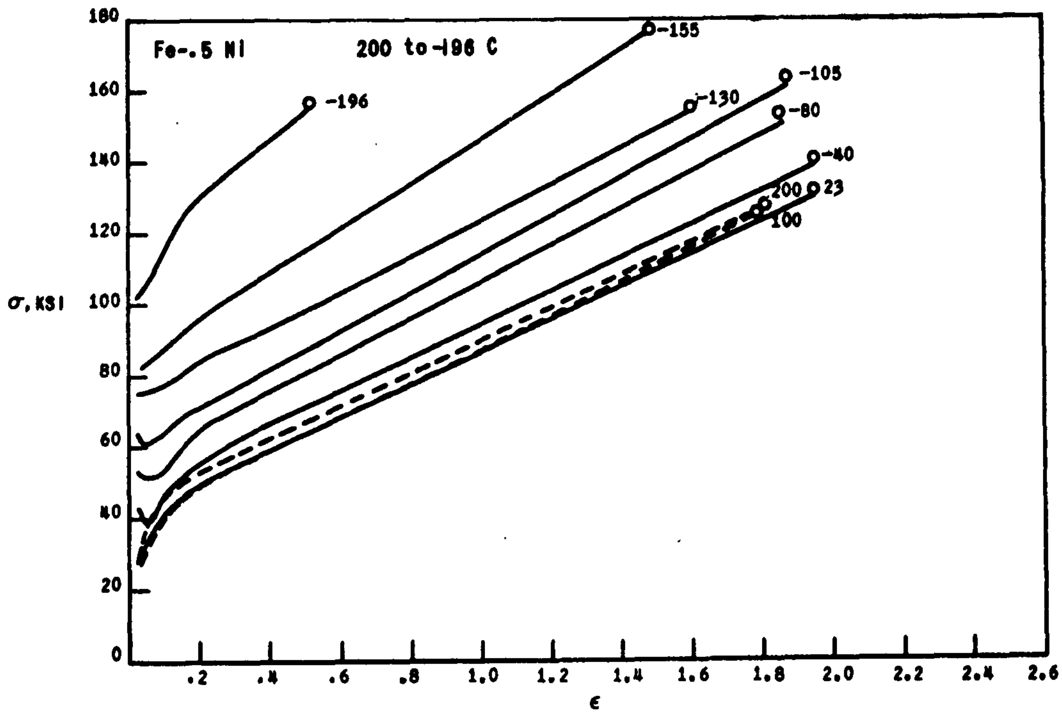

Figure A-17

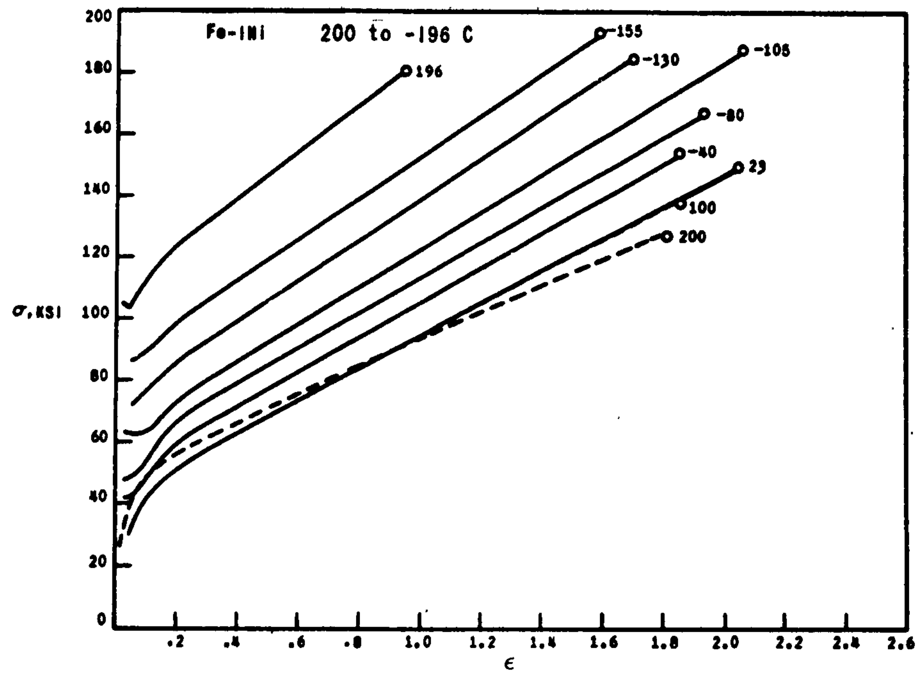

Figure A-18

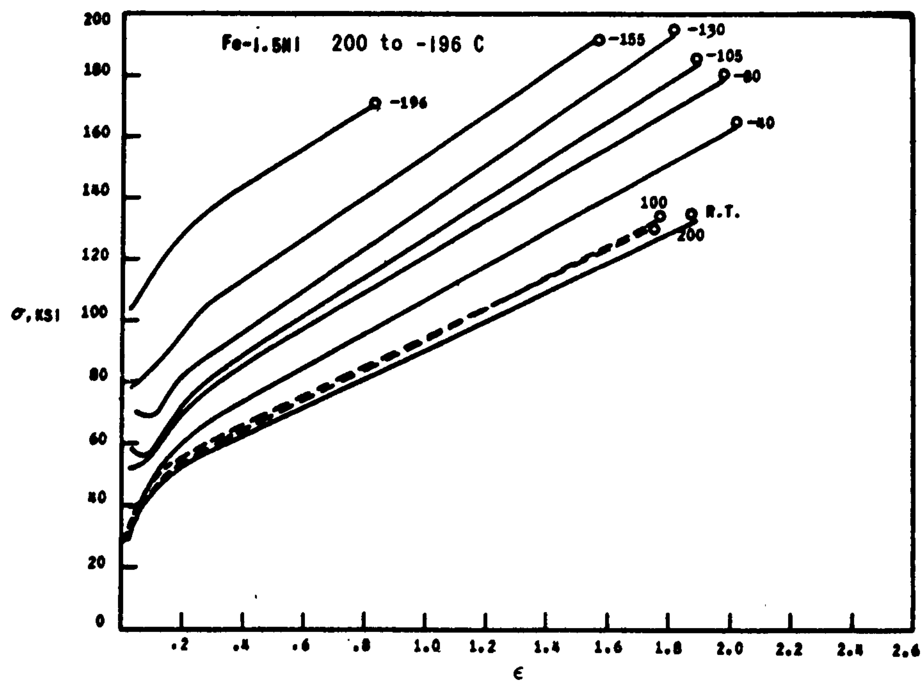

Figure A-19

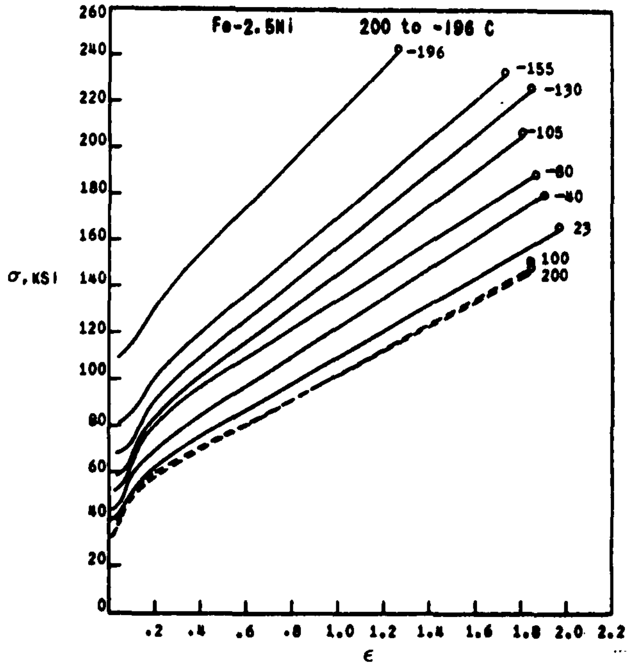

Figure A-20

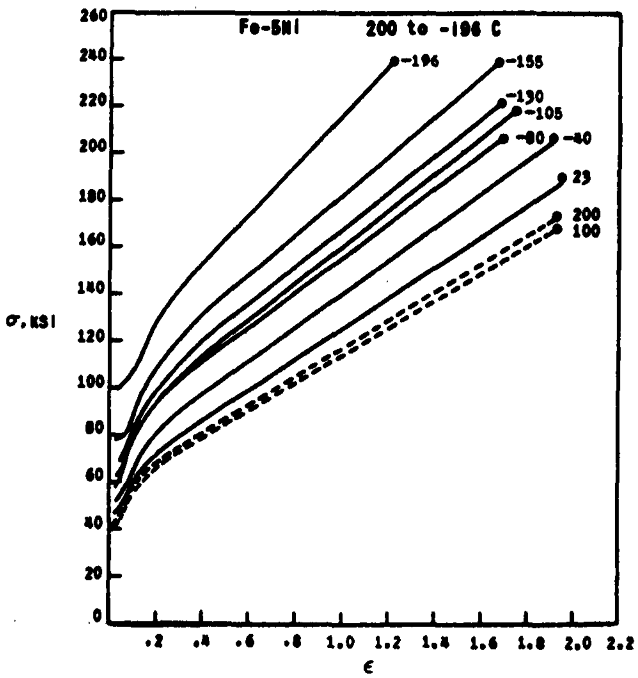

Figure A-21

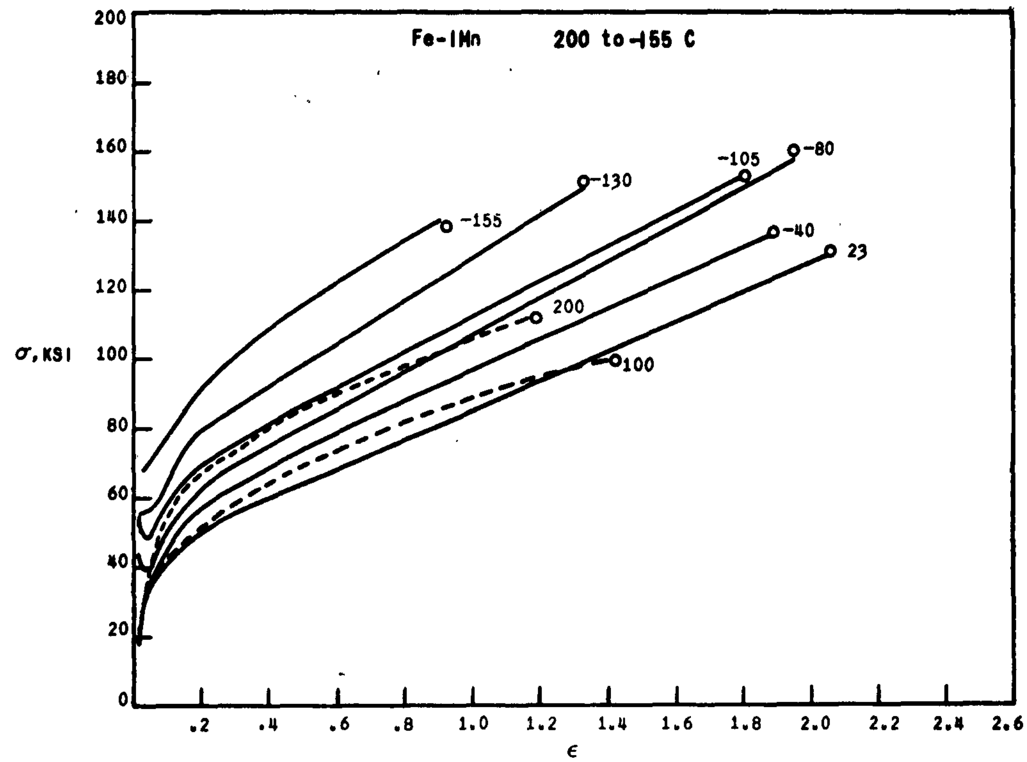

Figure A-22. TRUE STRESS-TRUE STRAIN TENSION CURVES FOR THE ORIGINAL ALLOY CONTAINING A RELATIVELY HIGH AMOUNT OF NITROGEN (50 ppm)

APPENDIX B

FIGURES B-1 THROUGH B-21. SELECTED FLOW STRESS, STRAIN AND STRAIN HARDENING PARAMETERS VERSUS RECIPROCAL ABSOLUTE TEMPERATURE FOR VARIOUS IRON-BASE ALLOYS.

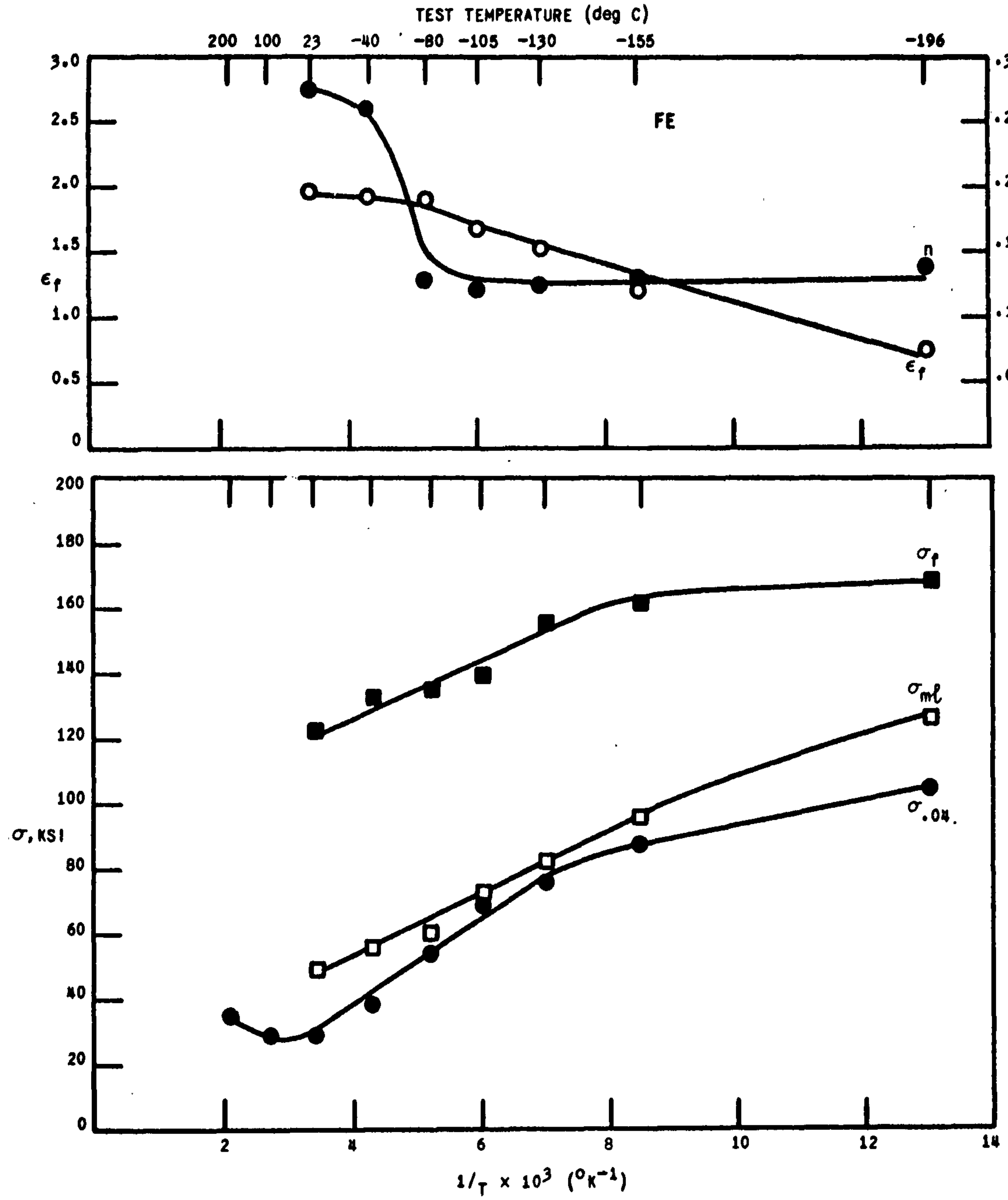

Figure B-1

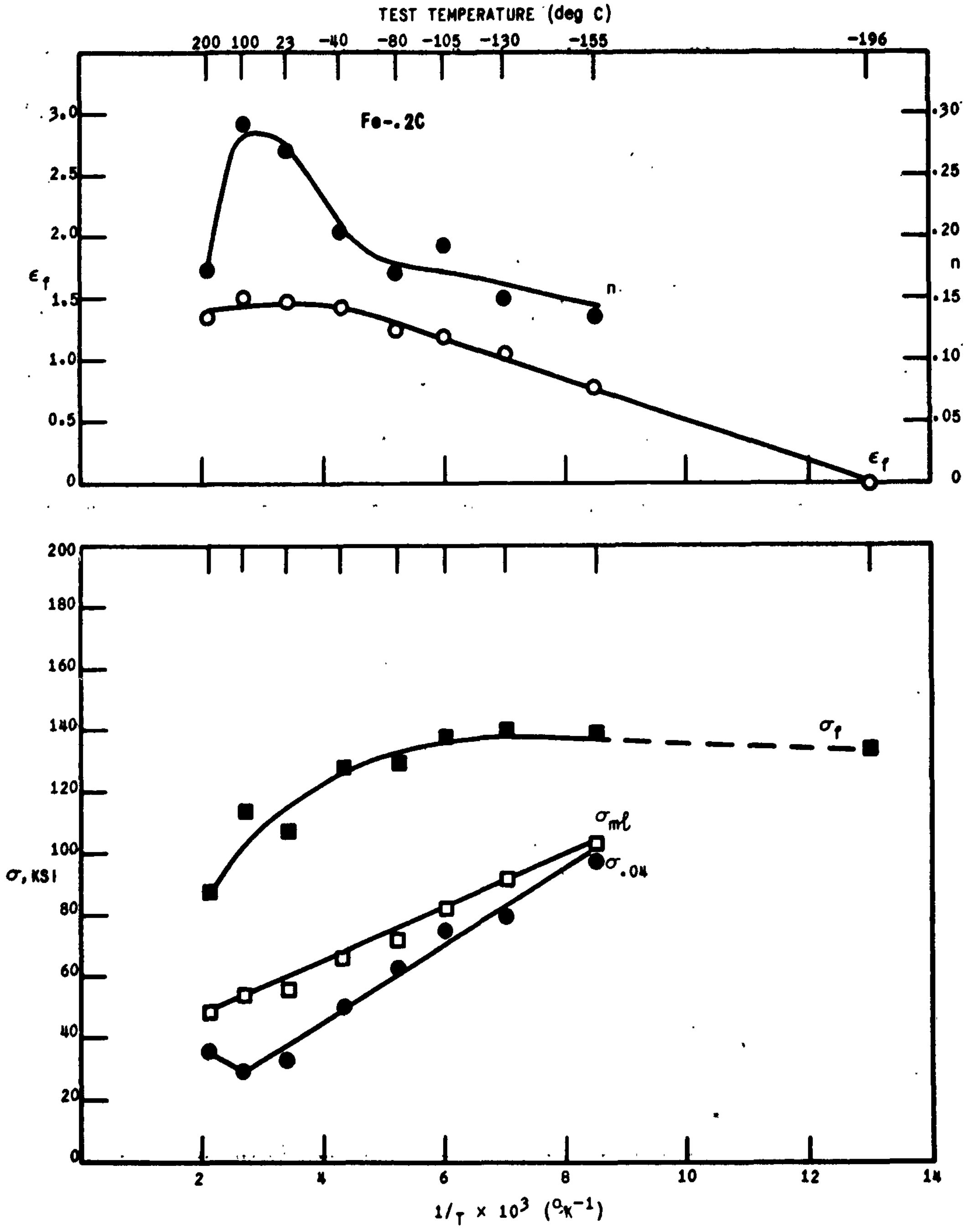

TEST TEMPERATURE (deg C)
200 100 23 -40 -80 -105 -130 -155 -196
Fe-.2C
ϵ_f
n
3.0
2.5
2.0
1.5
1.0
0.5
0
.30
.25
.20
.15
.10
.05
0
200
180
160
140
120
100
80
60
40
20
0
σ, KSI
σ_f
$\sigma_{m\ell}$
$\sigma_{.04}$
2
4
6
8
10
12
14
$1/_T \times 10^3$ ($^oK^{-1}$)

Figure B-2

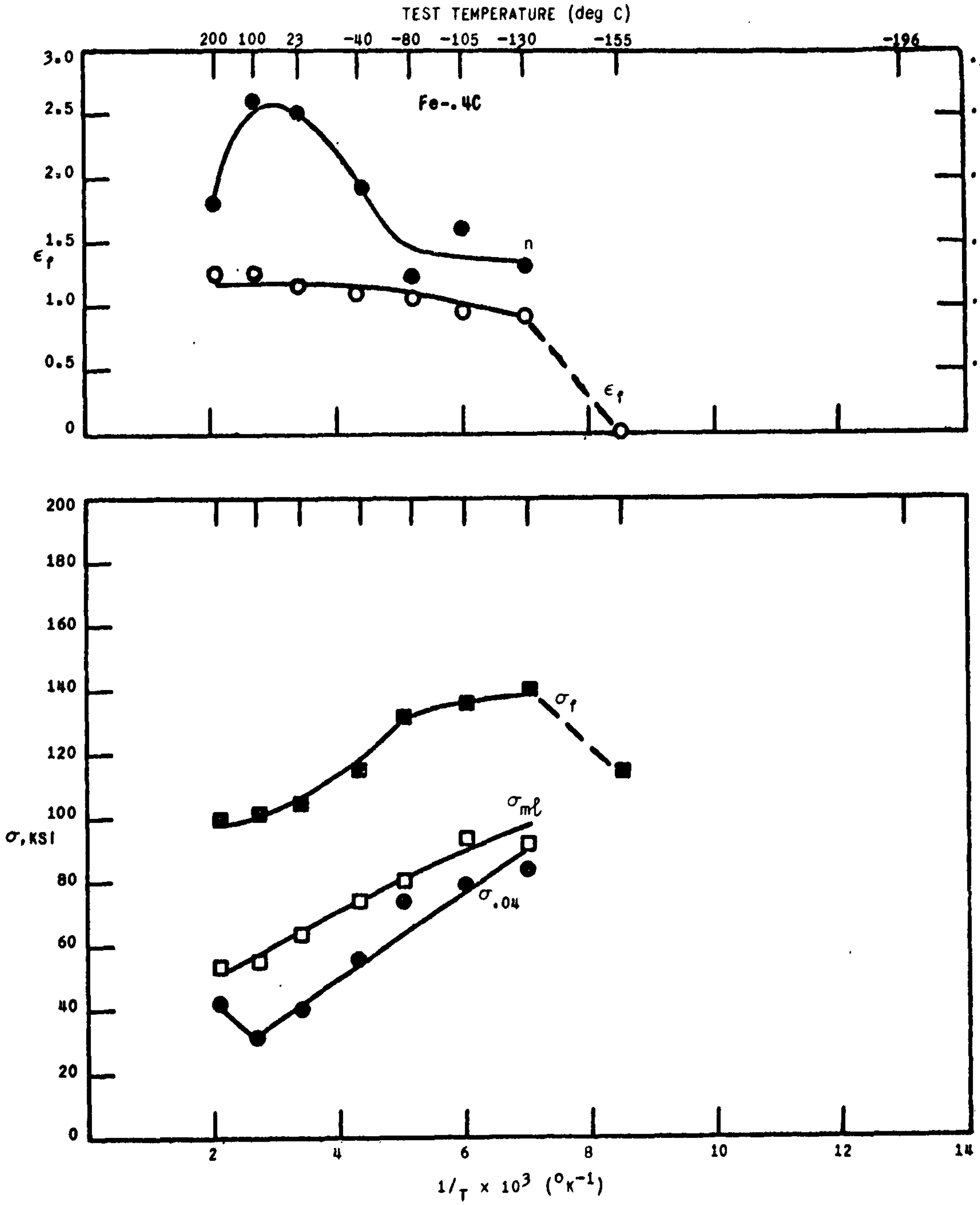

TEST TEMPERATURE (deg C)
200
100
23
-40
-80
-105
-130
-155
-196
Fe-.4C
n
ϵ_f
n
3.0
2.5
2.0
1.5
1.0
0.5
0
.30
.25
.20
.15
.10
.05
0
σ_f
σ_{ml}
$\sigma_{.04}$
σ, KSI
200
180
160
140
120
100
80
60
40
20
0
2
4
6
8
10
12
14
$1/_T \times 10^3$ ($^oK^{-1}$)

Figure B-3

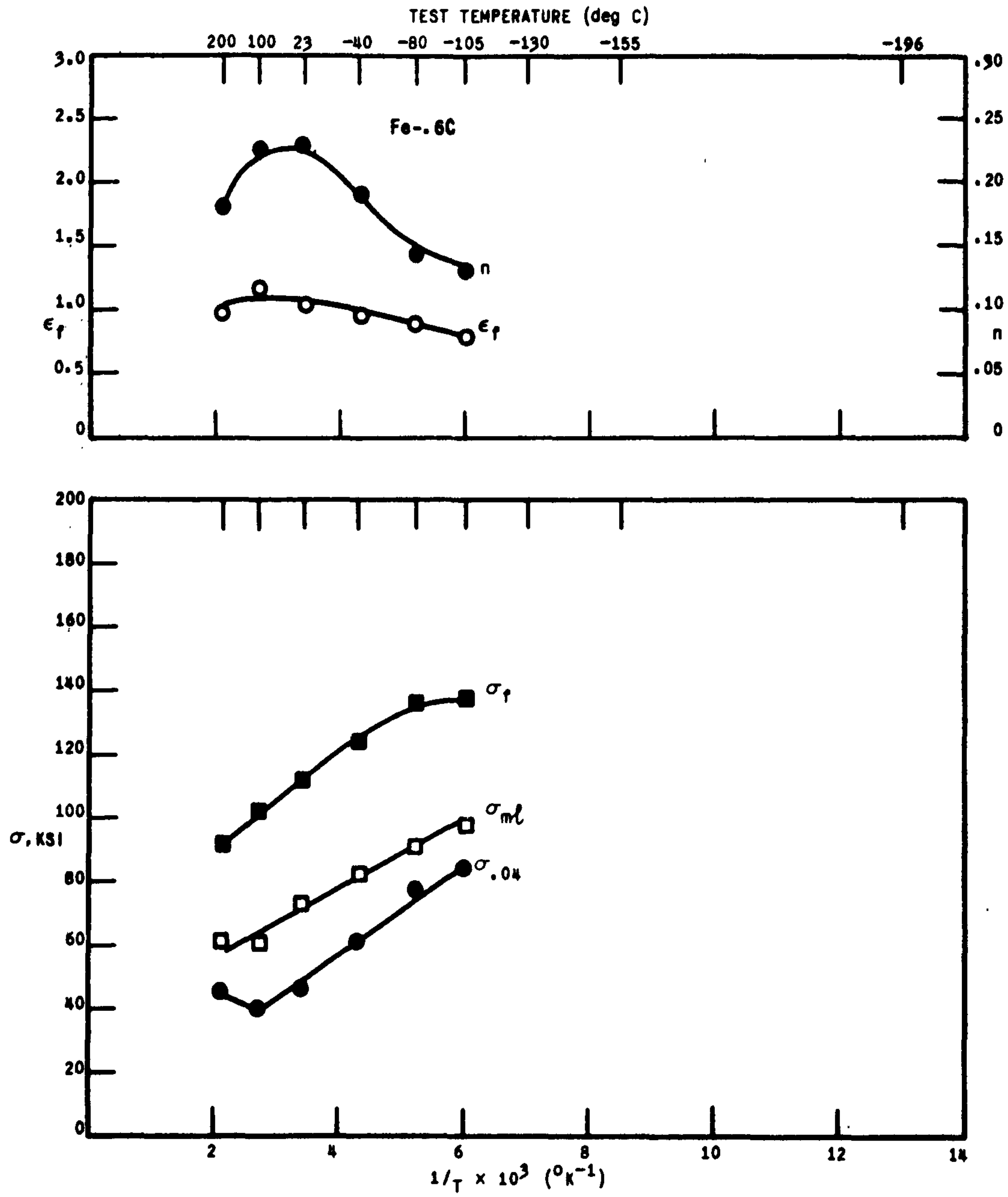
TEST TEMPERATURE (deg C)
200 100 23 -40 -80 -105 -130 -155 -196
3.0
2.5
2.0
1.5
1.0
0.5
0
.30
.25
.20
.15
.10
.05
0
n
Fe-.6C
ϵ_f
σ_f
σ_{ml}
$\sigma_{.04}$
200
180
160
140
120
100
80
60
40
20
0
σ, KSI
2
4
6
8
10
12
14
$1/T \times 10^3$ ($^oK^{-1}$)

Figure B-4

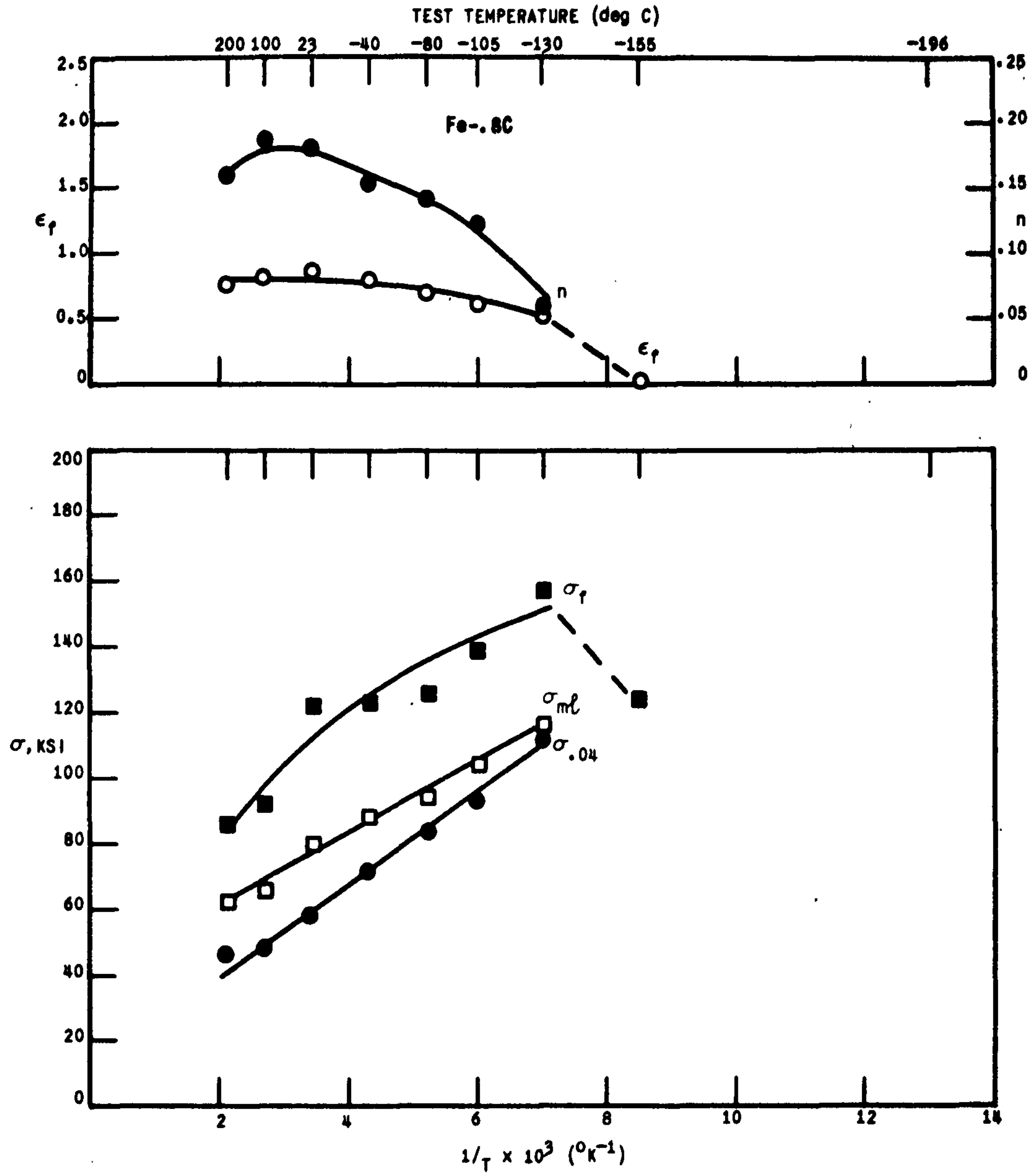
TEST TEMPERATURE (deg C)
200 100 23 −40 −80 −105 −130 −155 −196
Fe-.8C
ϵ_f
n
2.5
2.0
1.5
1.0
0.5
0
.25
.20
.15
.10
.05
0
σ, KSI
200
180
160
140
120
100
80
60
40
20
0
σ_f
σ_{ml}
$\sigma_{.04}$
2
4
6
8
10
12
14
$1/_T \times 10^3$ ($^oK^{-1}$)

Figure B-6

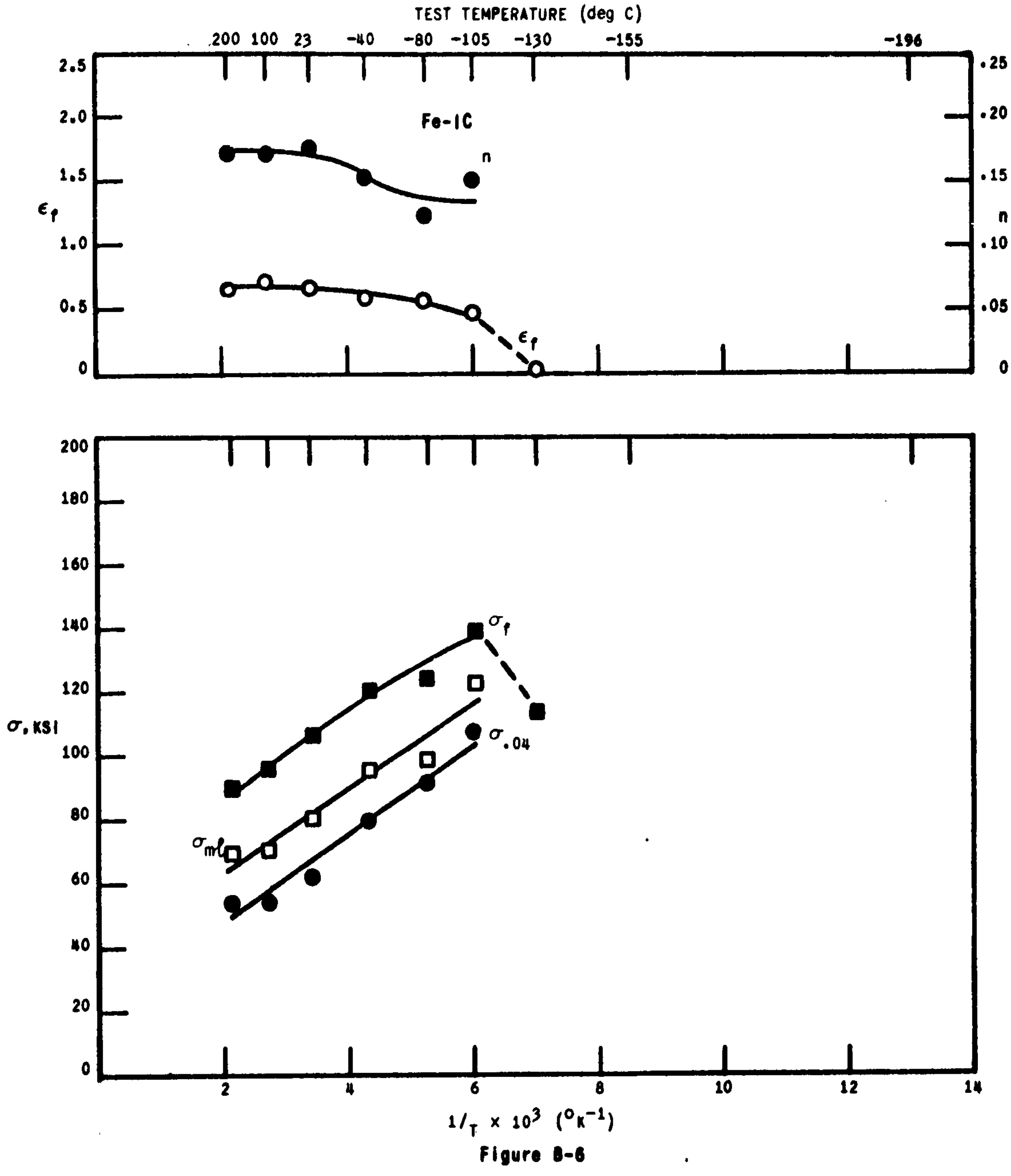

TEST TEMPERATURE (deg C)
200 100 23 -40 -80 -105 -130 -155 -196
Fe-1C
n
ϵ_f
n
ϵ_f
σ_f
$\sigma_{.04}$
σ_{ml}
σ, KSI
$1/_T \times 10^3$ ($^oK^{-1}$)

Figure 8-6

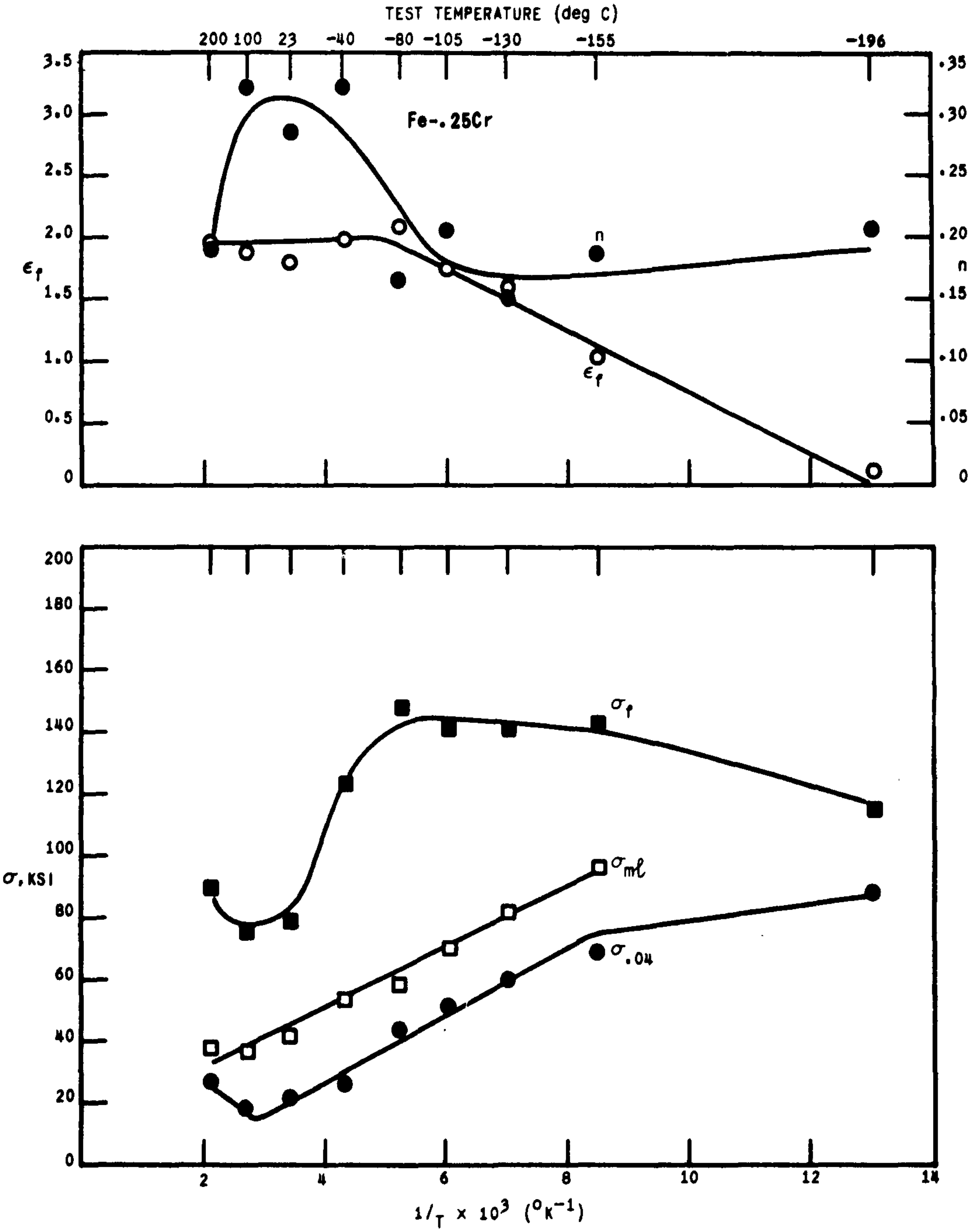

TEST TEMPERATURE (deg C)
200 100 23 -40 -80 -105 -130 -155 -196
3.5
3.0
2.5
2.0
1.5
1.0
0.5
0
ϵ_f
.35
.30
.25
.20
.15
.10
.05
0
n
Fe-.25Cr
n
ϵ_f
200
180
160
140
120
100
80
60
40
20
0
σ, KSI
σ_f
$\sigma_{m\ell}$
$\sigma_{.04}$
2
4
6
8
10
12
14
$1/_T \times 10^3$ ($^oK^{-1}$)

Figure B-7

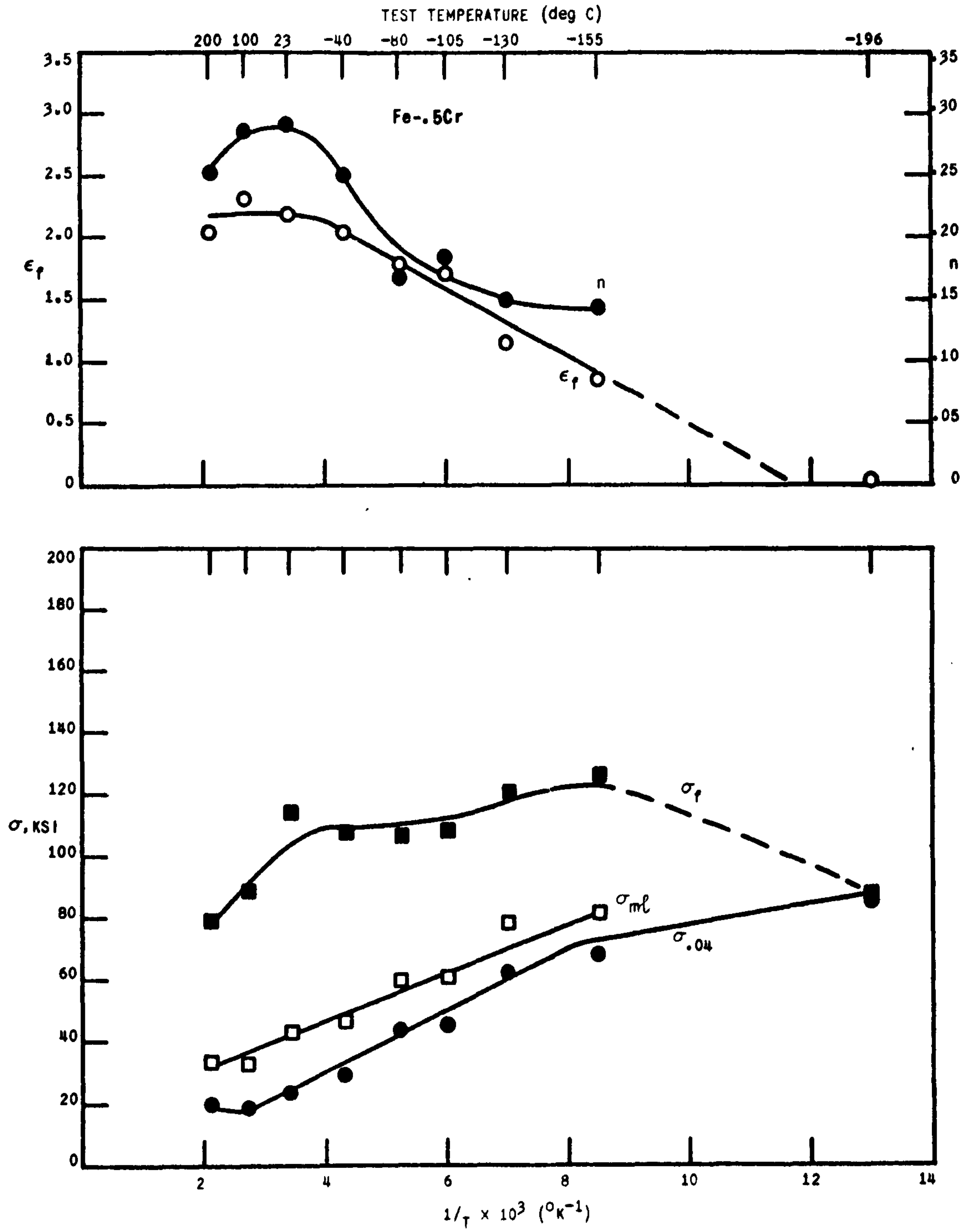

TEST TEMPERATURE (deg C)
200 100 23 -40 -80 -105 -130 -155 -196
Fe-.5Cr
ϵ_f
n
σ_f
σ, KSI
σ_{ml}
$\sigma_{.04}$
$1/_T \times 10^3$ ($^oK^{-1}$)

Figure B-8

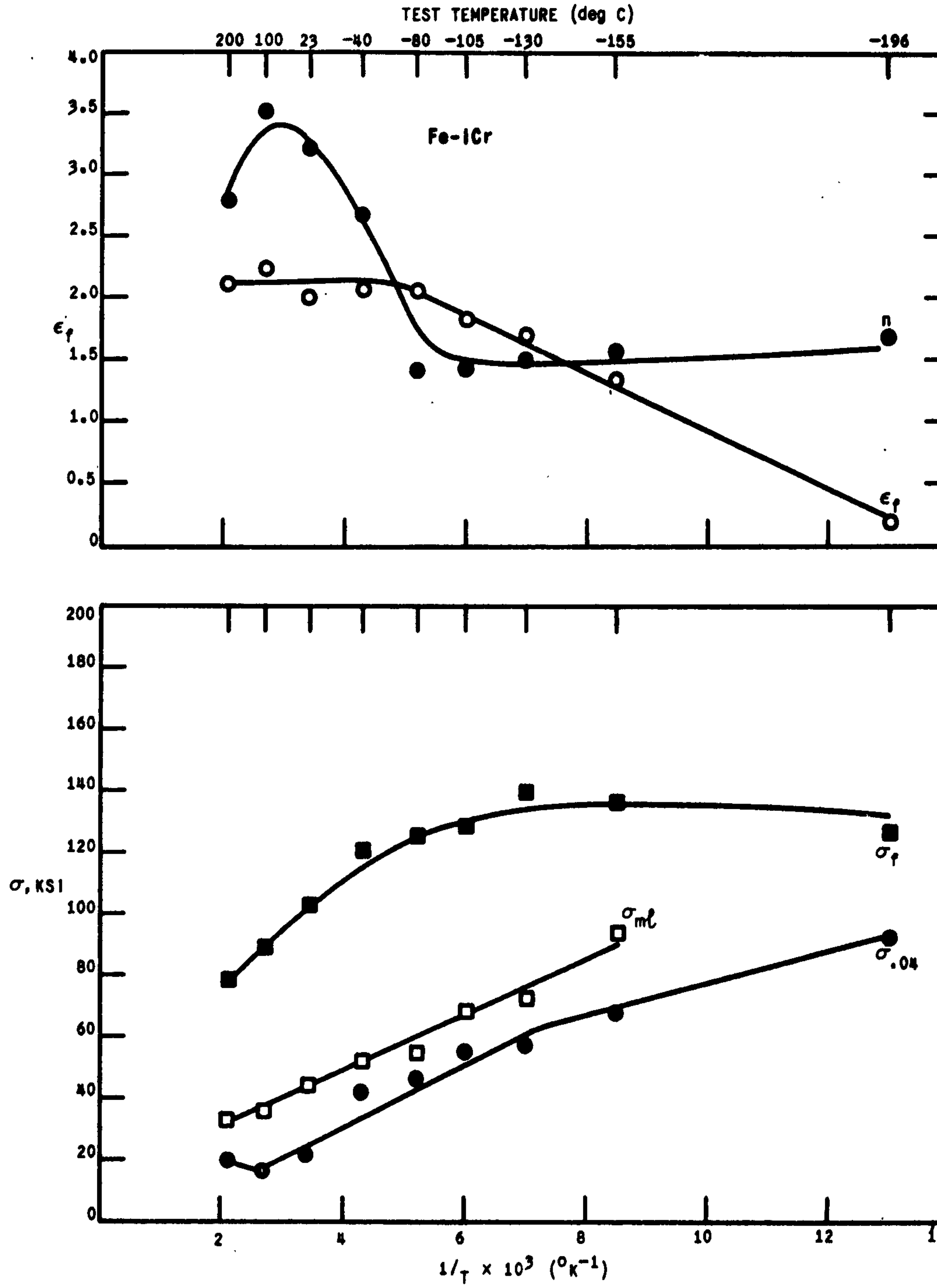
TEST TEMPERATURE (deg C)
200 100 23 -40 -80 -105 -130 -155 -196
Fe-1Cr
ϵ_f
n
σ, KSI
σ_f
$\sigma_{m\ell}$
$\sigma_{.04}$
$1/_T \times 10^3$ ($^oK^{-1}$)

Figure B-9

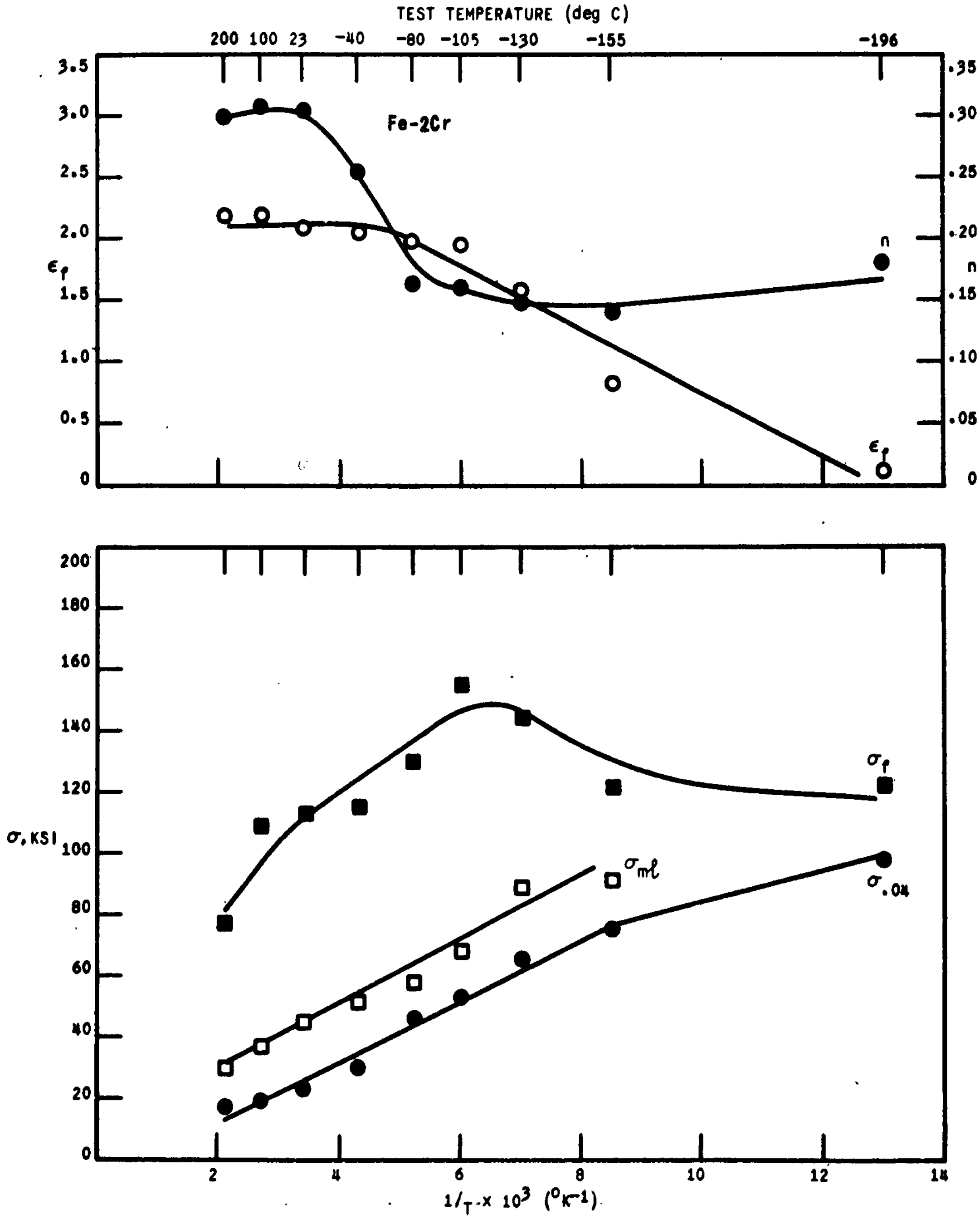

TEST TEMPERATURE (deg C)
200 100 23 -40 -80 -105 -130 -155 -196
Fe-2Cr
ϵ_f
n
3.5
3.0
2.5
2.0
1.5
1.0
0.5
0
.35
.30
.25
.20
.15
.10
.05
0
σ, KSI
200
180
160
140
120
100
80
60
40
20
0
σ_f
$\sigma_{m\ell}$
$\sigma_{.04}$
2
4
6
8
10
12
14
$1/_T \times 10^3$ ($^oK^{-1}$)

Figure 8-10

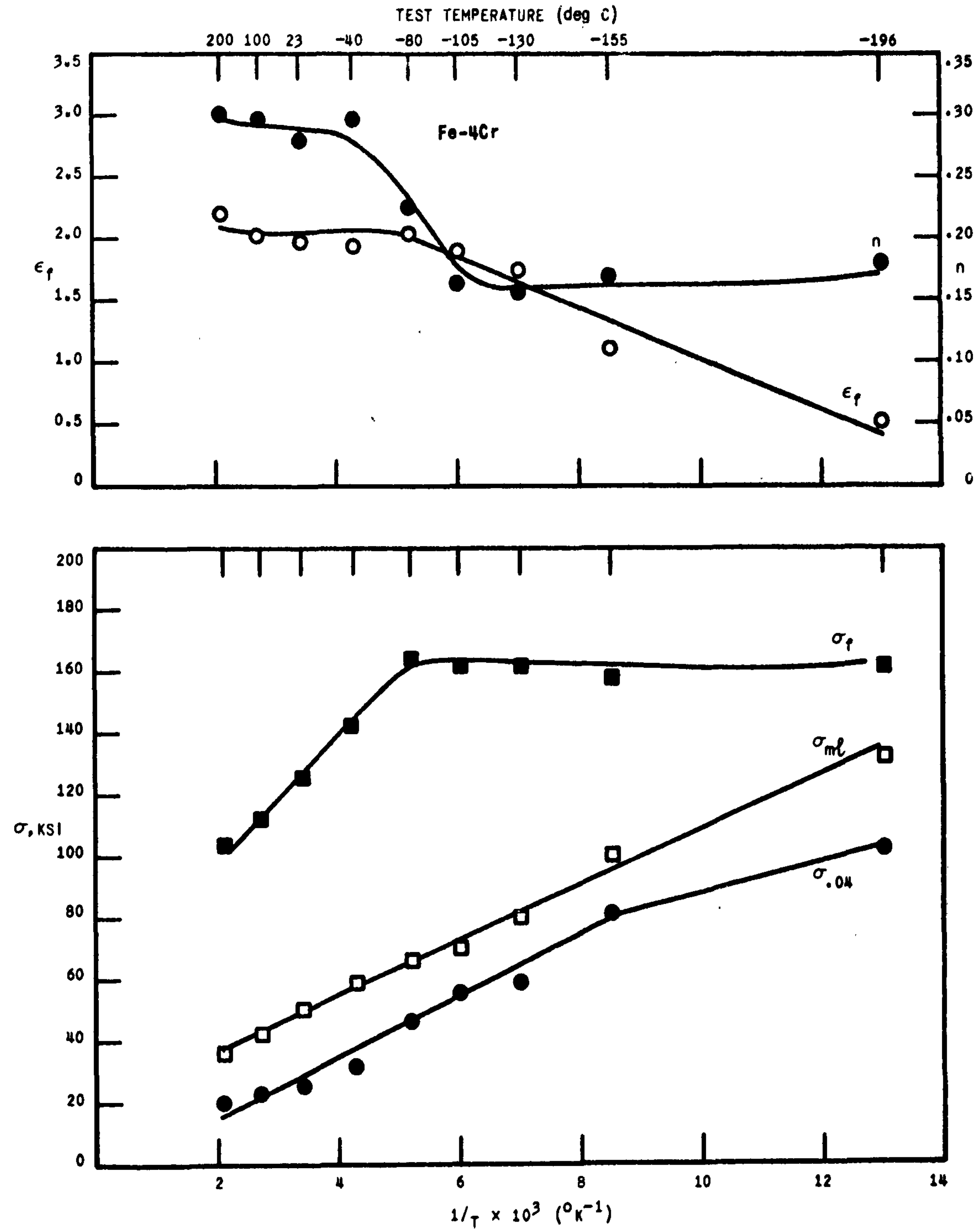
TEST TEMPERATURE (deg C)
200 100 23 -40 -80 -105 -130 -155 -196
Fe-4Cr
ϵ_f
n
3.5
3.0
2.5
2.0
1.5
1.0
0.5
0
.35
.30
.25
.20
.15
.10
.05
0
σ, KSI
200
180
160
140
120
100
80
60
40
20
0
σ_f
$\sigma_{m\ell}$
$\sigma_{.04}$
2
4
6
8
10
12
14
$1/_T \times 10^3$ ($^oK^{-1}$)

Figure B-11

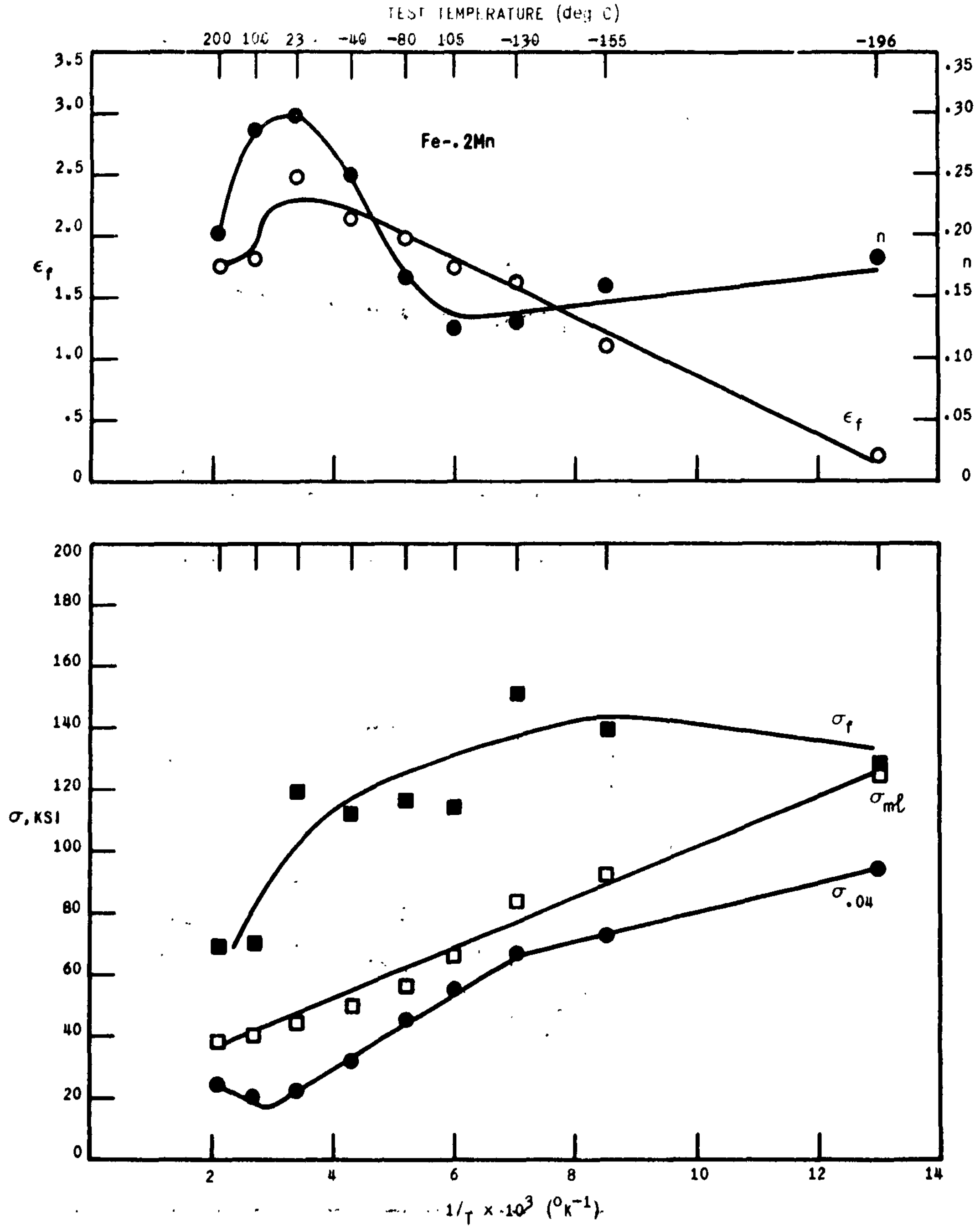
TEST TEMPERATURE (deg C)
200 100 23 -40 -80 105 -130 -155 -196
Fe-.2Mn
ϵ_f
n
σ, KSI
σ_f
$\sigma_{m\ell}$
$\sigma_{.04}$
2 4 6 8 10 12 14
1/T x 10³ (°K⁻¹)

Figure B-12

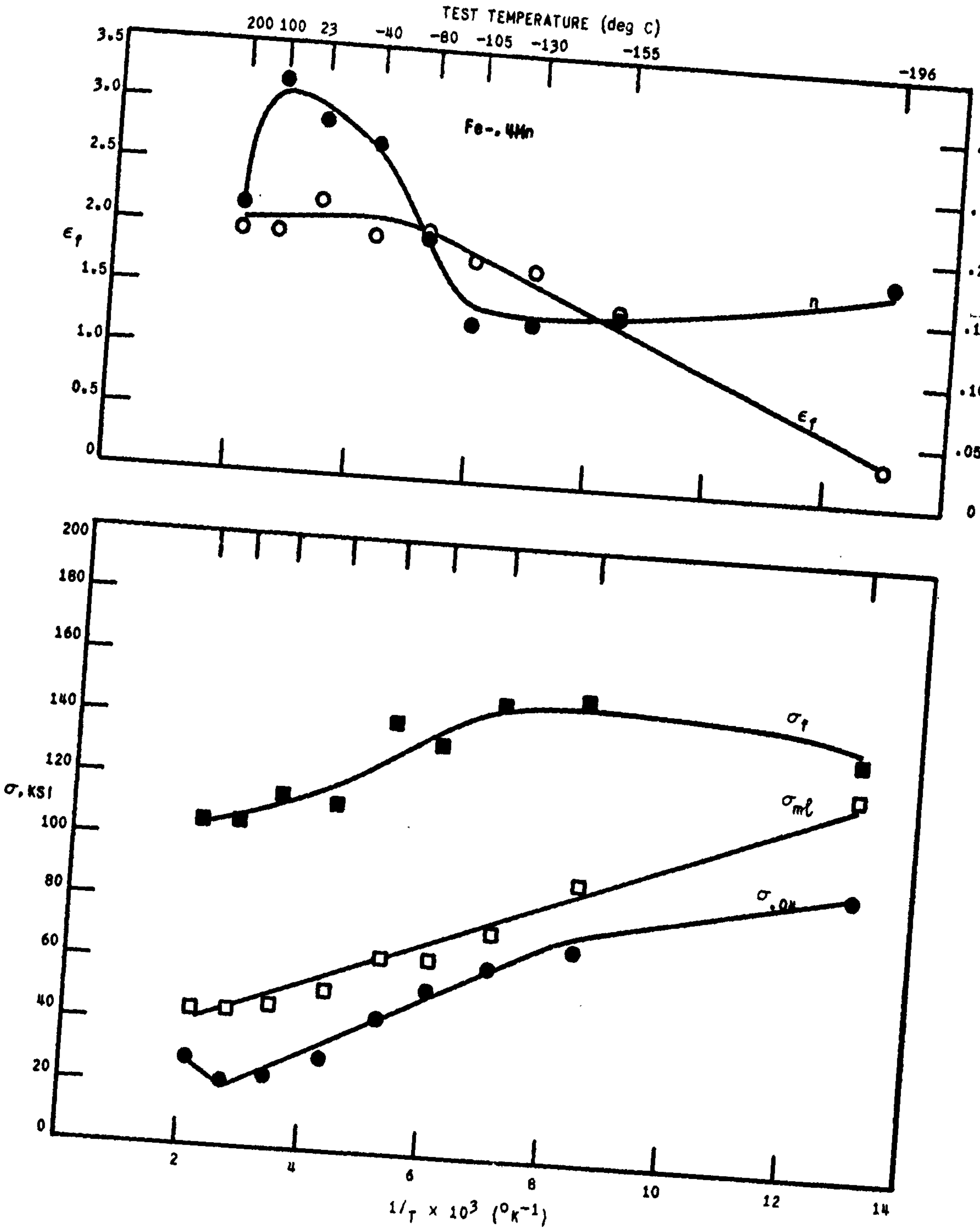
TEST TEMPERATURE (deg C)
200 100 23 -40 -80 -105 -130 -155 -196
Fe-.4Mn
3.5
3.0
2.5
2.0
1.5
1.0
0.5
0
ϵ_f
n
.35
.30
.25
.20
.15
.10
.05
0
200
180
160
140
120
100
80
60
40
20
0
σ, KSI
σ_f
σ_{ml}
$\sigma_{.04}$
2
4
6
8
10
12
14
$1/T \times 10^3$ ($^oK^{-1}$)

Figure B-13

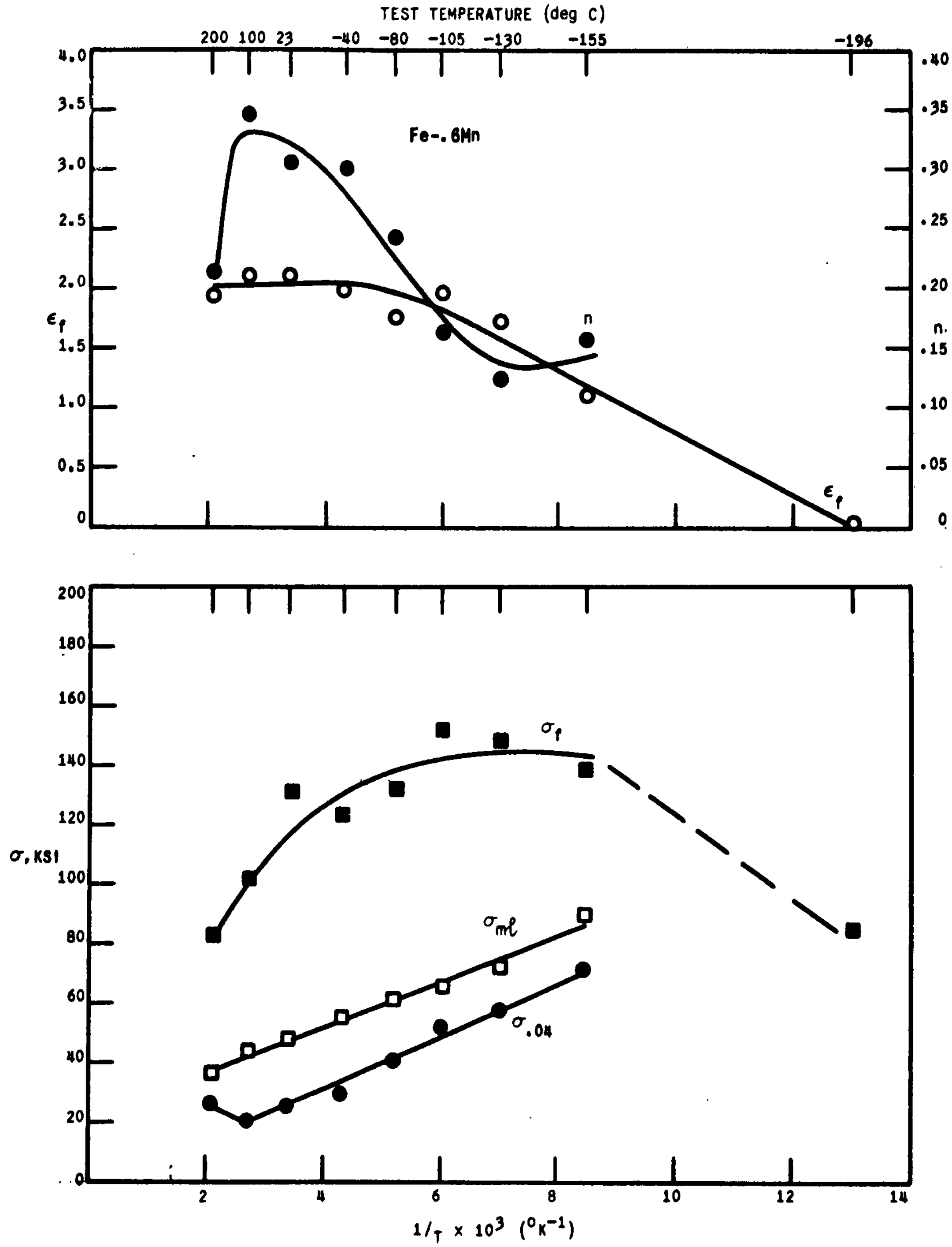

TEST TEMPERATURE (deg C)
200 100 23 -40 -80 -105 -130 -155 -196
Fe-.6Mn
4.0
3.5
3.0
2.5
2.0
1.5
1.0
0.5
0
ϵ_f
n
ϵ_f
.40
.35
.30
.25
.20
n.
.15
.10
.05
0
200
180
160
140
120
100
80
60
40
20
0
σ, KSI
σ_f
$\sigma_{m\ell}$
$\sigma_{.04}$
2
4
6
8
10
12
14
$1/_T \times 10^3$ ($^oK^{-1}$)

Figure B-14

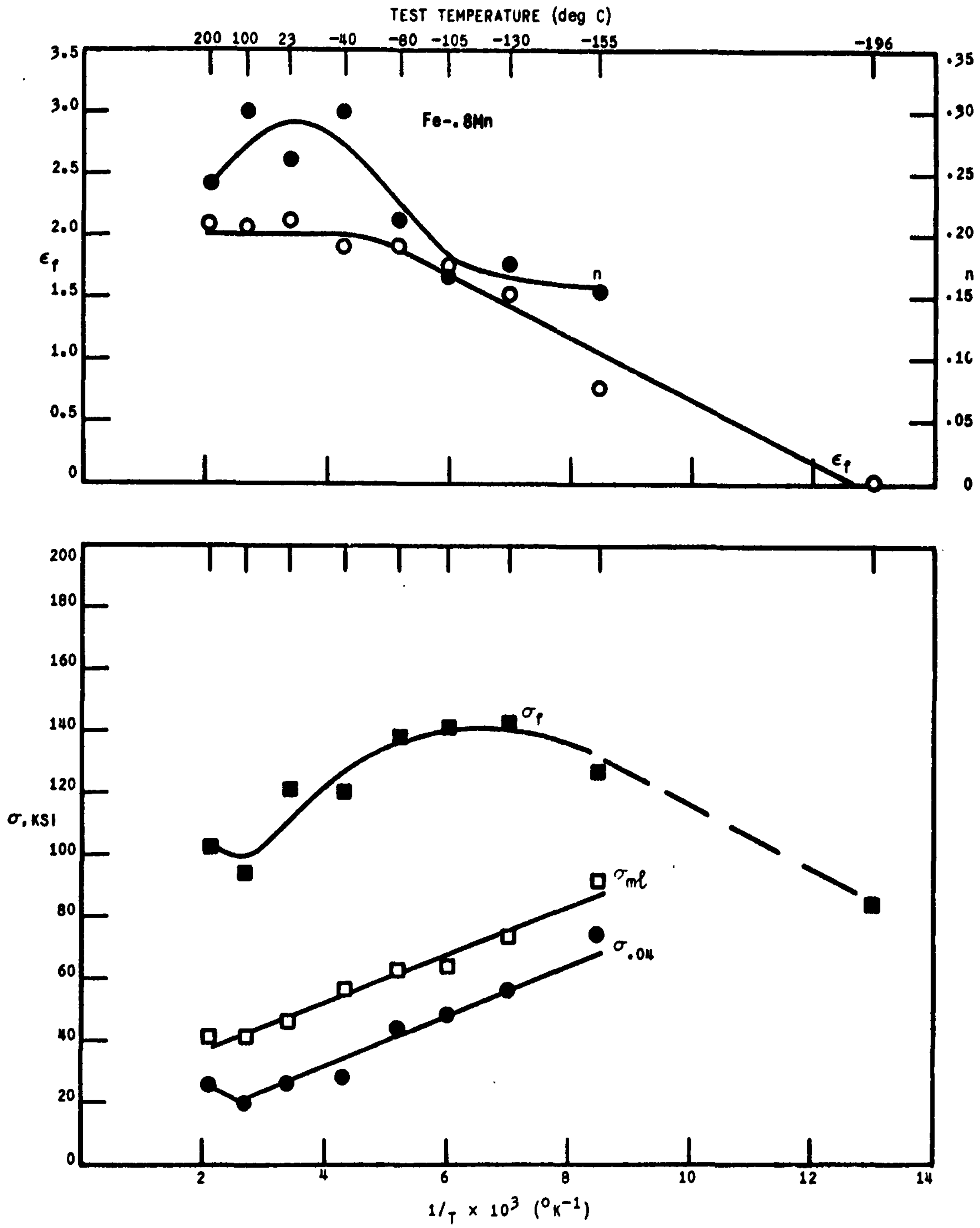

TEST TEMPERATURE (deg C)
200 100 23 -40 -80 -105 -130 -155 -196
Fe-.8Mn
3.5
3.0
2.5
2.0
1.5
1.0
0.5
0
ϵ_f
.35
.30
.25
.20
.15
.10
.05
0
n
n
ϵ_f
200
180
160
140
120
100
80
60
40
20
0
σ, KSI
σ_f
$\sigma_{m\ell}$
$\sigma_{.04}$
2
4
6
8
10
12
14
$1/_T \times 10^3$ ($^oK^{-1}$)

Figure 8-15

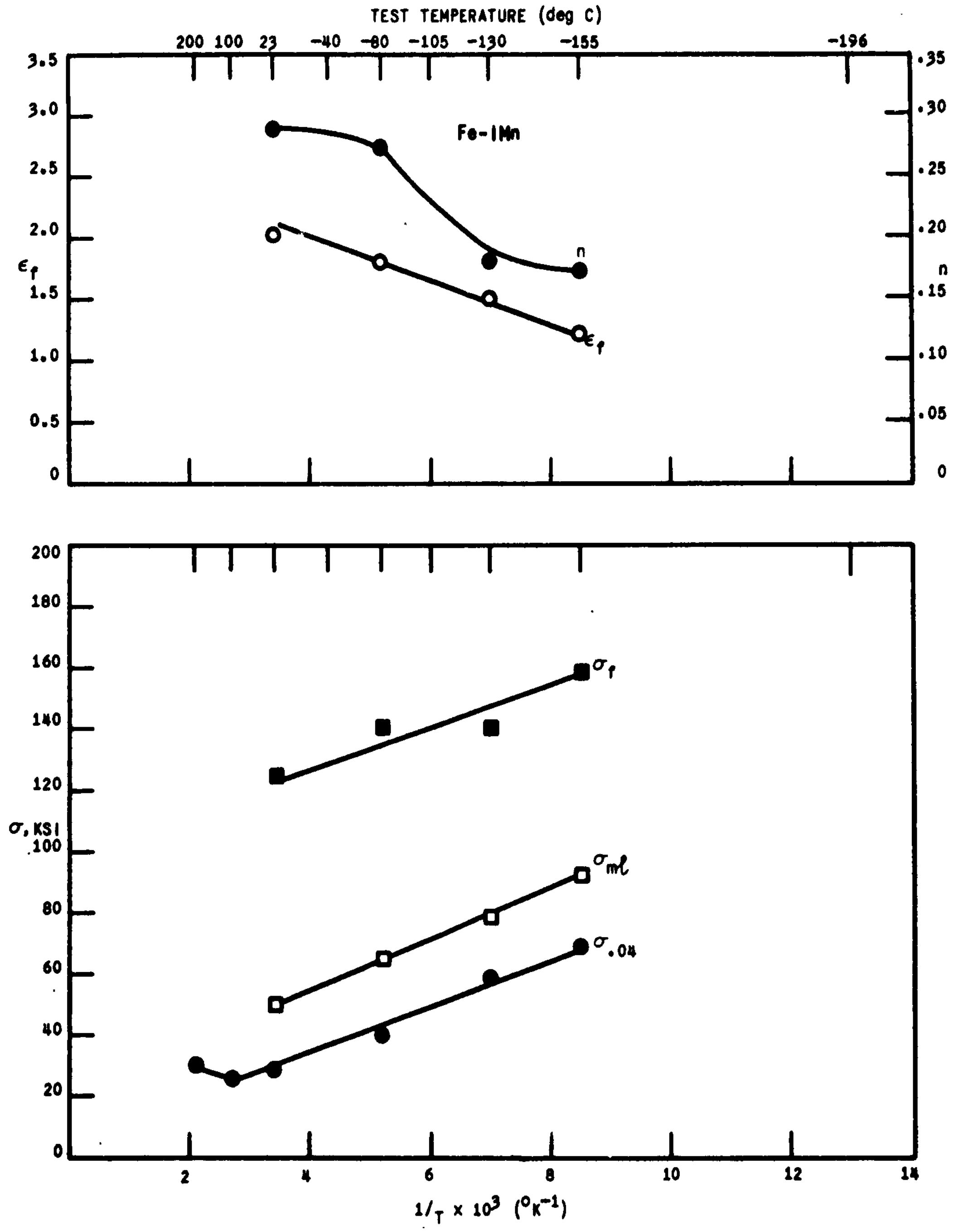
TEST TEMPERATURE (deg C)
200 100 23 -40 -80 -105 -130 -155 -196
3.5
3.0
2.5
2.0
1.5
1.0
0.5
0
ϵ_f
Fe-1Mn
n
ϵ_f
.35
.30
.25
.20
.15
.10
.05
0
n
200
180
160
140
120
100
80
60
40
20
0
σ, KSI
σ_f
$\sigma_{m\ell}$
$\sigma_{.04}$
2
4
6
8
10
12
14
$1/_T \times 10^3$ ($^oK^{-1}$)

Figure B-16

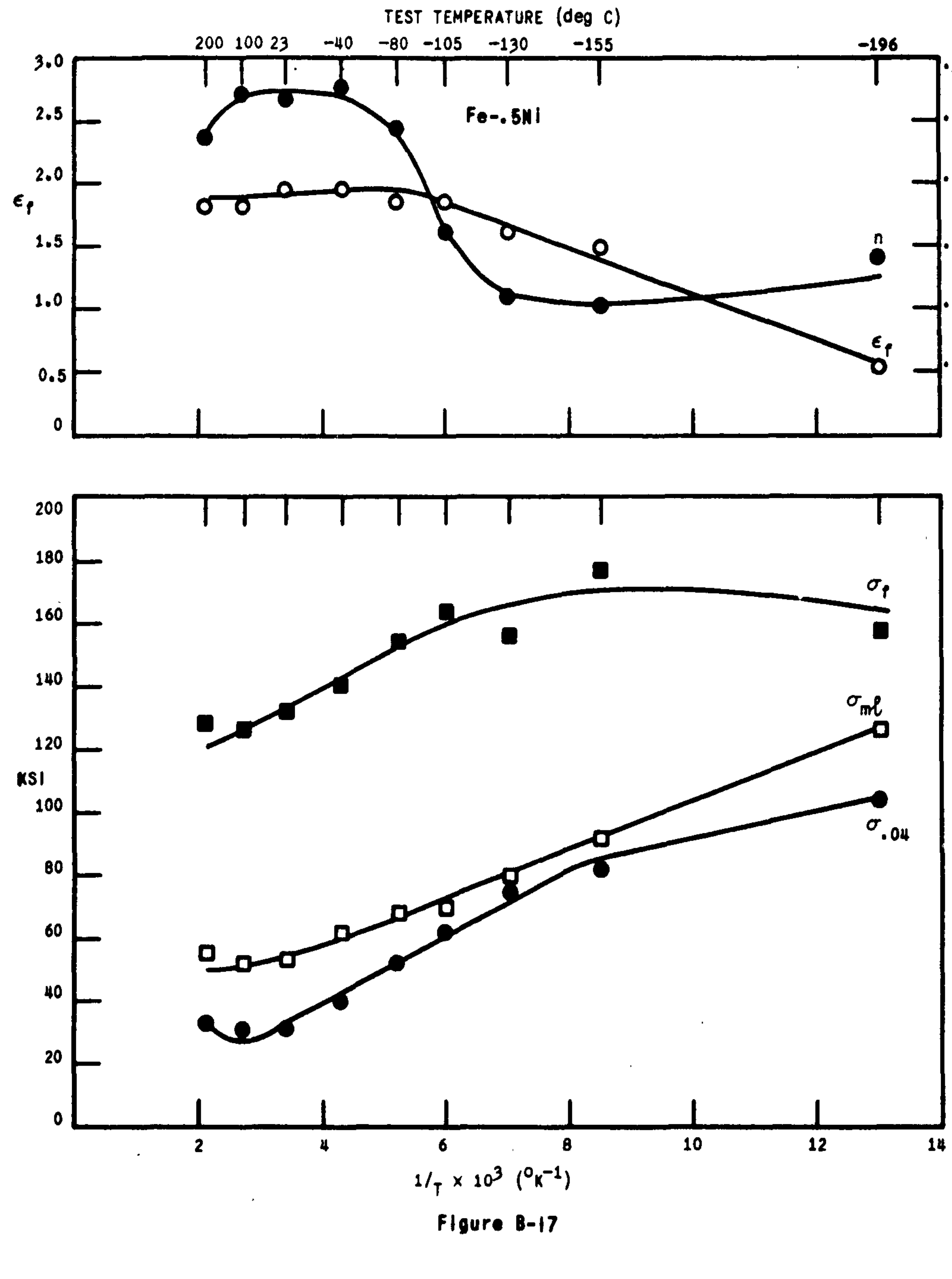
TEST TEMPERATURE (deg C)
200 100 23 -40 -80 -105 -130 -155 -196
3.0
2.5
2.0
1.5
1.0
0.5
0
.30
.25
.20
.15
.10
.05
0
Fe-.5Ni
ϵ_f
n
n
ϵ_f
200
180
160
140
120
100
80
60
40
20
0
KSI
σ_f
$\sigma_{m\ell}$
$\sigma_{.04}$
2
4
6
8
10
12
14
$1/_T \times 10^3$ ($^oK^{-1}$)

Figure B-17

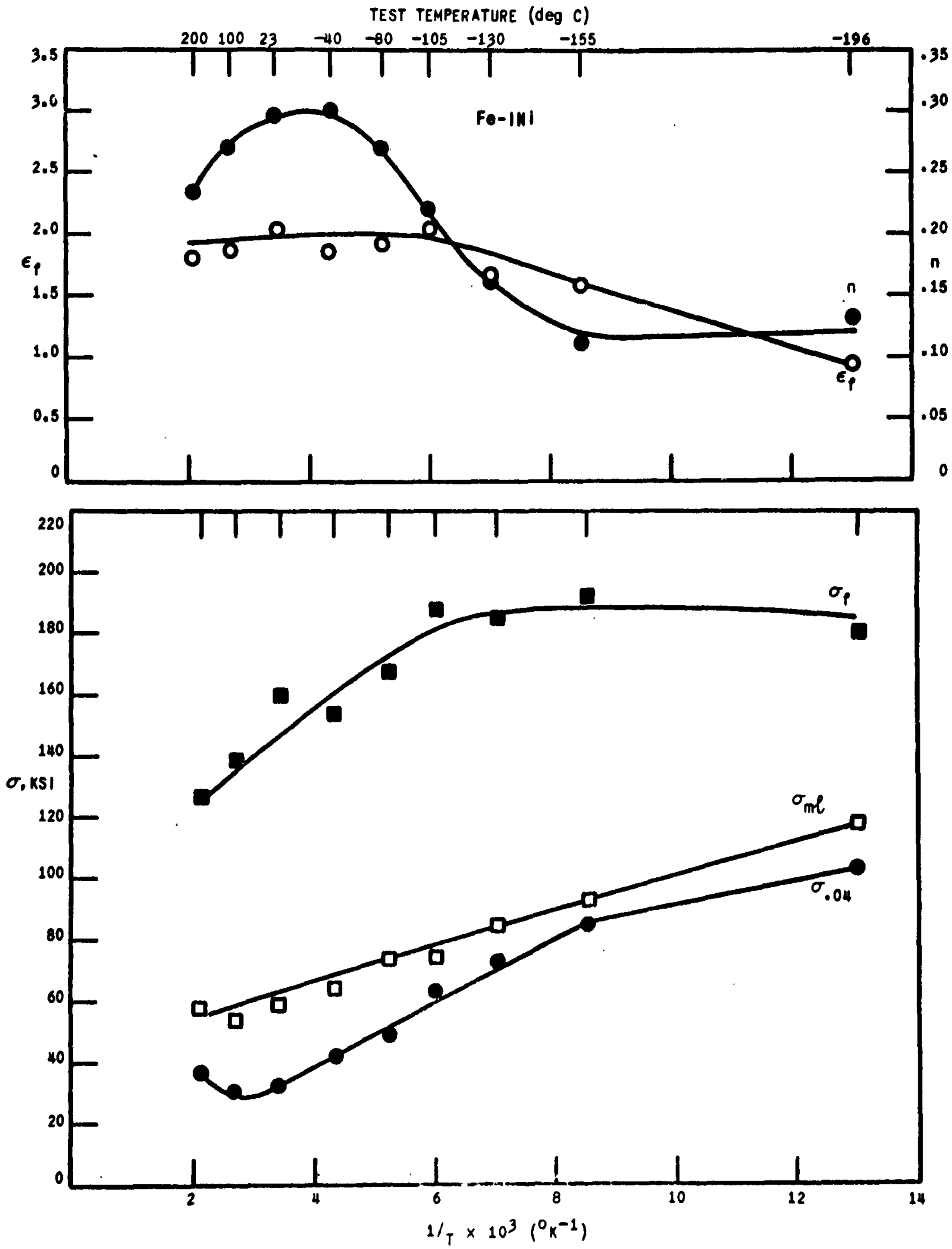
TEST TEMPERATURE (deg C)
200 100 23 -40 -80 -105 -130 -155 -196
Fe-1Ni
ϵ_f
n
σ, KSI
σ_f
σ_{ml}
$\sigma_{.04}$
$1/T \times 10^3$ ($^oK^{-1}$)

Figure B-18

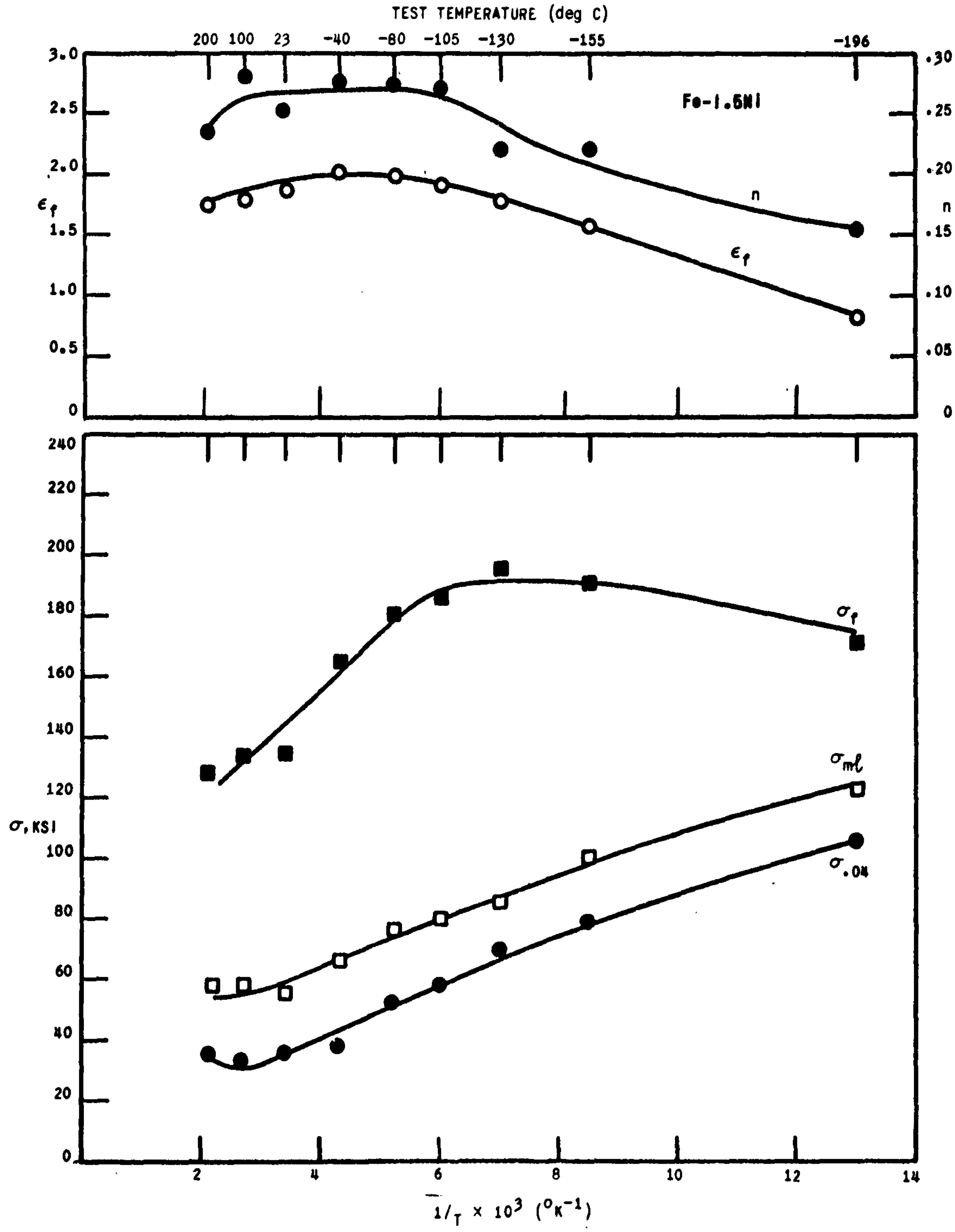
TEST TEMPERATURE (deg C)
200 100 23 -40 -80 -105 -130 -155 -196
3.0
2.5
2.0
1.5
1.0
0.5
0
ϵ_f
Fe-1.5Ni
n
ϵ_f
.30
.25
.20
.15
.10
.05
0
n
240
220
200
180
160
140
120
100
80
60
40
20
0
σ, KSI
σ_f
σ_{ml}
$\sigma_{.04}$
2
4
6
8
10
12
14
$\overline{1/_T} \times 10^3$ ($^{\circ}K^{-1}$)

Figure B-19

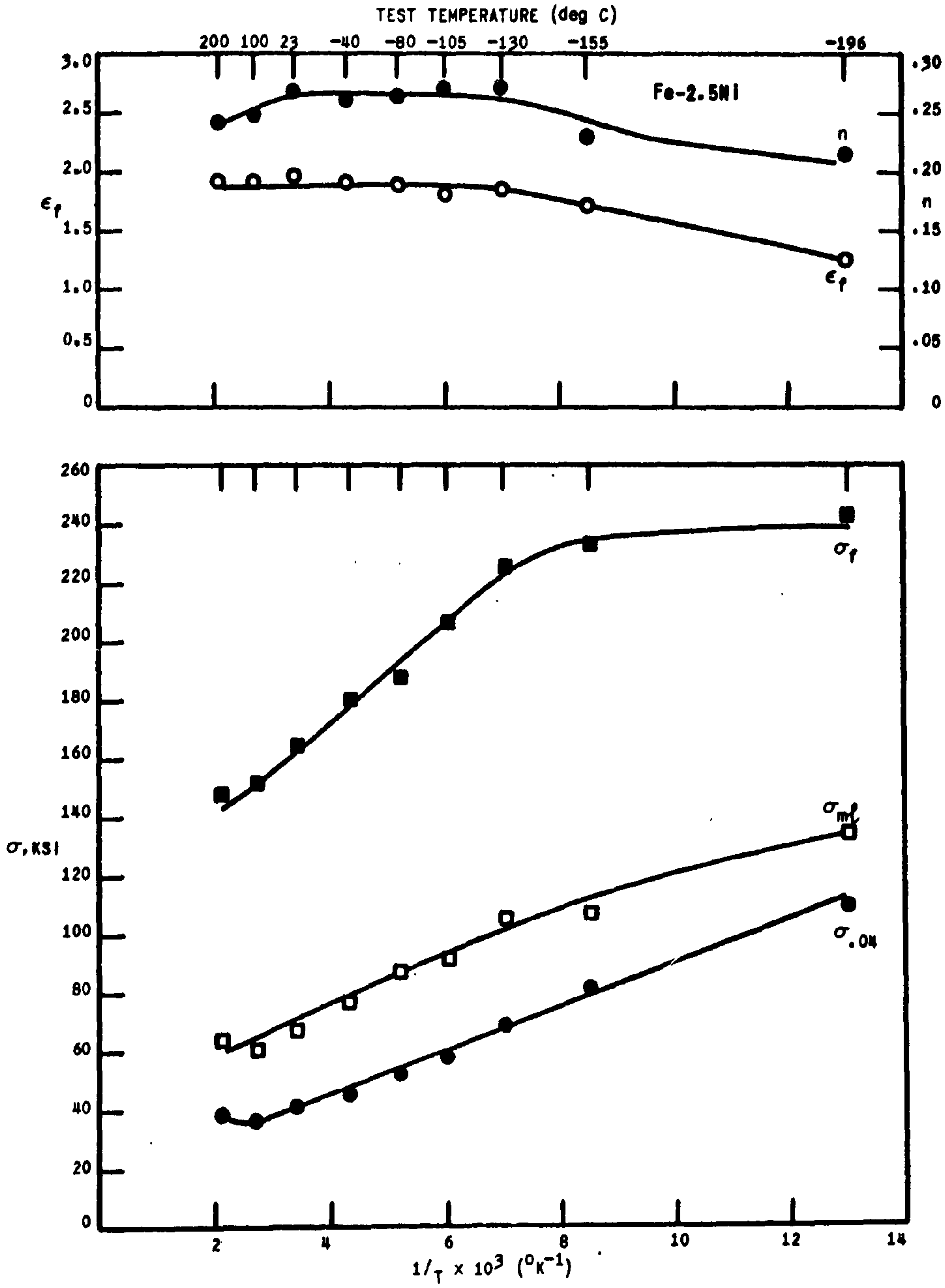
TEST TEMPERATURE (deg C)
200 100 23 -40 -80 -105 -130 -155 -196
Fe-2.5Ni
n
ϵ_f
σ, KSI
σ_f
σ_{mf}
$\sigma_{.04}$
$1/_T \times 10^3$ ($^oK^{-1}$)

Figure B-20

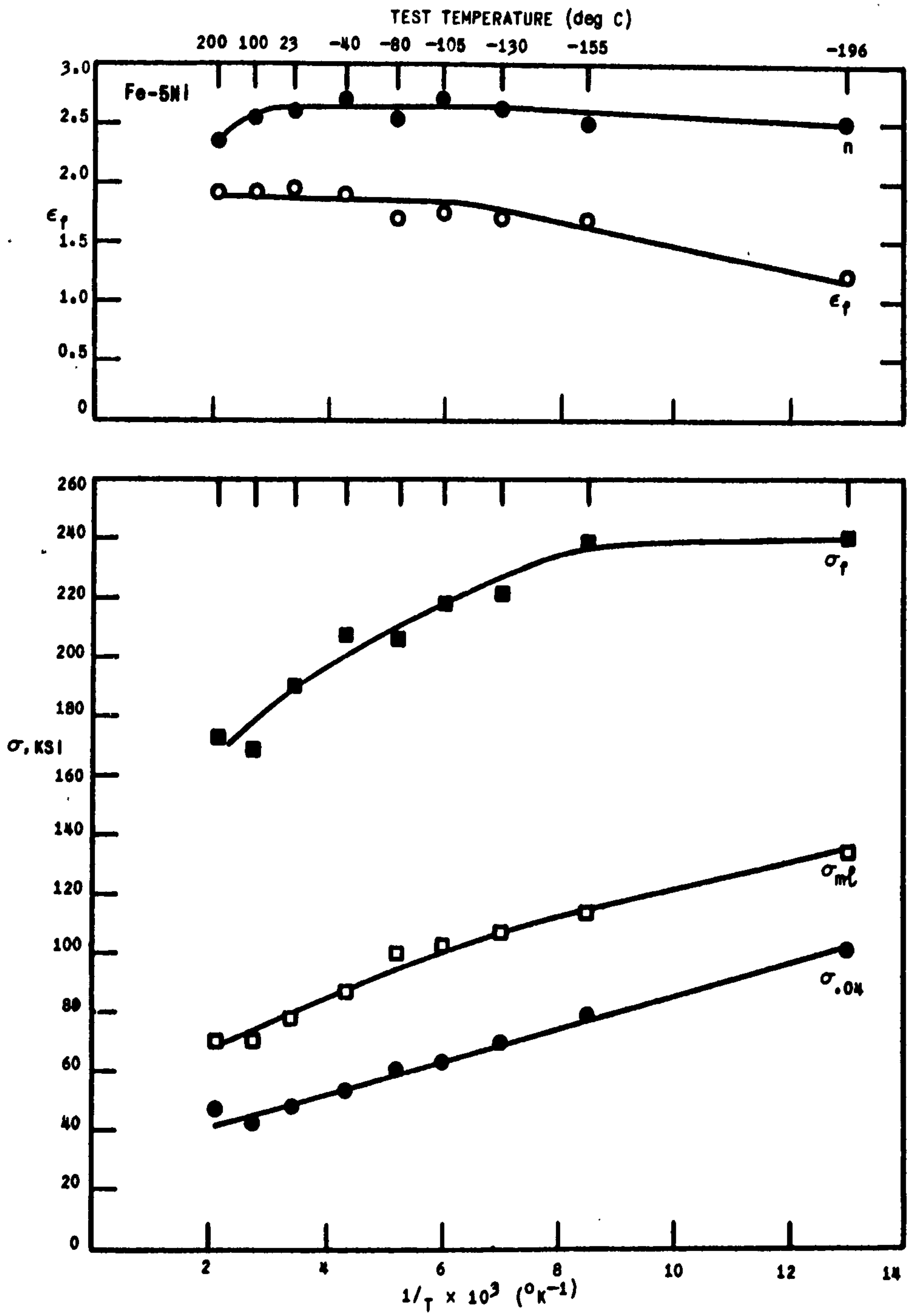

TEST TEMPERATURE (deg C)
200 100 23 -40 -80 -105 -130 -155 -196
Fe-5Ni
3.0
2.5
2.0
1.5
1.0
0.5
0
ϵ_f
n
.30
.25
.20
.15
.10
.05
0
ϵ_f
260
240
220
200
180
160
140
120
100
80
60
40
20
0
σ, KSI
σ_f
$\sigma_{m\ell}$
$\sigma_{.04}$
2
4
6
8
10
12
14
$1/T \times 10^3$ ($^{o}K^{-1}$)

Figure B-21

REFERENCES

1. GENSAMER, M., General Survey of the Problem of Fatigue and Fracture, Fatigue and Fracture of Metals, Technical Press of MIT, and John Wiley and Son, Inc., 1952, p. 1-17.

2. OROWON, E., Fundamentals of Brittle Behavior in Metals, ibid, p. 139-167.

3. BECHTOLD, J. H., Tensile Properties of Annealed Tantalum at Low Temperatures, Acta Metallurgica, v. 3, May 1955, p. 249-254.

4. INGRAM, A. G., et al., Notch Sensitivity of Refractory Metals, Transactions of the Metallurgical Society of AIME, v. 221, June 1961, p. 517-527.

5. LARSON, F. R., and NUNES, J., Low Temperature Flow and Fracture Tension Properties of Heat-Treated SAE 4340 Steel, Transactions, ASM, v. 53, 1961, p. 663-682.

6. NUNES, J., and LARSON, F. R., Low Temperature Hardness and Flow Stress Relationships of Metals, Watertown Arsenal Laboratories, WAL TR 834.2/5, October 1961. To be published in the Journal of the Institute of Metals.

7. LOUAT, N., and WAIN, H. L., Brittle Fracture and Yield Point Phenomenon, Proceedings of an International Conference on the Atomic Mechanisms of Fracture, Conducted by National Academy of Sciences, National Research Council, New Ocean House, Swampscott, Massachusetts, 12-14 April 1959. John Wiley and Son, Inc., New York.

8. FISHER, J. C., Application of Cottrell's Theory of Yielding to Delayed Yield in Steel, Transactions, ASM, v. 47, 1955, p. 451-462.

9. CLOUGH, W. R., and PAVLOVIC, A. S., The Flow, Fracture and Twinning of Commercially Pure Vanadium, Transactions, ASM, v. 52, 1960, p. 948-970.

10. BAIN, E. C., Functions of the Alloying Elements in Steel, American Society for Metals, Cleveland, Ohio, 1939.

11. AUSTIN, C. R., Effect of Elements in Solid Solutions on Hardness and Response to Heat Treatment of Iron Binary Alloys, Transactions, ASM, v. 31, 1943, p. 321-339.

12. AUSTIN, C. R., LUINI, L. A., and LINDSAY, R. W., Annealing Studies of Cold-Rolled Iron and Iron Binary Alloys, Transactions, ASM, v. 35, 1945, p. 446-484.

13. LACY, C. E., and GENSAMER, M., The Tensile Properties of Alloyed Ferrites, Transactions, ASM, v. 32, 1944, p. 88-110.

14. SMITH, R. L., SPANGLER, G., and BRICK, R. M., Effect of Grain Size and Carbon Content on the Low Temperature Tensile Properties of High Purity Fe-C Alloys, Transactions, ASM, v. 46, 1954, p. 973-977.

15. ALLEN, N. P., et al., Tensile and Impact Properties of High Purity Iron-Carbon and Iron-Carbon-Manganese Alloys of Low Carbon Content, Journal of the Iron and Steel Institute, v. 174, 1953, p. 108-120.

16. LONDON, G. J., SPANGLER, G., and BRICK, R. M., Mechanical Properties of High Purity Fe-C Alloys at Low Temperatures, Ship Structure Committee Report, SSC-93, National Academy of Sciences, National Research Council, Washington, D. C., 31 March 1959.

17. LESLIE, W. C., WILLIAMS, G. B., and HUTTON, D. S., The Tensile Properties of High Purity Low-Carbon Iron and Iron-Manganese Alloys, Journal of the Iron and Steel Institute, v. 198, May 1961, p. 21-29.

18. KAYSER, F. X., Iron-Aluminum Systems, Part I. Fundamental Studies and Alloy Development, Ford Motor Company, WADC TR 57-298, Contract No. AF 33(600)-32448, May 1957.

19. REES, W. P., and HOPKINS, B. E., Intergranular Brittleness in Iron-Oxygen Alloys, Journal of the Iron and Steel Institute, v. 172, December 1952, p. 403-409.

20. HOPKINS, B. E., and TIPLER, H. R., The Effect of Phosphorus on the Tensile and Notch-Impact Properties of High-Purity Iron and Iron-Carbon Alloys, Journal of the Iron and Steel Institute, v. 188, March 1958, p. 218-232.

21. RARING, R., RINEBOLT, J. A., and BRICK, W. J., JR., Effect of Alloying Elements on True Stress-True-Strain Flow Curves of Pearlitic Steel, Transactions, AIME, v. 191, 1951, p. 395-400.

22. GLEN, J., Effect of Alloying Elements on the High-Temperature Tensile Strength of Normalized Low-Carbon Steel, Journal of the Iron and Steel Institute, v. 186, May 1957, p. 21-48.

23. HAYNES, A. G., Low Alloy Constructional Steels - The Influence of Chemical Composition on their Mechanical Properties, Research Applied in Industry, v. 14, September 1961, p. 367-376.

24. COTTRELL, A. H., and BILBY, B. A., Dislocation Theory of Yielding and Strain Ageing of Iron, Proceedings of the Physical Society, v. 62, 1949, p. 49-62.

25. ROBBINS, J. L., SHEPARD, O. C., and SHERBY, O. D., Role of Crystal Structure on the Ductility of Pure Iron at Elevated Temperatures, Journal of the Iron and Steel Institute, v. 199, October 1961, p. 175-180.

26. GIBBONS, D. F., Plastic Deformation of Iron Between 300-77.2°K, Transactions, AIME, v. 197, 1953, p. 1245-1250.

27. SMITH, R. L., and RUTHERFORD, J. L., Tensile Properties of Zone Refined Iron in the Temperature Range from 298° to 4.2°K, Transactions, AIME, v. 209, 1957, p. 857-864.

28. SCHOECK, G., and SEEGER, A., The Flow Stress of Iron and Its Dependence on Impurities, Acta Metallurgica, v. 7, July 1959, p. 469-477.

29. HESLOP, J., and PETCH, N. J., The Stress to Move a Free Dislocation in Alpha Iron, The Philosophical Magazine, v. 1, September 1956, p. 866-873.

30. CONRAD, H., and SCHOECK, G., Cottrell Locking and the Flow Stress in Iron, Acta Metallurgica, v. 8, November 1960, p. 791-796.

31. PETCH, N. J., The Cleavage Strength of Polycrystals, Journal of the Iron and Steel Institute, v. 174, 1953, p. 25-28.

32. BIGGS, W. D., and PRATT, P. L., The Deformation and Fracture of Alpha-Iron at Low Temperatures, Acta Metallurgica, v. 6, 1958, p. 694-703.

33. COTTRELL, A. H., Theory of Brittle Fracture in Steel and Similar Metals, Transactions, AIME, v. 212, April 1958, p. 192-203.

34. NUNES, J., and LARSON, F. R., A Method for Determining the Plastic Flow Properties of Sheet and Round Tension Test Specimens, Watertown Arsenal Laboratories, WAL TR 111.1/1, March 1961; also Proceedings, ASTM, v. 61, 1961, p. 1349-1361.

35. GENSAMER, M., Strength and Ductility, Campbell Memorial Lecture, Transactions, ASM, v. 36, 1946, p. 30-60.

36. BEEUWKES, R., JR., Discussion, 7th Sagamore Ordnance Materials Conference, Syracuse, New York, 16 August 1960.

37. HAMAKER, J. C., JR., Discussion of Strain Hardening Properties of High Strength Sheet Materials, by F. R. Larson and J. Nunes, Transactions, ASM, v. 54, 1961, p. 837-840.

38. AMERICAN SOCIETY FOR METALS, Properties and Selection of Metals, Metals Handbook, v. 1, 1961, p. 227.

39. LARSON, F. R., and NUNES, J., Relationships Between Energy, Fibrosity and Temperature in Charpy Impact Tests of AISI 4340 Steel, Watertown Arsenal Laboratories, WAL TR 834.2/3, December 1961; also Proceedings, ASTM, v. 62, 1962.

40. BENNETT, P. E., and SINCLAIR, G. M., An Analysis of the Time and Temperature Dependence of the Upper Yield Point in Iron, Transactions, ASME, Journal of Basic Engineering, v. 83, December 1961, p. 557.

WATERTOWN ARSENAL
WATERTOWN 72, MASSACHUSETTS

TECHNICAL REPORT DISTRIBUTION

Report No.: WAL TR 834.2/9 May 1963 Title: Low Temperature Flow and Fracture Characteristics of Some Iron-Base Alloys

No. of Copies	TO
	Advanced Research Projects Agency, The Pentagon, Washington 25, D. C.
1	ATTN: Mr. Charles Yost
10	Armed Services Technical Information Agency, Arlington Hall Station, Arlington 12, Virginia
1	Defense Metals Information Center, Battelle Memorial Institute, Columbus 1, Ohio
1	Commanding Officer, U. S. Army Research Office, Arlington Hall Station, Arlington 12, Virginia
	Commanding Officer, Army Research Office (Durham), Box CM, Duke Station, Durham, North Carolina
1	ATTN: Physics Division
	Commanding General, U. S. Army Materiel Command, Washington 25, D. C.
1	ATTN: AMCRD-RS, Research Division
1	AMCRD-DE, Development Division
1	AMCRD-RS-CM-M, Dr. P. Kosting
1	AMCRD-RS-CM, Mr. J. Kaufman
1	AMCRD-RS, Scientific Deputy
	Commanding General, U. S. Army Electronics Command, Fort Monmouth, New Jersey
1	ATTN: Institute for Fundamental Research
	Commanding General, U. S. Army Missile Command, Redstone Arsenal, Huntsville, Alabama
1	ATTN: AMSMI-RB, Redstone Scientific Information Center
1	Directorate of R&D
1	Chief Scientist, Dr. W. W. Carter
1	Dr. B. Steverding

No. of Copies	TO
1	Commanding General, U. S. Army Mobility Command, 28251 Van Dyke Avenue, Center Line, Michigan
	Commanding General, U. S. Army Munitions Command, Dover, New Jersey
1	ATTN: Chief Scientist
	Commanding General, U. S. Army Tank-Automotive Center, Detroit Arsenal, Center Line, Michigan
1	ATTN: SMOTA-RCM.1
	Commanding General, U. S. Army Test and Evaluation Command, Aberdeen Proving Ground, Maryland
1	ATTN: AMSTE-IM, Technical Library, Building 313
	Commanding General, U. S. Army Transportation Research Command, Fort Eustis, Virginia
1	ATTN: Physical Sciences Division, Dr. G. D. Sands
	Commanding General, U. S. Army Weapons Command, Rock Island, Illinois
1	ATTN: Chief Scientist
	Commanding Officer, U. S. Army Ballistics Research Laboratories, Aberdeen Proving Ground, Maryland
1	ATTN: Dr. Coy Glass
	Commanding Officer, U. S. Army Chemical Corps Nuclear Defense Laboratories, Army Chemical Center, Maryland
1	ATTN: Nuclear Physics Division
1	Commanding Officer, U. S. Army Engineer Research and Development Laboratories, Fort Belvoir, Virginia
	Commanding Officer, U. S. Army Quartermaster Research and Engineering Laboratories, Natick, Massachusetts
1	ATTN: Pioneering Research Division, Dr. S. D. Bailey
	Commanding Officer, Harry Diamond Laboratories, Washington 25, D. C.
1	ATTN: AMXDO-TIB
	Commanding Officer, Frankford Arsenal, Bridge and Tacony Streets, Philadelphia 37, Pennsylvania
1	ATTN: Pitman-Dunn Laboratories
1	Research Institute

No. of Copies	TO
	Commanding Officer, Picatinny Arsenal, Dover, New Jersey
1	ATTN: Feltman Research Laboratories
1	Technical Library
	Commanding Officer, Rock Island Arsenal, Rock Island, Illinois
1	ATTN: 9320, Research and Development Division
	Commanding Officer, Springfield Armory, Springfield 1, Massachusetts
1	ATTN: SWESP-TX, Research and Development Division
	Commanding Officer, Watervliet Arsenal, Watervliet, New York
1	ATTN: Research Branch
1	Director, Naval Research Laboratory, Anacostia Station, Washington 25, D. C.
1	Commander, Office of Naval Research, Department of the Navy, Washington 25, D. C.
1	Commander, U. S. Naval Ordnance Laboratory, White Oak, Silver Spring, Maryland
	Commanding General, Air Force Cambridge Research Laboratories, Hanscom Field, Bedford, Massachusetts
1	ATTN: Electronic Research Directorate
	Commanding General, Air Force Materials Central, Wright-Patterson Air Force Base, Ohio
1	ATTN: Physics Laboratory
1	Aeronautical Research Laboratories
1	Commander, Office of Scientific Research, Air R&D Command, Temporary Building T, Washington 25, D. C.
	U. S. Atomic Energy Commission, Washington 25, D. C.
1	ATTN: Office of Technical Information
1	U. S. Atomic Energy Commission, Office of Technical Information Extension, P. O. Box 62, Oak Rodge, Tennessee
	Director, George C. Marshall Space Flight Center, Huntsville, Alabama
1	ATTN: M-S&M-M, Dr. W. Lucas

No. of Copies	TO
	Director, Jet Propulsion Laboratory,
	California Institute of Technology, Pasadena 3, California
1	ATTN: Dr. L. Jaffe
1	Director, Lewis Flight Laboratories, Cleveland Airport, Cleveland, Ohio
1	Director, National Bureau of Standards, Washington 25, D. C
1	Director, Research Analysis Corporation, 6935 Arlington Road, Bethesda, Maryland
	Commanding Officer, U. S. Army Materials Research Agency,
	Watertown 72, Massachusetts
5	ATTN: AMXMR-LXM, Technical Information Section
1	AMXMR-OPT
1	AMXMR, Dr. R. Beeuwkes, Jr.
2	Authors

65 -- TOTAL COPIES DISTRIBUTED

OTS Price $1.75

AD ______________ Accession No. ______________

Watertown Arsenal Laboratories, Watertown 72, Mass.
LOW TEMPERATURE FLOW AND FRACTURE CHARACTERISTICS OF SOME IRON-BASE ALLOYS - John Nunes and Frank R. Larson

WAL TR 834.2/9, May 1963, 62 pp - illus - tables - appendixes, AMS Code 5011.11.838, D/A Project 1-A-0-10501-B-010, Unclassified

Temperature dependent functions of various tensile flow stress and fracture parameters were investigated on Fe and low composition alloys of Fe-C, Fe-Cr, Fe-Mn and Fe-Ni. Data were obtained over a range of test temperatures from 200 to -196 C at an initial strain rate of .01 min^{-1}. It was found that the strain hardening exponent, n, for the Fe-Ni alloys exhibited a considerable improvement at very low testing temperature with increased alloy addition. Some anomalous yield point and strengthening effects were observed. The flow stress-temperature dependence was evaluated employing the relation $\sigma = \frac{M}{T} + \sigma_o$ where it is shown that along with crystallographic structure, composition can strongly influence the constant M. Some preliminary tests were run on several commercial sheets to test the generality of an empirical formula, $M = m_1$ (equivalent At. % Ni)$^{-1/3}$, describing this effect.

NO DISTRIBUTION LIMITATIONS

UNCLASSIFIED

1. Plastic flow
2. Fracture
3. Iron alloys

I. Nunes, John
II. Larson, Frank R.
III. AMS Code 5011.11.838
IV. D/A Project 1-A-0-10501-B-010

OTS Price $1.75

AD ______________ Accession No. ______________

Watertown Arsenal Laboratories, Watertown 72, Mass.
LOW TEMPERATURE FLOW AND FRACTURE CHARACTERISTICS OF SOME IRON-BASE ALLOYS - John Nunes and Frank R. Larson

WAL TR 834.2/9, May 1963, 62 pp - illus - tables - appendixes, AMS Code 5011.11.838, D/A Project 1-A-0-10501-B-010, Unclassified

Temperature dependent functions of various tensile flow stress and fracture parameters were investigated on Fe and low composition alloys of Fe-C, Fe-Cr, Fe-Mn and Fe-Ni. Data were obtained over a range of test temperatures from 200 to -196 C at an initial strain rate of .01 min^{-1}. It was found that the strain hardening exponent, n, for the Fe-Ni alloys exhibited a considerable improvement at very low testing temperature with increased alloy addition. Some anomalous yield point and strengthening effects were observed. The flow stress-temperature dependence was evaluated employing the relation $\sigma = \frac{M}{T} + \sigma_o$ where it is shown that along with crystallographic structure, composition can strongly influence the constant M. Some preliminary tests were run on several commercial sheets to test the generality of an empirical formula, $M = m_1$ (equivalent At. % Ni)$^{-1/3}$, describing this effect.

NO DISTRIBUTION LIMITATIONS

UNCLASSIFIED

1. Plastic flow
2. Fracture
3. Iron alloys

I. Nunes, John
II. Larson, Frank R.
III. AMS Code 5011.11.838
IV. D/A Project 1-A-0-10501-B-010

OTS Price $1.75

AD ______________ Accession No. ______________

Watertown Arsenal Laboratories, Watertown 72, Mass.
LOW TEMPERATURE FLOW AND FRACTURE CHARACTERISTICS OF SOME IRON-BASE ALLOYS - John Nunes and Frank R. Larson

WAL TR 834.2/9, May 1963, 62 pp - illus - tables - appendixes, AMS Code 5011.11.838, D/A Project 1-A-0-10501-B-010, Unclassified

Temperature dependent functions of various tensile flow stress and fracture parameters were investigated on Fe and low composition alloys of Fe-C, Fe-Cr, Fe-Mn and Fe-Ni. Data were obtained over a range of test temperatures from 200 to -196 C at an initial strain rate of .01 min^{-1}. It was found that the strain hardening exponent, n, for the Fe-Ni alloys exhibited a considerable improvement at very low testing temperature with increased alloy addition. Some anomalous yield point and strengthening effects were observed. The flow stress-temperature dependence was evaluated employing the relation $\sigma = \frac{M}{T} + \sigma_o$ where it is shown that along with crystallographic structure, composition can strongly influence the constant M. Some preliminary tests were run on several commercial sheets to test the generality of an empirical formula, $M = m_1$ (equivalent At. % Ni)$^{-1/3}$, describing this effect.

NO DISTRIBUTION LIMITATIONS

UNCLASSIFIED

1. Plastic flow
2. Fracture
3. Iron alloys

I. Nunes, John
II. Larson, Frank R.
III. AMS Code 5011.11.838
IV. D/A Project 1-A-0-10501-B-010

OTS Price $1.75

AD ______________ Accession No. ______________

Watertown Arsenal Laboratories, Watertown 72, Mass.
LOW TEMPERATURE FLOW AND FRACTURE CHARACTERISTICS OF SOME IRON-BASE ALLOYS - John Nunes and Frank R. Larson

WAL TR 834.2/9, May 1963, 62 pp - illus - tables - appendixes, AMS Code 5011.11.838, D/A Project 1-A-0-10501-B-010, Unclassified

Temperature dependent functions of various tensile flow stress and fracture parameters were investigated on Fe and low composition alloys of Fe-C, Fe-Cr, Fe-Mn and Fe-Ni. Data were obtained over a range of test temperatures from 200 to -196 C at an initial strain rate of .01 min^{-1}. It was found that the strain hardening exponent, n, for the Fe-Ni alloys exhibited a considerable improvement at very low testing temperature with increased alloy addition. Some anomalous yield point and strengthening effects were observed. The flow stress-temperature dependence was evaluated employing the relation $\sigma = \frac{M}{T} + \sigma_o$ where it is shown that along with crystallographic structure, composition can strongly influence the constant M. Some preliminary tests were run on several commercial sheets to test the generality of an empirical formula, $M = m_1$ (equivalent At. % Ni)$^{-1/3}$, describing this effect.

NO DISTRIBUTION LIMITATIONS

UNCLASSIFIED

1. Plastic flow
2. Fracture
3. Iron alloys

I. Nunes, John
II. Larson, Frank R.
III. AMS Code 5011.11.838
IV. D/A Project 1-A-0-10501-B-010